1982

Synthesis and characterization of multiply metal-metal bonded complexes of molybdenum and tungsten

Richard Trotter Carlin
Iowa State University

Carlin, Richard Trotter

SYNTHESIS AND CHARACTERIZATION OF MULTIPLY METAL-METAL BONDED COMPLEXES OF MOLYBDENUM AND TUNGSTEN

Iowa State University PH.D. 1982

PLEASE NOTE:

In all cases this material has been filmed in the best possible way from the available copy. Problems encountered with this document have been identified here with a check mark __✓__.

1. Glossy photographs or pages _____
2. Colored illustrations, paper or print _____
3. Photographs with dark background _____
4. Illustrations are poor copy _____
5. Pages with black marks, not original copy _____
6. Print shows through as there is text on both sides of page _____
7. Indistinct, broken or small print on several pages ✓
8. Print exceeds margin requirements _____
9. Tightly bound copy with print lost in spine _____
10. Computer printout pages with indistinct print _____
11. Page(s) _____ lacking when material received, and not available from school or author.
12. Page(s) _____ seem to be missing in numbering only as text follows.
13. Two pages numbered _____. Text follows.
14. Curling and wrinkled pages _____
15. Other _____

Synthesis and characterization of multiply metal-metal bonded complexes of molybdenum and tungsten

by

Richard Trotter Carlin

A Dissertation Submitted to the
Graduate Faculty in Partial Fulfillment of the
Requirements for the Degree of
DOCTOR OF PHILOSOPHY

Department: Chemistry
Major: Inorganic Chemistry

Approved:

Signature was redacted for privacy.

In Charge of Major Work

Signature was redacted for privacy.

For the Major Department

Signature was redacted for privacy.

For the Graduate College

Iowa State University
Ames, Iowa

1982

TABLE OF CONTENTS

LIST OF FIGURES

LIST OF TABLES

GENERAL INTRODUCTION

The synthesis of a large number of quadruply bonded molybdenum dimers has been accomplished (1). Despite the relative ease with which the molybdenum complexes can be obtained, analogous quadruply bonded tungsten dimers eluded chemists for a long time. It is only within the past several years that a few quadruply bonded tungsten dimers have been prepared. Because of this, knowledge of the chemistry and physical properties of these tungsten dimers is limited.

The first readily available and synthetically useful quadruply bonded tungsten dimer was $W_2(mhp)_4$ (mhp = anion of 2-hydroxy-6-methylpyridine) (2), in which the four mhp ligands bridge between the two metals. It was hoped that this dimer would behave in a similar fashion as the quadruply bonded molybdenum dimer, $Mo_2(O_2CCH_3)_4$ (3) which is the starting material for the synthesis of most of the other molybdenum quadruply bonded dimers (1). Ligand exchange reactions of $W_2(mhp)_4$ using the lithium salt of 2-amino-6-methylpyridine (Hmap) or trifluoroacetic acid (HTFA) give $W_2(map)_4$ (4) and $W_2(mhp)_2(TFA)_2$ (5), respectively, in which the tungsten-tungsten quadruple bonds are retained. Attempts to produce the unbridged species $W_2X_8^{4-}$ or $W_2Cl_4(PEt_3)_4$ (X = Cl or Br) resulted in oxidation of the tungstens to produce the previously synthesized complexes $Cs_3W_2X_9$ and $W_2X_4(OR)_4(HOR)_2$ (R = Me or Et), respectively (6,7). It is this oxidation of tungsten(II) which is the stumbling block for the synthesis of other quadruply bonded tungsten dimers from $W_2(mhp)_4$.

This oxidation of tungsten has been circumvented recently by Sharp and Schrock by reducing WCL_4 with a stoichiometric quantity of Na/Hg in

THF to give tungsten(II), which in the presence of a phosphine ligand, gives $W_2Cl_4(PR_3)_4$ (PR_3 = PMe_3, PBu_3, PMe_2Ph or $PMePh_2$) (8). These were the first well-characterized unbridged tungsten dimers containing a tungsten-tungsten quadruple bond. The previously synthesized octamethyl complexes, $Li_4W_2(Me)_8 \cdot 4Et_2O$ and $Li_4W_2(Me)_{8-x}Cl_x$, have also been shown to possess tungsten-tungsten quadruple bonds; however, their extreme sensitivity to air and thermal instability have hampered their thorough characterization (9,10,11). Very recent work using similar synthetic techniques as those used to prepare the $W_2Cl_4(PR_3)_4$ compounds has made possible the synthesis of several $W_2(O_2CR)_4$ (R = CF_3 (12), CMe_3 (13) or C_6H_5 (14)) complexes, all of which possess tungsten-tungsten quadruple bonds.

Before the synthesis of the quadruply bonded tungsten dimers was accomplished, the heteronuclear dimer $MoW(O_2CCMe_3)_4$ was prepared (15). This was the first compound in which tungsten participated in a metal-metal quadruple bond. The molybdenum-tungsten bond distance of 2.080(1) Å (16) raised some questions as to the nature of the heteronuclear quadruple bond, since it was 0.01 Å shorter than the molybdenum-molybdenum bond distance found for $Mo_2(O_2CCMe_3)_4$ (17). Efforts to use $MoW(O_2CCMe_3)_4$ as a starting material to obtain other heteronuclear quadruply bonded dimers were thwarted by the oxidation of both the molybdenum and tungsten atoms to the +3 oxidation state (18), a problem very similar to that which would later confront workers experimenting with the quadruply bonded tungsten dimer.

This project was begun in an effort to synthesize other dimers containing tungsten-tungsten and molybdenum-tungsten quadruple bonds. It was hoped that using less oxidizing conditions, preparation of complexes of the formula $W_2Cl_4L_4$ or $MoWCl_4L_4$ (L = neutral donor ligand such as trialkylphosphine or pyridine) could be accomplished starting with $W_2(mhp)_4$ and $MoW(O_2CCMe_3)_4$. By analogy with the dimolybdenum complexes with this formulation, these complexes would possess an unbridged metal-metal quadruple bond with an eclipsed arrangement of ligands (1). Although work with $W_2(mhp)_4$ has failed to give the desired quadruply bonded product, an interesting oxidative addition product has been prepared and characterized. Using $MoW(O_2CCMe_3)_4$, it has been possible to synthesize an unbridged heteronuclear dimer containing a molybdenum-tungsten quadruple bond. In addition, rectangular molybdenum-tungsten tetramers, for which homonuclear molybdenum and tungsten analogs are known (19,20), have also been synthesized.

Explanation of Dissertation Format

This dissertation consists of three sections, each of which is formatted for publication in a technical journal. At the end of each section is found a listing of references cited in that section.

SECTION I. TETRAKIS(PYRIDINE)TETRACHLORO-μ-CHLORO-μ-HYDRIDO DITUNGSTEN(W-W) AND ITS 4-ETHYLPYRIDINE HOMOLOG. COMPOUNDS DERIVED FROM A QUADRUPLY BONDED DIMER BY LIGAND EXCHANGE AND OXIDATIVE ADDITION OF HYDROGEN CHLORIDE

INTRODUCTION

The chemistry of quadruply bonded tungsten dimers is a relatively new area of study. Of particular interest is the readily obtained $W_2(mhp)_4$, where mhp is the 2-hydroxy-6-methylpyridine anion (1). This compound has been found to undergo a number of reactions including ligand exchange with bidentate ligands in which the quadruple bond remains intact (2-4), and metal-metal bond cleavage by π-acceptor ligands to form monomeric tungsten(II) derivatives. Intermediate between these two extremes are the reactions in which the W_2^{4+} core is oxidized to form a compound with a metal-metal bond of order less than four. This has been observed when $W_2(mhp)_4$ is treated with gaseous HX in alcohol solutions to form the tungsten(III) compound $Cs_3W_2X_9$ (5) and the tungsten(IV) complex $W_2X_4(OR)_4(ROH)_2$ (6), and in this laboratory when $W_2(mhp)_4$ is reacted with $AlCl_3$ in diglyme to produce the one electron oxidized species $W_2Cl_2(mhp)_3$ with a bond order of 3.5 (7).

In this paper, we wish to report the synthesis and structure of another W(III) dimer. The preparation involves the oxidation of the quadruple bond to a bond of lower order.

EXPERIMENTAL SECTION

Materials

$W_2(mhp)_4$ was prepared by the established procedure (1). Pyridine and 4-ethylpyridine were dried by refluxing over CaH_2 followed by distillation. Absolute ethanol and anhydrous diethylether were used from the bottles without further purification.

Analyses

Tungsten analyses were performed by decomposing samples with nitric acid and igniting in tared porcelain crucibles to tungsten trioxide. Chlorine analyses were carried out by first decomposing samples in absolute ethanol using KOH/H_2O_2. The resulting solutions were evaporated to near dryness, water was added, and the remainder of the ethanol was boiled off. Following acidification with dilute nitric acid, potentiometric titrations with a standard silver nitrate solution were performed.

Physical Measurements

Standard infrared spectra were obtained on a Beckman IR 4250 spectrometer using both nujol and fluorocarbon mulls on CsI or KBr plates. Fourier transform infrared spectra were obtained on an IBM IR/90 spectrometer using nujol mulls on either CsI plates or polyethylene discs. X-ray photoelectron spectra were measured with an AEI-200B instrument using Al K_α radiation (1486.6 eV). Beckman DU and Cary 14 spectrophotometers were used to measure the reflectance and solution uv-visible spectra, respectively.

Syntheses

$W_2(\mu\text{-}H)(\mu\text{-}Cl)Cl_4(py)_4$

In a typical reaction, 3 g (3.75 mmol) $W_2(mhp)_4$ and a magnetic stirring bar were introduced under nitrogen atmosphere into a 100 mL reaction flask equipped with a water jacket. Approximately 30 mL dry pyridine was added either by syringe from a storage flask or by fresh distillation from CaH_2. The reaction flask was then evacuated on a vacuum line and 6 mL (47.2 mmol) trimethylchlorosilane was vacuum distilled into the flask. The mixture was refluxed under nitrogen for ca. 6 h. It was then cooled to below reflux and 1 mL methanol was added by syringe while maintaining a nitrogen flush. The mixture was refluxed for an additional 10 h, cooled to room temperature, and filtered. The resulting solid was washed with absolute ethanol and anhydrous diethylether and then vacuum dried, giving the desired product, $W_2HCl_5(pyridine)_4$, as a light-brown powder in ca. 65% yield.

Anal. Calcd. for $W_2Cl_5C_{20}H_{21}N_4$: W, 42.64; Cl, 20.55; C, 27.86; H, 2.45; N, 6.50. Found: W, 42.1; Cl, 20.6; C, 27.80; H, 2.42; N, 6.46.

An oxidation state determination was also performed by decomposing samples in a standard acidic Ce(IV) solution to oxidize tungsten to W(VI) and then titrating the excess Ce(IV) with a standard Fe(II) solution using ferroin indicator. An average of 7.13 mol Ce(IV) was needed per mol of compound. Since one mol Ce(IV) is required to oxidize H^- to H_2, the average oxidation state of each tungsten is found to be +2.94 compared to the expected +3.0.

The compound is stable in air showing no signs of decomposition after several days, although samples are stored under nitrogen. It is essentially insoluble in most common organic solvents and is only slightly soluble in pyridine, acetonitrile, and methylene chloride; however, acetonitrile and methylene chloride solutions rapidly decompose, changing from faint yellow to light green.

$W_2(\mu\text{-}D)(\mu\text{-}Cl)Cl_4(py)_4$

The preparation of the deuteride analog was carried out in the same fashion as the hydride compound except CD_3OD was added to the reaction mixture after the initial refluxing step in place of normal methanol. Anal. Found: Cl, 20.64; C, 28.2; H, 2.50; N, 6.64.

$W_2(\mu\text{-}H)(\mu\text{-}Cl)Cl_4(Etpy)_4$

The 4-ethylpyridine substituted compound was obtained by loading a sample of $W_2HCl_5(pyridine)_4$ and ca. 5 mL 4-ethylpyridine into a 1 x 10 cm Pyrex reaction tube and sealing the tube under vacuum. The tube was then heated to ca. 100°C in a sand bath for several days. The tube was opened in the air, and the product washed with anhydrous diethylether and dried in the air. The compound was obtained as well-formed brown crystals of parallelepiped geometry suitable for X-ray crystallographic studies.

$W_2(\mu\text{-}D)(\mu\text{-}Cl)Cl_4(Etpy)_4$

The deuteride analog was prepared in the same manner as the corresponding hydride compound above except $W_2DCl_5(py)_4$ was used as starting material.

Collection and Treatment of X-ray Data

A 0.30 x 0.25 x 0.20 mm single crystal of $W_2HCl_5(Etpy)_4$ was sealed in a glass capillary. From four ω-oscillation photographs at $\chi = 0°$ and various ϕ angles, 15 reflections were chosen and were input into the automatic indexing program ALICE (8). The resulting reduced cell and reduced scalars indicated a C-centered monoclinic cell. This was confirmed by ω-oscillation photographs about the cell axes.

Data were collected at 25°C using graphite-monochromated Mo K_α radiation on a DATEX automated four-circle diffractometer. Four octants of data were collected, hkl, $\bar{h}\bar{k}\bar{l}$, $\bar{h}k\bar{l}$, and $h\bar{k}\bar{l}$, within a 2θ sphere of 50° using an ω-scan technique, giving a total of 6759 reflections. The intensities of three standard reflections were measured every 75 reflections. The instrument retuned on the standards numerous times during data collection. The intensities of the standards fluctuated by ca. 10%, but showed no consistent decrease which would have indicated crystal decay. Instead, these fluctuations were probably the result of instrument vibrations or movement of the crystal in the capillary.

Early examination of data revealed systematic absences of hkl for h + k = 2n + 1 confirming the C-centering. In addition, systematic absences for ℓ = 2n + 1 led to the choice of two possible space groups, C2/c (centric) or Cc (accentric). An HPR plot (9) favored the centric space group.

Final lattice parameters were obtained by using least-squares refinements on 15 independent reflections with $|2\theta| > 20°$. The results were

$a = 11.883(3)$Å, $b = 13.213(3)$Å, $c = 21.727(4)$Å, and $\beta = 96.39(3)°$ with $V = 3391(1)$Å^3.

For the final structural refinement, the intensities of the 6759 reflections were corrected for Lorentz and polarization effects and standard deviations calculated (10). An empirical absorption correction ($\mu = 77.6$ cm^{-1}) was applied using a ϕ-scan technique at $\chi = 90°$ (11). After removal of extinctions, averaging of the four octants to the two unique octants, hkl and $\bar{h}\bar{k}l$, yielded 1982 independent reflections. Reflections 110 and 002 were eliminated because of secondary extinction effects. The final data set consisted of 1980 independent reflections with $I>3\sigma_I$.

Structure Solution and Refinement

The structure was initially solved in the centric space group C2/c using a data set consisting of the two full octants hkl and $\bar{h}\bar{k}l$ (3622 reflections with $|2\theta|<50°$), plus 87 $\bar{h}k0$ and 87 $\bar{h}k\bar{l}$ reflections. These reflections were reduced and averaged without an absorption correction to 1947 independent reflections with $I>3\sigma_I$. All refinements on positional and thermal parameters were carried out using a block-matrix least-squares procedure (12) minimizing the function $\Sigma\omega(|F_o|-|F_c|)^2$, where $\omega = 1/\sigma_F^2$. Scattering factors used were those of Hanson *et al.* (13), modified for tungsten by the real and imaginary parts of anomalous dispersion (14).

From the experimentally determined density of 1.95 g/cm^3, it was calculated that the unit cell was composed of four molecules of formula W_2HCl_5(4-ethylpyridine)$_4$. In the space group C2/c, the molecule had to reside on a special position (inversion center or 2-fold axis).

Examination of a three dimensional sharpened Patterson map (15) indicated that there was only one unique tungsten atom in the unit cell, and it was related by an inversion center to the other tungsten atom in the dimeric molecule, thus, imposing inversion symmetry on the molecule.

Refinement of the positional and thermal parameters of the tungsten atom yielded a conventional residual index of $R = \Sigma||F_o|-|F_c||/\Sigma|F_o| = 0.219$ and $R_w = \Sigma[\omega(|F_o|-|F_c|)^2/\Sigma\omega|F_o|^2]^{1/2} = 0.289$, where $\omega = 1/\sigma_F 2$. An electron density map (15) phased on the refined tungsten atom revealed the positions of the chlorine atoms. It became apparent at this stage that there was no true inversion center in the molecule; instead, a pseudo inversion center was resulting from disorder in the crystal or from near inversion symmetry of the molecule. The bridging chlorine atom would refine to a reasonable isotropic thermal parameter only when an atom multiplier of 0.5 was used indicating only one bridging chlorine atom in the molecule. Each terminal chlorine atom appeared in the electron density map as two overlapping peaks of about equal intensities with separations of ca. 0.8 Å, again showing that the terminal chlorine atoms which should have been equivalent in true C2/c symmetry were in fact not inversion related. It was necessary to refine the four terminal chlorines separately using an atomic multiplier of 0.5 for each.

The ring atoms of the 4-ethylpyridine groups were located on an electron density map phased on the tungsten and chlorine atoms. These ring atoms appeared as single peaks, so that it was necessary to refine on only two rings with the other two rings in the molecule being generated by the pseudo inversion center. Although the peaks were essentially single,

they were in fact composed of two close, overlapping peaks which could not be distinguished as was done for the terminal chlorine atoms. Elongated peaks were observed for the carbon atoms farthest from the center of the molecule. Upon anisotropic refinement of all ring atoms, larger and/or more anisotropic ellipsoids were obtained for carbon atoms more removed from the nitrogen atoms.

Location and refinement of both ethyl groups posed significant problems. The methylene carbon (C6) of the first ethyl group was refined as a single atom with a large isotropic thermal parameter. The methyl carbon bonded to C6, however, was seen on electron density maps as two equal-intensity, diffuse peaks on either side of C6. It was necessary to refine it as two methyl carbons (C7 and C7A) possessing large isotropic thermal parameters with atomic multipliers of 0.5. Location of the second ethyl group proved to be more difficult since the two carbon atoms appeared as at least six overlapping peaks on the electron density map. Close examination revealed that the methylene carbon appeared as two overlapping peaks, while the methyl carbon was disordered in two positions about each of these two methylene carbon peaks producing two additional pairs of overlapping peaks. Convergence was achieved by refining the methylene carbon with an atomic multiplier of 1.0 and the methyl carbons as two disordered atoms with atomic multipliers of 0.5. The resulting positional and thermal parameters are only an approximation and are not to be taken as the true arrangement of this ethyl group.

Final convergence was obtained with $R = 0.069$ and $R_w = 0.091$ using full-matrix least-squares refinement and employing the averaged,

absorption corrected data discussed in the previous section. A final difference Fourier synthesis showed no features greater than 0.9 $e^-/Å^3$ or less than -0.8 $e^-/Å^3$ with the largest discrepancies found near the tungsten atom (16).

Extensive efforts were made to solve the structure in the accentric space group Cc using the same data set as that used to initially solve the centric structure (17). It was possible to obtain convergence with a model consisting of only the tungsten and chlorine atoms which was essentially the same as that found for the centric model. Attempts to introduce the 4-ethylpyridine ligands, however, resulted in correlation problems and divergence. Using block-matrix least-squares refinement methods, unreasonable bond distances and angles within the rings were obtained. The pseudo inversion center of the molecule prevented an accentric solution.

Deconvolution of Molecular Structure

The pseudo inversion center in the molecule results in two superimposed inversion-related images of the dimeric molecule. Since the 4-ethylpyridine ligands and tungsten atoms were refined as truly inversion related, it was necessary only to sort out the chlorine atoms of the two images.

The molecule can be considered as two edge-sharing octahedra bridged by one chlorine atom and one hydride ligand, which was not located in the refined model. All terminal chlorine atoms are in equatorial positions, so that the portion of the dimeric molecule without the axial 4-ethylpyridine ligands is essentially planar. A representation of the

planar fragment including all inversion generated atoms, but excluding the bridging hydride, is shown in Figure I-1. Primed atoms are related to their counterpart unprimed atoms by the pseudo inversion center.

Assuming a chlorine-chlorine van der Waal contact of ca. 3.4Å(17), it is found that Cℓ3A and Cℓ2′ are much too close to Cℓ1 at distances of 2.63(2) and 2.61(2)Å, respectively, while Cℓ3 and Cℓ2A′ are at reasonable distances of 3.29(2) and 3.32(2)Å, respectively. This leads to the conclusion that Cℓ2, Cℓ2A′, Cℓ3 and Cℓ3A′ belong to the image with Cℓ1 as the bridging atom. All chlorine atoms of this image are shown as solid circles in Figure I-1. Although this image is a correct one and bond distances and angles are referred to it, the inverted image composed of Cℓ1′, Cℓ2′, Cℓ2A, Cℓ3′, and Cℓ3A (dotted circles) is also correct and would give an identical mirror image structure. If the true space group is Cc (accentric), then either image could be found in the crystal; the only difference would arise from the choice of coordinates, x,y,z or -x,-y,-z, which would determine the orientation of the molecule in relation to the crystal axes (the handedness). From the structure determination, it is possible to ascertain the molecular geometry but not the absolute crystalline orientation. In fact, if there actually is disorder in the crystal, both orientations of the molecule are randomly distributed throughout the crystal. This may be the case since the bulk of the 4-ethylpyridine ligands, the coordinates of which would be the same in both orientations, should greatly influence the packing of the molecules, thus reducing the possible ordering influence of the chlorine atoms.

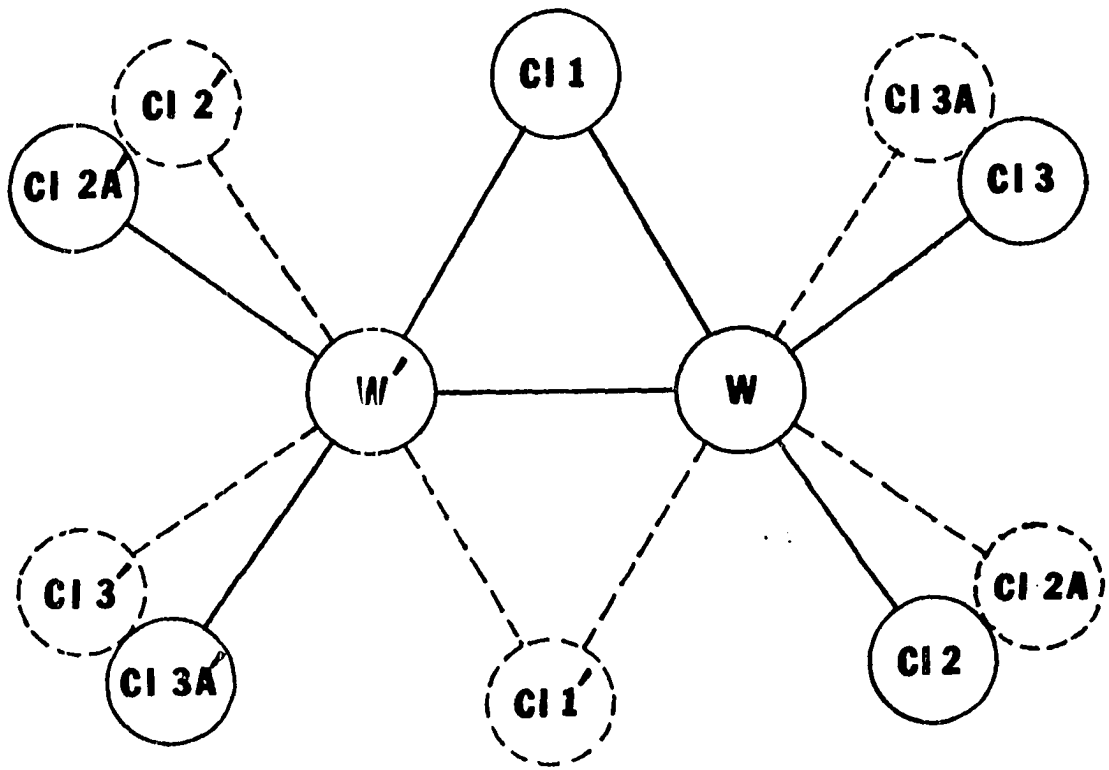

Figure I-1. Diagram showing the coplanar tungsten and chlorine atoms, and the effect of the pseudo inversion center in the structure of $W_2HCl_5(Etpy)_4$

Atomic coordinates and thermal parameters are presented in Tables I-1 and I-2, respectively.

Table I-1. Positional parameters[a] for $W_2HCl_5(4\text{-ethylpyridine})_4$

Atom	Multiplier	x	y	z
W	1.0	0.42430(6)	0.52680(6)	0.45806(4)
Cl1	0.5	0.5057(9)	0.3547(7)	0.4587(5)
Cl2	0.5	0.3538(14)	0.6927(11)	0.4445(8)
Cl2A	0.5	0.2981(13)	0.6683(13)	0.4207(7)
Cl3	0.5	0.3026(11)	0.4666(11)	0.3679(7)
Cl3A	0.5	0.3385(12)	0.4168(11)	0.3777(7)
N1	1.0	0.2803(14)	0.4930(11)	0.5075(8)
C1	1.0	0.2315(18)	0.4026(15)	0.5026(10)
C2	1.0	0.1328(25)	0.3754(18)	0.5338(13)
C3	1.0	0.0893(19)	0.4539(25)	0.5641(14)
C4	1.0	0.1409(19)	0.5438(22)	0.5743(12)
C5	1.0	0.2340(16)	0.5600(22)	0.5425(10)
C6	1.0	-0.0210(25)	0.4206(26)	0.5958(15)
C7	0.5	-0.0091(66)	0.3604(70)	0.6494(38)
C7A	0.5	-0.0123(62)	0.4796(54)	0.6648(35)
N2	1.0	0.5382(13)	0.5793(16)	0.3917(7)
C21	1.0	0.5706(20)	0.6741(18)	0.3921(11)
C22	1.0	0.6368(2)	0.7158(19)	0.3455(12)
C23	1.0	0.6604(21)	0.6428(23)	0.2975(11)
C24	1.0	0.6269(22)	0.5446(19)	0.2994(11)
C25	1.0	0.5677(18)	0.5133(17)	0.3451(10)
C26	1.0	0.7242(34)	0.6832(36)	0.2428(20)
C27	0.5	0.7586(38)	0.7595(38)	0.2462(21)
C27A	0.5	0.6794(36)	0.7968(35)	0.2218(20)

[a]Estimated standard deviations are in parentheses.

Table I-2. Thermal parameters[a] for $W_2HCl_5(4\text{-ethylpyridine})_4$

Atom	B_{11}	B_{22}	B_{33}	B_{12}	B_{13}	B_{23}
W	4.64(4)	3.57(4)	4.12(4)	-0.23(4)	0.30(3)	-0.23(3)
Cℓ1	5.8(5)	3.0(4)	5.5(5)	-0.5(4)	0.5(4)	-1.6(4)
Cℓ2	7.5(9)	4.3(6)	7.0(9)	2.5(7)	2.7(7)	1.4(6)
Cℓ2A	6.2(8)	6.9(9)	5.9(8)	0.8(6)	0.0(6)	1.8(6)
Cℓ3	4.5(6)	6.0(7)	4.6(5)	0.0(6)	-1.1(4)	-1.8(6)
Cℓ3A	4.6(7)	5.9(8)	6.1(7)	-1.0(5)	0.8(6)	-2.0(7)
N1	5.4(8)	3.0(7)	5.8(9)	0.6(6)	1.2(7)	-0.4(6)
C1	6.4(12)	3.5(9)	6.3(11)	-0.3(8)	-0.1(9)	1.0(8)
C2	10.4(18)	3.9(11)	9.4(12)	0.9(12)	1.7(15)	1.9(11)
C3	3.7(10)	10.0(20)	10.6(19)	-3.4(12)	0.7(11)	-3.1(15)
C4	4.4(10)	11.1(21)	6.6(13)	0.5(12)	1.9(10)	0.2(13)
C5	3.7(9)	11.1(18)	5.1(11)	0.8(10)	1.0(8)	0.4(11)
C6	9.4(7)					
C7	13.5(23)					
C7A	11.0(19)					
N2	4.4(8)	7.6(11)	4.1(8)	-1.3(8)	0.0(6)	0.2(8)
C21	7.9(14)	5.8(13)	6.5(13)	-3.0(11)	-1.3(11)	2.3(10)
C22	7.2(14)	7.4(15)	6.6(13)	-2.6(12)	-0.5(11)	0.4(12)
C23	7.6(14)	8.3(16)	5.6(13)	-0.8(13)	1.0(11)	0.6(12)
C24	7.3(13)	6.3(13)	5.8(12)	0.1(11)	2.0(10)	0.8(10)
C25	5.3(10)	5.6(11)	5.3(11)	0.4(9)	1.0(9)	1.2(9)
C26	13.7(12)					
C27	6.1(10)					
C27A	5.6(9)					

[a]Estimated standard deviations are in parentheses. The anisotropic thermal parameter expression used is $\exp[-1/4(B_{11}h^2a^{*2} + B_{22}k^2b^{*2} + 2\ B_{23}klb^*c^*)]$ with B's in $Å^2$. Isotropic thermal parameters are given as B_{11} and are in $Å^2$.

RESULTS AND DISCUSSION

Crystal Structure of $W_2HCl_5(4\text{-ethylpyridine})_4$

The deconvoluted molecule is shown in Figure I-2. The disordered methyl groups are shown in their two half-occupancy sites as unshaded spheres. Also, the hydride ligand has been included in its proposed position. A view of the unit cell is provided in Figure I-3 with molecules ordered according to the Cc space group for simplicity.

Table I-3 provides the important angles and distances (both bonding and nonbonding) for the skeletal atoms about the two tungsten atoms. As noted earlier, the molecular structure consists of two edge sharing octahedra distorted in such a manner to allow for a W-W bond distance of 2.516(2) Å. The tungsten atoms and the five chlorine atoms are essentially coplanar with the greatest deviation from the least-squares plane being only 0.10 Å. The close approach of the two tungsten atoms reduces the W-Cℓ1-W′ angle to 61.3(2)° while the terminal chlorine atoms are forced towards the hydride bridged side of the molecule as perceived from viewing the solid circles of Figure I-1. All Cl····Cl nonbonding distances are in accord with a van der Waal radius of 1.7 - 1.9 Å for chlorine (18). The axial nitrogen atoms are tilted away from each other with W-W-N angles of ca. 97° and a N1····N2′ nonbonding distance of 3.05(2)Å, the approximate distance expected for a Van der Waal contact (18) and 0.53Å longer than if the nitrogens were not bent back. The need for this distortion of the axial ligands may explain the occupancy of all axial positions by 4-ethylpyridine, because the chlorine atoms, having a

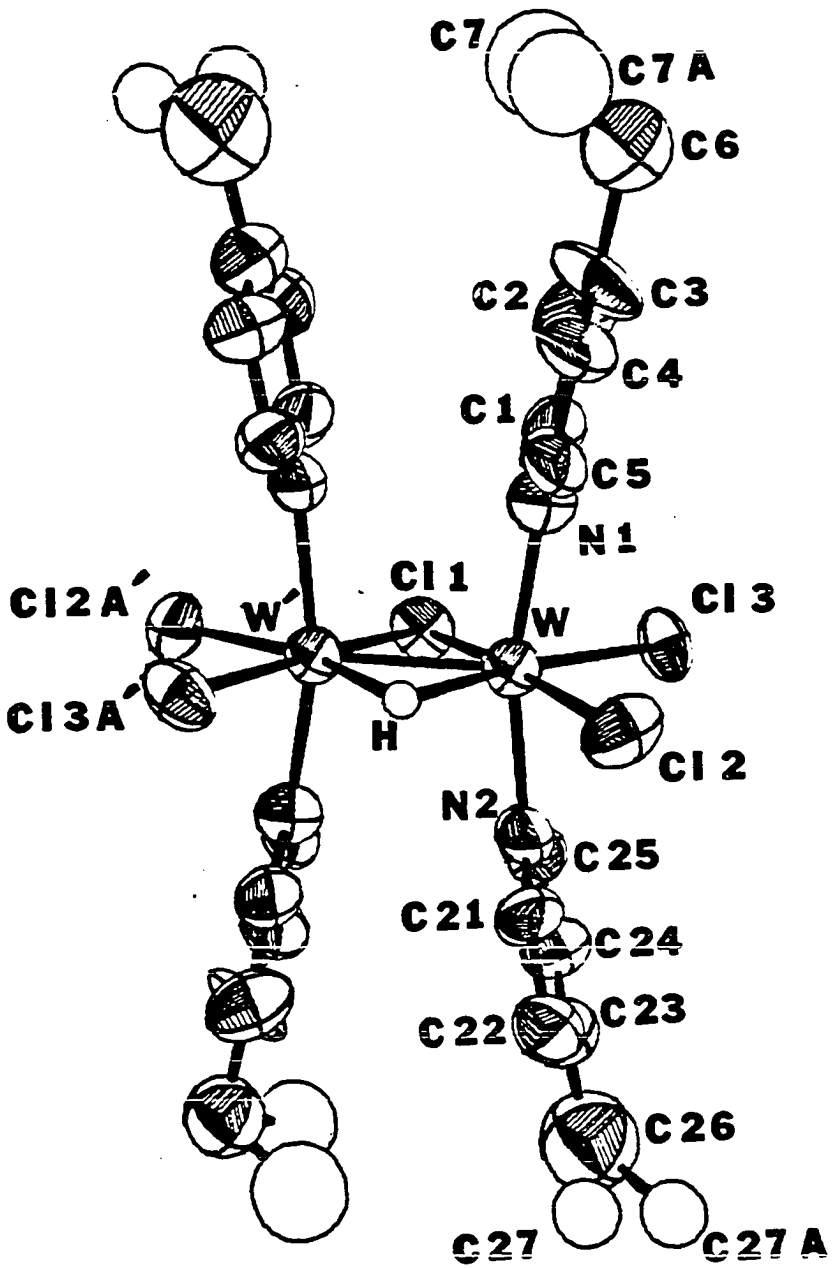

Figure I-2. ORTEP drawing of $W_2HCl_5(Etpy)_4$ with the bridging H-atom placed in its estimated location. Disordered methyl groups are shown in both half-occupancy positions

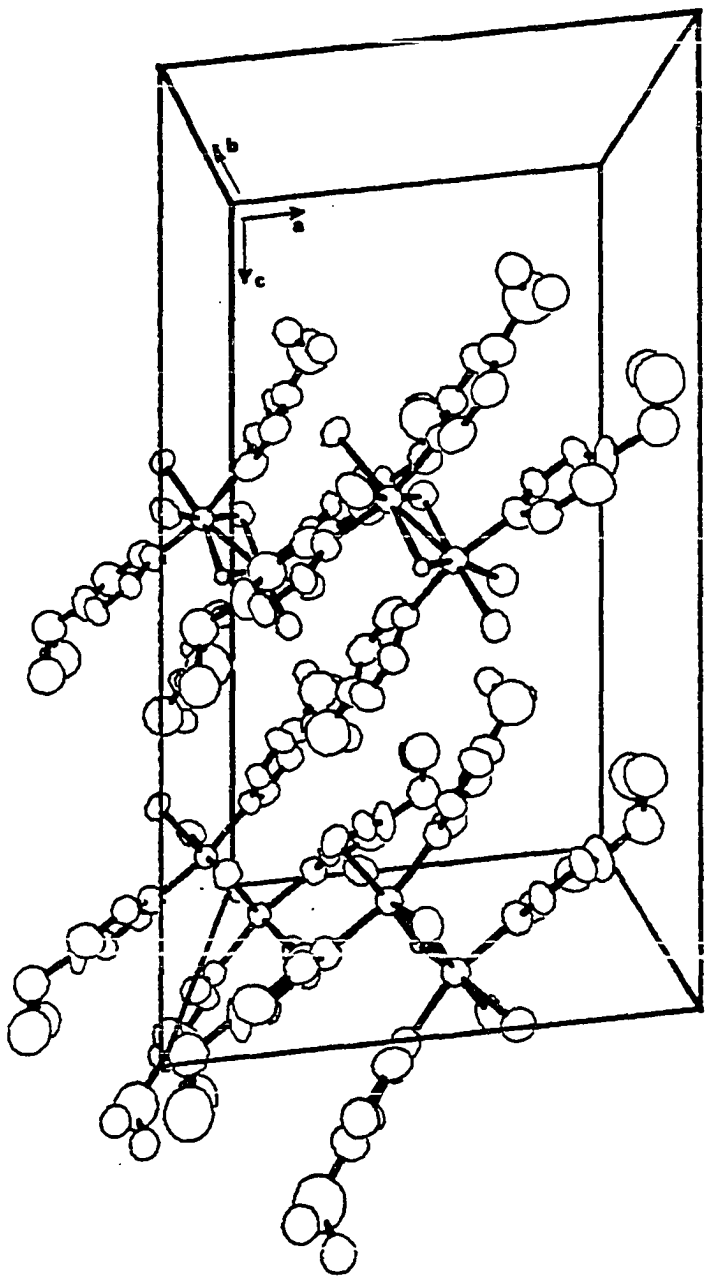

Figure I-3. The unit cell of $W_2HCl_5(Etpy)_4$ as viewed down the b-axis

Table I-3. Interatomic distances and angles around tungsten atoms for $W_2HCl_5(4\text{-ethylpyridine})_4$

Bond Distances (Å)		Bond Angles (Deg)	
W - W′	2.516(2)	W - W′ - Cℓ1	59.5(2)
W - Cℓ1	2.471(9)	W′ - W - Cℓ1	59.3(2)
W′ - Cℓ1	2.466(10)	W - Cℓ1 - W′	61.3(2)
W - Cℓ2	2.354(15)	Cℓ1 - W - Cℓ3	84.3(4)
W - Cℓ3	2.436(14)	Cℓ3 - W - Cℓ2	91.9(5)
W′ - Cℓ2A′	2.476(17)	Cℓ1 - W′ - Cℓ2A′	84.5(4)
W′ - Cℓ3A′	2.409(15)	Cℓ2A′ - W′ - Cℓ3A′	91.5(5)
W - N1	2.166(16)	W′ - W - Cℓ2	124.6(4)
W - N2	2.197(16)	W - W′ - Cℓ3A′	124.5(4)
		W′ - W - N1	97.1(4)
		W′ - W - N2	97.0(4)
		N1 - W - N2	165.7(6)

Intramolecular Nonbonding Distances (Å)	
N1 ··· N2′	3.05(2)
Cℓ3 ··· Cℓ2	3.44(2)
Cℓ2A′ ··· Cℓ3′	3.50(2)
Cℓ1 ··· Cℓ3	3.29(2)
Cℓ1 ··· Cℓ2A′	3.32(2)

larger van der Waal radius, would require an even greater axial distortion. Instead, by occupying equatorial positions the chlorine atoms are able to distort in the manner already described to alleviate steric crowding in the equatorial plane.

The W-W bond distance of 2.516(2)Å is difficult to reconcile on electronic considerations alone. A formal oxidation state of +3 for each tungsten would seem to require the formulation of a triple bond between the metal atoms; however, the bond is considerably longer than the average W-W triple bond distance of ca. 2.29Å found for the W(III) compounds studied extensively by Chisholm (19). It is also substantially shorter than in the closely related compound $W_2Cl_6(pyridine)_4$, with d(W-W) = 2.737(3)Å(20), for which calculations performed by Shaik and co-workers (21) lead to the assignment of a net single bond between the tungsten atoms, resulting from the ordering of the three HOMO's $\sigma^2\ \pi^2\ \delta^{*2}$. From bond length comparisons, it becomes apparent that the W-W bond in $W_2HCl_5(4\text{-ethylpyridine})_4$ falls in the range found for a formal double bond. Comparison to W(IV) compounds which are assumed to possess double bonds between tungsten atoms bears this out: $W_2(\mu\text{-}S)_2(\mu\text{-}Et_2NCX_2)_2(Et_2NCS_2)_2$, d(W=W) = 2.530(2)Å(22); $W_4(OPr^i)_{14}H_2$, d(W=W) = 2.446(1)Å(23); $W_2(\mu\text{-}S)(\mu\text{-}EtS)_2Cl_4(SC_4H_8)_2$, d(W=W) = 2.524(1)Å(24); $W_2Cl_4(OR)_4(ROH)_2$, d(W=W) = 2.481(1)Å for R = CH_3 and d(W=W) = 2.483(1)Å for R = C_2H_5 (6). In addition, another tungsten dimer formulated as $W_2H_4(\mu\text{-}H)(\mu\text{-}PMe_2)(PMe_3)_5$ in which the tungsten should be in an average oxidation state of +3 has d(W-W) = 2.588(1)Å, very near that found in this compound.

Probably the best view of the metal-metal bonding in $W_2HCl_5(Etpy)_4$ is that of a compromise between metal d-orbital overlap, M-L-M bridges and terminal ligand repulsions. The major repulsive forces arise from the axial 4-ethylpyridine ligands, since the Cl····Cl basal repulsions are minimized by the distortion, of the chlorine atoms towards the hydride bridged side of the molecule. Since the N····N axial repulsion will be less than the Cl····N repulsions in $W_2Cl_6(pyridine)_4$, a significant shortening of the metal-metal distance would result. Also, the bridging hydride will tend to pull the metals closer together. Apparently, a compromise is reached in which a distance near that observed for a W(IV)-W(IV) double bond is obtained. Similar arguments apply to $W_2H_4(\mu\text{-}H)(\mu\text{-}PMe_2)(PMe_3)_4$. These arguments make it difficult to assign an exact bond order for $W_2HCl_5(Etpy)_4$ and point out some of the intrinsic flaws in assigning bond orders based solely on electron counts.

Another noteworthy feature of the structure is that the average W-Cl bond distance of 2.46Å for the terminal chlorines <u>trans</u> to the bridging hydride ligand is 0.08Å longer than the average W-Cl distance of 2.38Å found for the chlorines <u>trans</u> to the bridging chlorine atom. This can be attributed to the stronger <u>trans</u> influence of the hydride ligand. The same <u>trans</u> effect is observed for $W_4(OPr^i)_{14}H_2$ (23), $(pyH)_3Mo_2Cl_8H$ (25) and $(pyH)_3(H_5O_2)[Mo_2Cl_8H][MoCl_4O(H_2O)]$ (26) in which the W-O and Mo-Cl distances are 0.06 and 0.10Å longer, respectively, for terminal ligands <u>trans</u> to the bridging hydride ligands. It should be noted, however, that the standard deviations for the W-Cl distances in $W_2HCl_5(Etpy)_4$ are higher than desired as a result of the difficulties encountered in the structure

solution. In fact, the difference between the average W-Cl distances for the two types of terminal chlorine atoms is not statistically significant but still highly suggestive that the trans effect is operative.

Finally, the bond distances for the 4-ethylpyridine ligands given in Table I-4 are in agreement with expected values in most cases. Variations from the norm, especially for the methyl groups, are again a result of the refinement difficulties.

Table I-4. Bond distances (Å) and angles (Deg) for 4-ethylpyridine ligands

N1 - C1	1.33(2)	N1 - C1 - C2	123.2(19)
C1 - C2	1.46(4)	C1 - C2 - C3	113.8(22)
C2 - C3	1.36(4)	C2 - C3 - C4	124.3(24)
C3 - C4	1.34(4)	C3 - C4 - C5	115.4(25)
C4 - C5	1.38(3)	C4 - C5 - N1	126.0(24)
C5 - N1	1.33(3)	C5 - N1 - C1	116.2(18)
C3 - C6	1.61(4)	C3 - C6 - C7	119.9(39)
C6 - C7	1.40(9)	C3 - C6 - C7A	106.5(32)
C6 - C7A	1.68(8)	C2 - C3 - C6	111.7(26)
		C4 - C3 - C6	123.3(26)
N2 - C21	1.31(3)	N2 - C21 - C22	122.5(21)
C21 - C22	1.46(3)	C21 - C22 - C23	113.9(22)
C22 - C23	1.47(4)	C22 - C23 - C24	121.6(23)
C23 - C24	1.36(4)	C23 - C24 - C25	119.7(23)
C24 - C25	1.34(3)	C24 - C25 - N2	122.1(21)
C25 - N2	1.41(3)	C25 - N2 - C21	120.0(18)
C23 - C26	1.57(5)	C23 - C26 - C27	118.2(42)
C26 - C27	1.09(7)	C23 - C26 - C27A	110.6(31)
C26 - C27A	1.64(7)	C22 - C23 - C26	117.4(28)
		C24 - C23 - C26	121.0(27)

Infrared Spectra

Infrared spectra were obtained on all compounds using both nujol and fluorocarbon mulls. A single, medium-intensity band indicative of a M-H-M stretching mode is found for $W_2HCl_5(py)_4$ at 1510 cm^{-1} and for $W_2HCl_5(Etpy)_4$ at 1545 cm^{-1}. Bands of the corresponding deuteride compounds, $W_2DCl_5(py)_4$ and $W_2DCl_5(Etpy)_4$, show the expected shifts to lower frequencies ($\nu_D = \nu_H/\sqrt{2}$) with the respective stretching modes coming at 1082 cm^{-1} and 1112 cm^{-1}, thus confirming the assignment. The intensities of these bands imply that they arise from the asymmetric M-H-M stretching mode. Evidently, the weaker symmetric stretching mode is not seen as a result of lower intensity or obscurement by other bands in the spectra. However, it is possible that the asymmetric and symmetric modes occur at approximately the same frequency, as would happen if the W-H-W bond angle were ca. 90° (27). Using the W-W bond distance of 2.516Å and assuming a symmetric hydride bridge bond arrangement with W-H bond distances of ca. 1.8 Å, the W-H-W angle is calculated to be ca. 89°, an angle which would require near coincidence of the two stretching modes. A comparison of the assumed asymmetric M-H-M stretching frequency observed here (1510-1545 cm^{-1}) with ν(sym), 1553 cm^{-1} and ν(asym), 1248 cm^{-1} found in $Cs_3Mo_2Cl_8H$ (27) indicates a much higher frequency for ν(asym) in $W_2HCl_5(py)_4$ or $W_2HCl_5(Etpy)_4$. Since this frequency approaches that for ν(sym) in $Cs_3Mo_2Cl_8H$, this may be taken as evidence that ν(sym) and ν(asym) are indeed nearly coincident.

Above 400 cm^{-1}, the spectra of $W_2HCl_5(py)_4$ and $W_2HCl_5(Etpy)_4$ were otherwise essentially those expected for coordinated pyridine and

4-ethylpyridine, respectively (28). The spectra below 400 cm^{-1}, where W-Cl stretching and deformation, and W-N stretching frequencies should be found (29), are shown in Figure I-4 for comparison. Assuming exact C_{2v} symmetry, six W-Cl (four terminal and two bridging) stretching modes and three W-N stretching modes should be active for both compounds. The spectrum of $W_2HCl_5(py)_4$ (spectrum a) shows five bands (relative intensity in parentheses) at 320(s), 309(sh), 299(s), 275(s), and 267(sh) which are assigned to W-Cl stretching modes. The assignment of the bands at 233(m), 223(w), and 203(w) is not certain since they may result from bridging W-Cl stretches, Cl-W-Cl deformations, and/or W-N stretches (29).

The spectrum of $W_2HCl_5(Etpy)_4$ below 400 cm^{-1} is very similar to that of $W_2HCl_5(py)_4$. The W-Cl stretching modes are found at 322(s), 304(s), and 276(s) cm^{-1}. These bands are slightly broader and not as well resolved as the same bands for $W_2HCl_5(py)_4$ but are almost identical in positions and relative intensities. The medium intensity band at 226 cm^{-1} and the weaker overlapping bands at 185 and 173 cm^{-1} may again be assigned to W-Cl-W bridge-stretching, Cl-W-Cl deformation, and/or W-N stretching modes.

The near identical infrared spectra and the method of preparation of $W_2HCl_5(Etpy)_4$ (simple ligand exchange) indicate that $W_2HCl_5(py)_4$ has the same basic structure as that determined for $W_2HCl_5(Etpy)_4$.

X-ray Photoelectron Spectra

Tungsten and chlorine X-ray photoelectron spectra (XPS) were obtained for both $W_2HCl_5(py)_4$ and $W_2HCl_5(Etpy)_4$. Binding energies were referenced

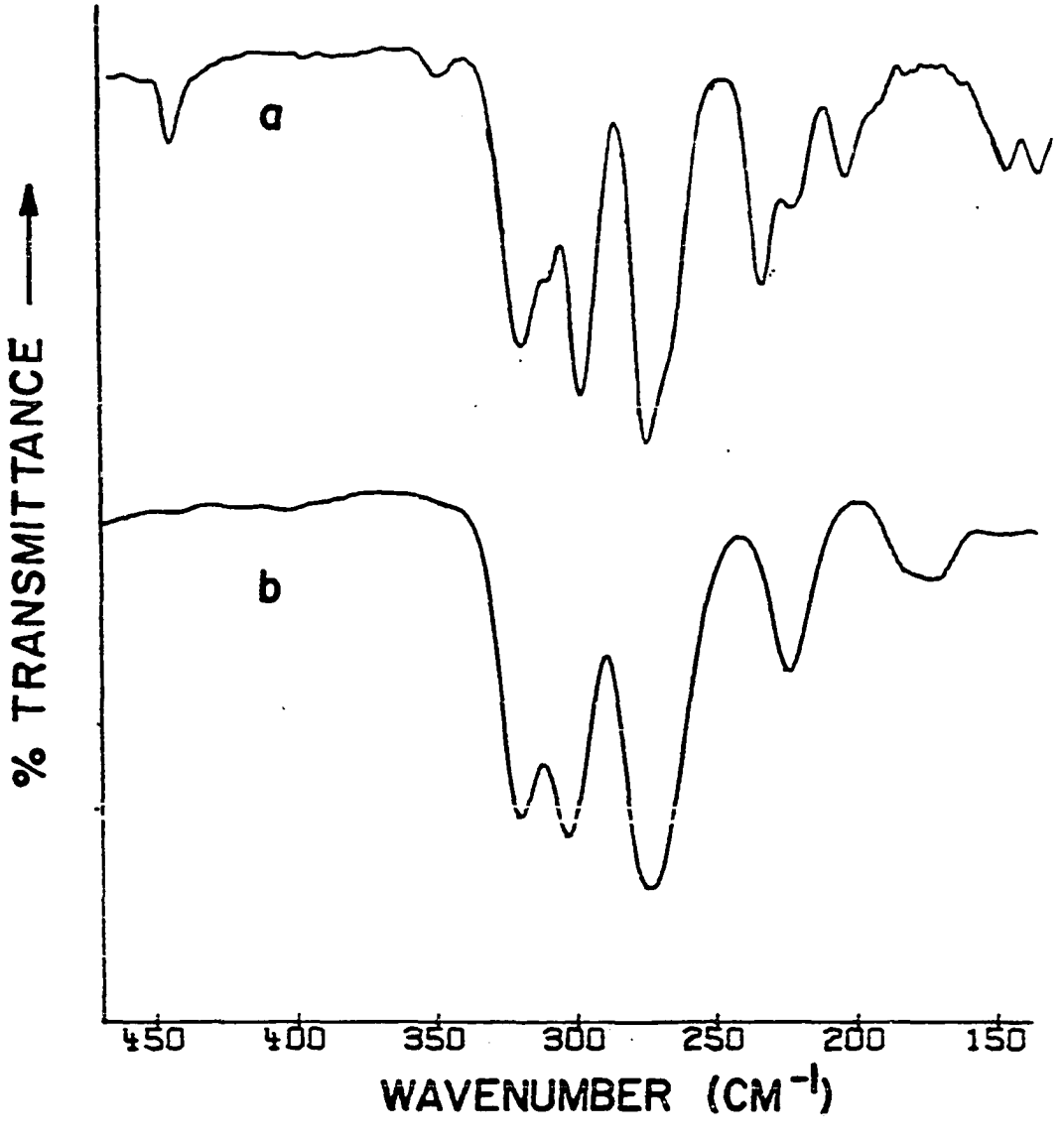

Figure I-4. Fourier transform infrared spectra of a) $W_2HCl_5(py)_4$ and b) $W_2HCl_5(Etpy)_4$

to the C1s binding energy taken as 285.0 eV (30). Spectra were deconvoluted using a program developed by M. H. Luly (31).

The W $4f_{5/2}$ and $4f_{7/2}$ energies are at 34.8 and 32.6 eV for $W_2HCl_5(py)_4$ and at 34.6 and 32.4 eV for $W_2HCl_5(Etpy)_4$. The values are in accord with those found for $K_3W_2Cl_9$ (W $4f_{5/2,7/2}$: 34.7, 32.5 eV) and $[Bu_4N]_3W_2Cl_9$ (W $4f_{5/2,7/2}$: 34.4, 32.3) (32).

The chlorine spectra were complex, and efforts to fit one or two types of chlorines to the peak profiles gave poor agreement factors. Using three nonequivalent chlorines for each compound and varying the appropriate parameters, good fits were obtained as shown in Table I-5. The χ^2 values provided for each least-squares fit are an indication of the goodness of fit and can only be used to compare fits to the same spectrum since it is dependent on the number of counts (31). The difference between fits 1 and 2 for each compound is that in fit 1 the chlorine atoms were constrained to the ratios 1:2:2 while in fit 2 their ratios were allowed to vary. The ratios 1:2:2 were chosen because there should be one bridging chlorine atom, Clb; two terminal chlorine atoms, Cl_t, trans to the bridging chlorine; and two terminal chlorine atoms, Cl_t', trans to the bridging hydride ligand. These structural assignments are based on results obtained for $K_3W_2Cl_9$ and $(Bu_4N)_3W_2Cl_9$ for which bridging Cl $2p_{3/2}$ binding energies are found at 198.7 and 198.9 eV and terminal Cl $2p_{3/2}$ at 198.2 and 197.9 eV, respectively (32). The terminal chlorines trans to the hydride ligand should have the lowest binding energy because their longer W-Cl bond distances would increase their effective negative charge; however, these assignments for the terminal chlorines are tentative,

Table I-5. Chlorine X-ray photoelectron spectra

Compound	Least-Squares Fit	Cl 2p$_{3/2}$ BE[a] (eV)			FWHM (eV)	Ratio	χ^2
		Cl_b	Cl_t	Cl_t'		Cl_b:Cl_t:Cl_t'	(x10^3)
$W_2HCl_5(py)_4$	1	199.4	198.4	197.8	1.4	1.0:2.0:2.0	0.47
	2	199.6	198.8	198.0	1.4	1.0:2.4:4.5	0.46
$W_2HCl_5(Etpy)_4$	1	199.3	198.3	197.8	1.4	1.0:2.0:2.0	1.29
	2	199.4	198.4	197.7	1.4	1.0:2.4:2.7	1.15

[a]Spin-orbit splitting is 1.55 eV in all cases.

especially since the terminal chlorine bond distances have a considerable amount of uncertainty associated with them as discussed earlier. When the chlorine ratios are allowed to vary, slight improvements in the fits are seen (lower χ^2's), and the ratios vary somewhat from the ideal 1:2:2, especially for $W_2HCl_5(py)_4$; however, the binding energies change insignificantly.

From these results, it can be concluded that the chlorine XPS spectra are in accord with the structure determined for $W_2HCl_5(Etpy)_4$. Also, the near identical profile of the two spectra as seen in Figure I-5 (fit 1 deconvolutions are shown for both spectra) serves to amplify the proposal that $W_2HCl_5(py)_4$ possesses the same structure as $W_2HCl_5(Etpy)_4$.

UV-Visible Spectra

Attainment of uv-visible spectra was hampered by insolubility and/or decomposition of the pyridine and the 4-ethylpypridine compounds in most common organic solvents. Reflectance spectra were obtained for both compounds, and are shown in Figure I-6. The spectra are essentially identical and are also quite similar to the spectra recorded by Saillant and co-workers for the compounds $W_2Cl_6L_4$ (L = pyridine, 4-picoline and 4-isopropylpyridine) (33) of which the pyridine compound has been discussed earlier in relation to structural comparisons.

An interesting effect is noted for $W_2HCl_5(py)_4$ in pyridine. The compound gives a pale yellow solution in pyridine at room temperature which shows a weak absorption at 708 nm and a medium intensity absorption at 475 nm with a shoulder at 580 nm. Upon warming the solution to ca. 50-60°C under vacuum, the pale yellow solution changes to an intense purple

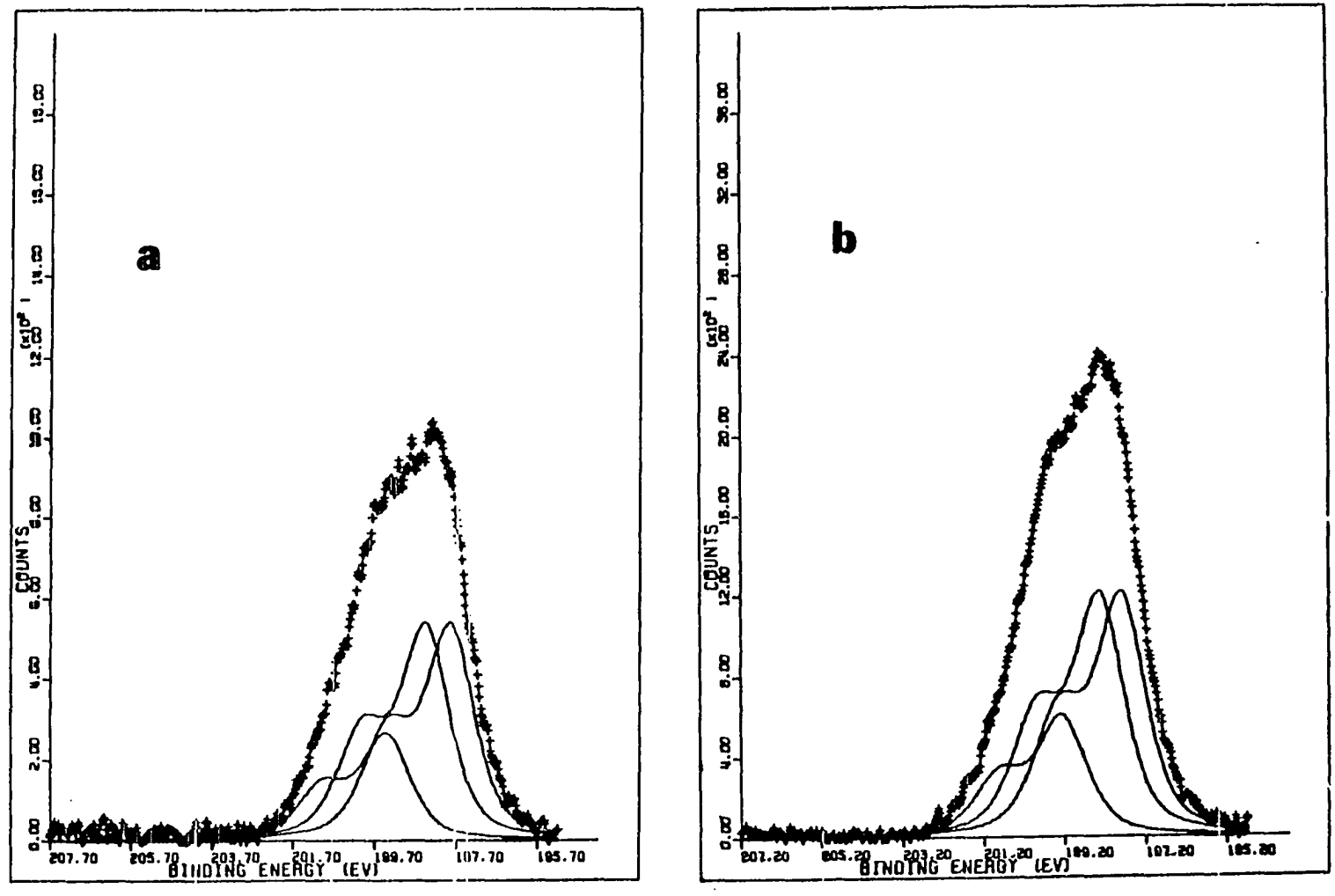

Figure I-5. Chlorine 2p binding energy spectra of a) $W_2HCl_5(py)_5$ and b) $W_2HCl_5(Etpy)_4$. Spectra are deconvoluted using the respective least-squares fit 1 parameters for both

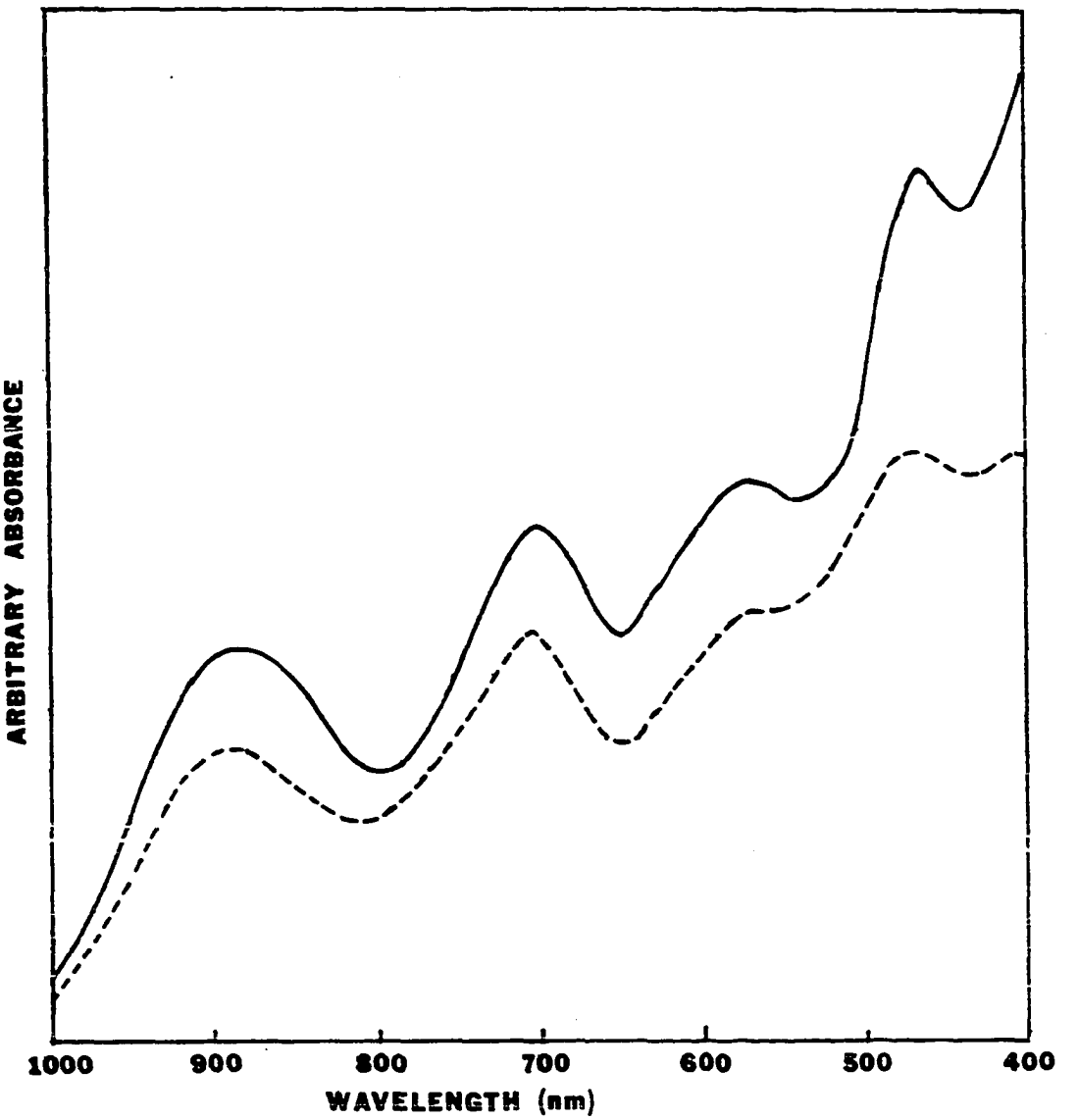

Figure I-6. Reflectance spectra for $W_2HCl_5(Etpy)_4$ (——) and $W_2HCl_5(py)_4$ (---)

with a strong absorption at 562 nm and a shoulder at 505 nm. These are six to eight times more intense than the 475 nm absorption observed at room temperature. Upon cooling to room temperature, the purple color persists unchanged for several weeks before gradually turning a yellow-orange. An almost identical effect is observed for the 4-ethylpyridine analog in 4-ethylpyridine solution.

The reason for this dramatic change in color is unclear. It is apparently reversible since heating powdered $W_2HCl_5(py)_4$ in pyridine or 4-ethylpyridine results in the formation of poor quality crystals of $W_2HCl_5(py)_4$ and well-formed crystals of $W_2HCl_5(Etpy)_4$, respectively. Also, vacuum distillation of the pyridine from a refluxed and filtered solution of $W_2HCl_5(py)_4$ yields a purple solid which shows broad bands in its infrared spectrum, but from which pyridinium ion can be identified. From this sketchy evidence, it is tentatively proposed that the color change is due to an equilibrium in which the hydride ligand is abstracted from the compound by pyridine as a proton producing the pyridinium cation and an unidentified soluble tungsten species. The equilibrium is such that only the characterized hydride species is precipitated and the quantities of compounds in solution are too small to allow recovery of useful amounts of the tungsten species responsible for the purple color.

CONCLUSIONS

The preparation of $W_2HCl_5(py)_4$ can be viewed as the product of the oxidative addition of HCl to a quadruple bond, as previously described in the formation of $Mo_2Cl_8H^{3-}$ (25) and $MoWCl_8H^{3-}$ (28). The HCl in this case results from the addition of methanol to $ClSiMe_3$. The reaction, however, is not straightforward in that the HCl generated would exist almost entirely as pyridinium chloride unless it reacted immediately with the ditungsten species in solution. Also, without the generation of HCl, numerous products with incomplete mhp replacement are obtained (34), indicating the need for HCl in order to completely replace all mhp ligands. Because of these complications, it is not possible at present to formulate a simple reaction scheme for the formation of $W_2HCl_5(py)_4$.

REFERENCES CITED

1. Cotton, F. A.; Fanwick, P. E.; Niswander, R. H.; Sekutowski, J. C. J. Am. Chem. Soc. 1978, 100, 4725.

2. Cotton, F. A.; Niswander, R. H.; Sekutowski, J. C. Inorg. Chem. 1978, 17, 3541.

3. Sattelberger, A. P.; McLaughlin, K. W. J. Amer. Chem. Soc. 1981, 103, 2880.

4. Mailki, W. S.; Wild, R. E.; Walton, R. A. Inorg. Chem. 1981, 20, 1380.

5. DeMarco, D.; Nimry, T.; Walton, R. A. Inorg. Chem. 1980, 19, 575.

6. Anderson, L. B.; Cotton, F. A.; DeMarco, D.; Fang, A.; Ilsley, W. H.; Kolthammer, B. W. S.; Walton, R. A. J. Am. Chem. Soc. 1981, 103, 5078.

7. Ryan, T. and McCarley, R. E., Iowa State University, Ames, Iowa, to be published.

8. Jacobson, R. A. J. Appl. Crystallogr. 1976, 9, 115.

9. Howells, E. R.; Phillips, D. C.; Rodgers, D. Acta Cryst. 1950, 3, 210.

10. Lawton, S. L.; Jacobson, R. A. Inorg. Chem. 1968, 7, 2124.

11. Karcher, B. A. Ph.D. Dissertation, Iowa State University, Ames, IA, 1981.

12. Lapp, R. L.; Jacobson, R. A. "ALLS, A Generalized Crystallographic Least Squares Program", 1979, U. S. DOE Report IS-4737.

13. Hanson, H. P.; Herman, F.; Lea, J. D.; Skillman, S. Acta Crystallogr. 1960, 17, 1040.

14. Templeton, D. H. In "International Tables for X-ray Crystallography", 1st ed.; Macgillary, C. H. and Rieck, G. D., Eds.; Kynock Press: Birmingham, England, 1962; Vol. III, page 215.

15. Powell, D. R.; Jacobson, R. A. "FOUR: A General Crystallographic Fourier Program", 1980, U. S. DOE Report IS-4737.

16. The largest peak in the difference map was 0.9 $e^-/Å^3$ and was located in the place of the tungstens and chlorines at distances of 2.6 and 1.5Å from W and W′, respectively. This peak may be due to the hydride although attempts to refine on it were unsuccessful as might be expected because of the close proximity to the tungstens and the presence of the pseudo inversion center.

17. Since in an accentric space group Friedel's law does not hold when anomalous scattering is included, refinement was also attempted in the space group Cc using the four unique octants hkl, $\bar{h}\bar{k}l$, $\bar{h}k\bar{l}$, and $h\bar{k}\bar{l}$ after an empirical absorption correction; however, correlation of the 4-ethylpyridine groups again resulted in divergence.

18. Bondi, A. J. Phys. Chem. 1964, 68, 441.

19. Chisholm, M. H. Transition Met. Chem. 1978, 3, 321, and references therein.

20. Jackson, R. B.; Strieb, W. E. Inorg. Chem. 1971, 10, 1760.

21. Shaik, S.; Hoffmann, R.; Fisel, C. R.; Summerville, R. H. J. Am. Chem. Soc. 1980, 102, 4555.

22. Bino, A.; Cotton, F. A.; Dori, Z.; Sekutowski, J. C. Inorg. Chem. 1978, 17, 2946.

23. Akiyama, M.; Little, D.; Chisholm, M. H.; Hoitko, D. A.; Cotton, F. A.; Extine, M. W. J. Am. Chem. Soc. 1979, 101, 2504.

24. Boorman, P. M.; Kerr, K. A.; Patel, V. D. J. Chem. Soc. Dalton Trans. 1981, 506.

25. Bino, A.; Cotton, F. A. Angew. Chem. Int. Ed. Engl. 1979, 18, 332.

26. Bino, A.; Cotton, F. A. J. Am. Chem. Soc. 1979, 101, 4150.

27. Katovic, V.; McCarley, R. E. Inorg. Chem. 1978, 17, 1268.

28. Gill, N. S.; Nutall, R. H.; Schaife, D. E.; Sharp, D. W. A. Inorg. Nucl. Chem. 1961, 18, 79.

29. Clark, R. J.; Williams, C. S. Inorg. Chem. 1964, 4, 350.

30. Best, S. A.; Brant, P.; Feltham, R. D.; Rauchfuss, T. B.; Roundhill, D. M.; Walton, R. A. Inorg. Chem. 1977, 16, 1976.

31. Luly, M. H. "APES, A Fortran Program to Analyze Photoelectron Spectra", 1979 U. S. DOE Report IS-4694.

32. Ebner, J. R.; McFadden, D. L.; Tyler, D. R.; Walton, R. A. Inorg. Chem. 1976, 15, 3014.

33. Saillant, R.; Hayden, J. L.; Wentworth, R. A. D. Inorg. Chem. 1967, 6, 1497.

34. Carlin, R. T.; McCarley, R. E., Iowa State University, Ames, Iowa, unpublished results.

SECTION II. SYNTHESIS, CRYSTAL STRUCTURE AND SPECTRAL CHARACTERIZATION OF TETRACHLOROTETRAKIS(TRIMETHYLPHOSPHINE)MOLYBDENUM(II)-TUNGSTEN(II). A HETERONUCLEAR DIMER POSSESSING A MOLYBDENUM-TUNGSTEN QUADRUPLE BOND

INTRODUCTION

Interest in the synthesis of an unbridged, quadruply-bonded, heteronuclear (Mo-W) dimer was sparked by the structural determination of $MoW(O_2CCMe_3)_4$ (1). The Mo-W bond length of 2.080(1) Å is considerably shorter than that expected from comparison to the homonuclear, quadruple bonds found in $Mo(O_2CCMe_3)_4$ and $W_2(O_2CCF_3)_4$, where d(MoMo) = 2.088(1) Å (2) and d(WW) = 2.211(2) Å and 2.207(2) Å (3), respectively. Because bridging carboxylate units are present in these compounds, the metal-metal bond cannot be viewed in terms of solely metal d orbital overlap; instead, the pertubation of the d orbitals by these carboxylate ligands must also be considered. This perturbation may be large since the carboxylate ligands have O-C-O π orbitals residing directly over the metal-metal bond. Additionally, these carboxylate ligands hold the two metal atoms in close approach, and so the metal-metal separation will be less than if non-bridging ligands were present. It is difficult, if not impossible, to determine how much of the closeness of the two metals is due to true metal-metal bonding and how much is a result of the carboxylates restraining them to close approach. By eliminating all bridging ligands it would be possible to draw conclusions about the metal-metal bond based solely on d-orbital overlap arguments with the ligand perturbations of these d orbitals being minimized.

The normal route from a carboxylate bridged dimolybdenum dimer to an unbridged species is represented below (4,5).

$$Mo_2(OAc)_4 \xrightarrow[0^0C]{HCl\ (aq.\ sat.)} Mo_2Cl_8^{4-} \xrightarrow[(L = \text{neutral donor } PR_3, \text{ pyr, } SR_2, \text{ etc.})]{+L} Mo_2Cl_4L_4$$

Efforts to duplicate these reactions with $MoW(O_2CCMe_3)_4$ were thwarted by oxidation of the metals in aqueous HCl from +2 to +3 and the formation of the $MoWCl_8H^{3-}$ anion (6). Reduction of the metal atoms in this dimer back to a +2 oxidation state proved to be impossible (7).

In an attempt to by-pass this unfortunate oxidation, use was made of the following single-step preparation of $Mo_2Cl_4(PR_3)_4$ (8).

$$Mo_2(OAc)_4 + 4\ ClSiMe_3 + 4\ L \xrightarrow[\Delta]{} Mo_2Cl_4L_4 + 4\ Me_3Si\text{-}OAc$$

$$Mo_2(OAc)_4 + 4\ AlCl_3 + 4\ L \xrightarrow{THF} Mo_2Cl_4L_4 + 4\ Cl_2Al\text{-}OAc$$

This preparative technique made possible the synthesis of the desired heteronuclear dimer $MoWCl_4(PMe_3)_4$. The synthetic details, the single-crystal x-ray structural determination and the spectral properties of this compound will be described here. Additionally, a discussion of the nature of this heteronuclear Mo-W bond in relation to its homonuclear analogs and of its possible intrinsic strength will be presented.

EXPERIMENTAL

Materials

The compounds discussed below were handled in Schlenk vessels under a nitrogen atmosphere or on a vacuum line.

Tetrahydrofuran was initially refluxed with copper(I) chloride to eliminate peroxides. After drying over CaH_2, the THF was then vacuum distilled onto Molecular Sieves (4Å) for storage in vacuo. Cyclohexane was refluxed over CaH_2 and vacuum distilled onto Molecular Sieves (4Å) for storage. Toluene was refluxed over CaH_2 and distilled under a nitrogen atmosphere into a 500 mL Schlenk flask for storage.

Trimethylphosphine was obtained from Alfa Products and was stored in a vacuum bulb without further purification. Chlorotrimethylsilane was obtained from the Fisher Scientific Company and was also stored in vacuo without further purification. To avoid getting any hydrolyzed or oxidized species into the reaction mixtures, both PMe_3 and $ClSiMe_3$ were vacuum distilled from their storage vessels either directly into the reaction flask or into a calibrated volume tube for measurement before vacuum distillation into the reaction flask.

Physical Measurements

Far infrared, uv-visible and x-ray photoelectron spectra were obtained as discussed earlier (9). X-ray photoelectron spectra were deconvoluted using a least-squares curve fitting program written at Ames Laboratory (10). Samples for ^{31}P NMR study were dissolved in $CDCl_3$ and either sealed in vacuo in 10 mm NMR tubes along with a capillary

containing a H_3PO_4 standard, or loaded into a 5 mm NMR tube under nitrogen to which was later added a capillary containing the H_3PO_4 standard. The spectra were obtained using a Bruker WM-300 Spectrometer.

Syntheses

$Mo_2(O_2CCMe_3)_4$

This compound was prepared by an established procedure (11).

$MoW(O_2CCMe_3)_4$

This extremely air sensitive compound was prepared in limited quantities by a multi-step procedure devised by V. Katovic *et al.* (12).

WCl_4

A facile preparation of this compound was achieved by reduction of WCl_6 with a stoichiometric amount of $W(CO)_6$ in refluxing chlorobenzene (13). The product was stored in a nitrogen atmosphere dry box.

$Mo_2Cl_4(PMe_3)_4$

Under a nitrogen atmosphere, $Mo_2(O_2CCMe_3)_4$ (0.7 g, 1.2 mmol) was added to a 100 mL reaction flask equipped with a condenser. The flask was evacuated on a vacuum line and $ClSiMe_3$ (*ca.* 15 mL) was vacuum distilled into the flask. An excess of PMe_3 (0.85 mL, 8.5 mmol) was then added. The reaction mixture was refluxed under nitrogen for two days. Upon filtration, a purple precipitate was obtained. Purification of this precipitate was achieved by first heating *in vacuo* to 70°C to eliminate

any silyl ester remaining and then extraction with cyclohexane to give red crystals.

$W_2Cl_4(PMe_3)_4$

This tungsten dimer was prepared by the literature method (14) with some modifications. Into a 100 mL Schlenk flask containing WCl_4 (0.90 g, 2.8 mmol) was vacuum distilled 70 mL of THF and an excess of PMe_3 (0.7 mL, 7.0 mmol). The mixture was maintained at or below -23°C using a chloroform slush bath while the requisite quantity (31.0 g) of sodium-amalgam (0.178 mmol Na/1 g Hg) was syringed into the flask. The reaction mixture was allowed to warm and was stirred at room temperature for 5 h. The resulting green solution was filtered through Celite, and the solvent was removed *in vacuo* leaving a dark green residue. This residue was redissolved in toluene and passed through a 1 x 6 cm Florisil column. The toluene was removed *in vacuo*, and the green residue was extracted with cyclohexane to obtain the final product.

$MoWCl_4(PMe_3)_4$

In a typical preparation, $MoW(O_2CCMe_3)_4$ (0.45 g, 0.7 mmol) and excess PMe_3 (0.5 g, 5.0 mmol) were refluxed in *ca.* 15 mL $ClSiMe_3$ for 2.5 days. After cooling, the mixture was filtered giving a dark green filtrate and a small quantity of a green solid. The $ClSiMe_3$ and excess PMe_3 were removed *in vacuo* leaving a blue-green, tarry residue. The green solid and filtrate residue were combined and were purified by heating *in vacuo* at 100°C to expel any silyl ester. Subsequent extraction with cyclohexane yielded crystals suitable for x-ray single-crystal structural analysis.

Collection and Treatment of X-ray Data

A single crystal of $MoWCl_4(PMe_3)_4$, determined to be free of $Mo_2Cl_4(PMe_3)_4$ by ^{31}P NMR (see discussion of ^{31}P NMR spectra), with dimensions 0.14 x 0.11 x 0.21 mm was glued to the end of a glass fiber and mounted on a 4-circle diffractometer designed at the Ames Laboratory (15). From four ω-oscillation photographs at $\chi = 0°$ and various ϕ angles, 14 reflections were chosen and were input into the automatic indexing program ALICE (16). The resulting reduced cell was C-centered monoclinic as expected from previous studies on the dimolybdenum and ditungsten homonuclear analogs (17).

Final lattice parameters were obtained by using least-squares refinements on 15 independent reflections with $2\theta > 30°$. The resulting lattice parameters were a = 18.377(4) Å, b = 9.206(2) Å, c = 17.323(6) Å, and $\beta = 115.40(2)°$ with V = 2647.6(1) $Å^3$.

Data were collected at 25°C using graphite-monochromated Mo K_α radiation (λ = 0.71034 Å). Four octants of data were collected with a 2θ sphere of 50° using an ω-scan technique giving a total of 5432 reflections. The intensities of three standards were measured after every 75 reflections and indicated no appreciable decay. The data were corrected for Lorentz and polarization effects and standard deviations were calculated (18). An empirical absorption correction (μ = 54.86 cm^{-1}) was applied using a ϕ-scan technique at $\chi = 90°$ (19). Averaging of these data gave 1887 independent reflections with $I > 3\sigma_I$.

Structure Solution and Refinement

Systematic extinctions of hkl for h+k = 2n+1 and of h0l for l = 2n+1 indicated the space group to be C2/c. All refinements were carried out using either block-matrix or full-matrix least-squares procedures minimizing the function $\Sigma\ \omega(|F_o|-|F_c|)^2$, where $\omega = 1/\sigma_F^2$. The scattering factors used for all atoms, except the metal atoms, were taken directly from Hanson et al. (20). The scattering factor tables for the metal atoms were calculated by averaging together the molybdenum and tungsten tables of Hanson et al. (20), including the tables correcting for anomalous dispersion (21).

In an earlier structural determination of $MoWCl_4(PMe_3)_4$ (22), the positional parameters of the metal atoms were determined from examination of a sharpened Patterson map (23). All other nonhydrogen atoms had been located in this earlier study using a combination of least-squares refinements (24) and Fourier syntheses (23) techniques. Using these previously determined positional parameters, block-matrix least-squares refinement on all nonhydrogen atoms gave residuals of $R = \Sigma\left||F_o|-|F_c|\right|/\Sigma|F_o| = 0.056$ and $Rw = [\Sigma\omega(|F_o|-|F_c|)^2/\omega|F_o|^2]^{1/2} = 0.082$. A difference Fourier synthesis at this point revealed the position of most of the methyl hydrogens. The positions were very near those determined for $Mo_2Cl_4(PMe_3)_4$ and $W_2Cl_4(PMe_3)_4$ (17); however, attempts to refine the hydrogen positional parameters were unsuccessful. Therefore, using several of the hydrogen positions determined from the Fourier difference map as starting points, idealized hydrogen positions were calculated with d(C-H) = 0.95 Å, and isotropic B values of 7.0 $Å^2$ were assigned to each

hydrogen atom. In subsequent refinements, the hydrogen atoms were included in the atom lists, but their positional and thermal parameters were fixed. A least-squares refinement now yielded residuals of R = 0.054 and Rw = 0.077.

It was observed that the data at low values of $\sin\theta/\lambda$ had unusually high Rw's; therefore, the data were sorted according to Fo and reweighed in 35 overlapping groups such that $\Delta\omega^2$ was essentially constant. A full-matrix least-squares refinement was carried out giving R = 0.053 and Rw = 0.063; however, a difference Fourier synthesis map revealed peaks ranging from -0.9 to +1.4 $e^-/\text{Å}^3$ about the metal atom positions.

Returning to a $1/\sigma_F^2$ weighting scheme, the multipliers of the metals were allowed to vary. Full-matrix least-squares refinement on all parameters (hydrogen parameters still fixed) resulted in a significant lowering of the residuals to R = 0.043 and Rw = 0.056. The multipliers on MoW1 and MoW2 shifted from their full occupancy values of 0.5 to values of 0.528(3) and 0.452(2), respectively. The final difference Fourier synthesis again showed peaks from -0.9 to +1.2 $e^-/\text{Å}^3$ near the metal atoms with the largest peaks, both positive and negative, falling between the metal centers. The number of such peaks, however, was considerably less than observed before the metal atom multipliers were allowed to vary. Also, the low angle data refined to considerably lower residuals, eliminating the need for a reweighting of these data. The resulting multipliers imply that there is some ordering of the metal atoms in the crystal. This point will be elaborated more fully later.

Positional and thermal parameters are given in Tables II-1, II-2 and II-3, and bond distances and angles are provided in Table II-4.

Table II-1. Positional parameters for $MoWCl_4(PMe_3)_4$ nonhydrogen atoms[a]

Atom	X	Y	Z	Multiplier
MoW1	0.0	0.09792(7)	0.25	0.5281(26)
MoW2	0.0	0.33894(8)	0.25	0.4519(24)
CL1	0.0853(1)	0.0012(3)	0.1892(2)	
P1	0.1154(1)	0.0427(3)	0.3928(1)	
P2	0.0953(2)	0.3938(3)	0.1831(2)	
C11	0.2163(6)	0.097(1)	0.4101(7)	
C12	0.1248(9)	-0.155(1)	0.4021(8)	
C13	0.1101(7)	0.095(1)	0.4909(7)	
C21	0.1009(8)	0.589(2)	0.1768(9)	
C22	0.2006(7)	0.340(2)	0.2384(9)	
C23	0.0675(8)	0.341(1)	0.0725(8)	

[a]Estimated standard deviations are given in parentheses for the last significant digits.

Table II-2. Thermal parameters for $MoWCl_4(PMe_3)_4$ nonhydrogen atoms[a,b]

Atom	B_{11}	B_{22}	B_{33}	B_{12}	B_{13}	B_{23}
MOW1	2.234(28)	2.565(30)	2.228(27)	0.0	0.866(20)	0.0
MOW2	2.211(33)	2.650(37)	2.504(35)	0.0	1.001(25)	0.0
CL1	3.99(11)	4.49(13)	4.29(12)	1.00(9)	2.37(9)	-0.20(10)
CL2	3.60(10)	4.07(12)	3.46(10)	-0.56(9)	0.56(8)	-0.76(9)
P1	3.22(10)	3.56(12)	2.68(10)	-0.07(9)	0.73(8)	0.23(9)
P2	3.25(11)	3.79(12)	4.15(12)	-0.20(9)	2.04(9)	0.53(9)
C11	2.8(4)	5.6(6)	4.7(5)	0.1(4)	0.8(4)	-0.3(5)
C12	7.0(7)	4.2(6)	5.3(6)	0.2(5)	0.9(5)	1.0(5)
C13	5.7(6)	7.1(7)	2.9(4)	0.4(5)	1.4(4)	0.4(5)
C21	6.3(7)	5.3(7)	7.4(7)	-0.9(5)	3.8(6)	0.9(6)
C22	4.0(5)	7.2(8)	6.7(7)	0.5(5)	2.9(5)	2.9(6)
C23	7.5(7)	5.6(6)	4.6(6)	0.3(6)	4.1(6)	0.4(5)

[a]The general thermal parameter expression used is $\exp[-1/4(B_{11}h^2a^{*2} + B_{22}k^2b^{*2} + \ldots 2B_{23}k\ell b^*c^*)]$.

[b]Estimated standard deviations are given in parentheses for the last significant figures.

Table II-3. Calculated positional parameters for $MoWCl_4(PMe_3)_4$ hydrogen atoms[a]

Atom	X	Y	Z
H111	0.25511	0.06080	0.46354
H112	0.22816	0.05820	0.36568
H113	0.21975	0.19962	0.40995
H121	0.14746	0.82519	0.46199
H122	0.16134	0.81832	0.37978
H123	0.08086	0.77770	0.37780
H131	0.05742	0.06676	0.48576
H132	0.11467	0.19907	0.49941
H133	0.15009	0.04988	0.53979

[a]All hydrogen atoms are assigned isotropic B values of 7.0$Å^2$.

Table II-4. Bond distances (Å) and angles (Deg) in $MoWCl_4(PMe_3)_4$[a]

Distances

MoW1-MoW2	2.219(1)
MoW1-C11	2.4036(25)
MoW1-P1	2.5245(25)
MoW2-C12	2.4105(25)
MoW2-P2	2.5317(26)
P1-C11	1.815(10)
P1-C12	1.829(13)
P1-C13	1.810(11)
P2-C21	1.807(14)
P2-C22	1.821(12)
P2-C23	1.824(12)

Angles

MoW2-MoW1-C11	111.76(7)
MoW2-MoW1-P1	101.62(6)
C11-MoW1-C11′	136.49(13)
C11-MoW1-P1	85.58(8)
C11-MoW1-P1′	85.86(8)
P1-MoW1-P1′	156.76(13)
MoW1-MoW2-C12	111.96(7)
MoW1-MoW2-P2	101.52(7)
C12-MoW2-C12′	136.08(13)
C12-MoW2-P2	85.74(9)
C12-MoW2-P2′	85.70(9)
P2-MoW2-P2′	156.97(13)
MoW1-P1-C11	118.4(4)
MoW1-P1-C12	107.2(4)
MoW1-P1-C13	120.3(4)
C11-P1-C12	101.9(6)
C11-P1-C13	103.5(5)
C12-P1-C13	103.0(6)
MoW2-P2-C21	107.1(4)
MoW2-P2-C22	119.5(4)
MoW2-P2-C23	119.3(4)
C21-P2-C22	103.1(6)
C21-P2-C23	101.6(6)
C22-P2-C23	103.7(6)

[a]Standard deviations are given in parentheses for the last significant figures.

RESULTS AND DISCUSSION

Crystal Structure

The structure of $MoWCl_4(PMe_3)_4$, as seen in Figure II-1, is isostructural with its homonuclear analogs (17). The electronic configuration of the quadruple metal-metal bond, $\sigma^2\pi^4\delta^2$, requires an eclipsed configuration of ligands to maintain the δ interaction. The arrangement of the ligands about each metal is essentially square planar with steric considerations requiring trans positioning of the trimethylphosphine ligands. Similar steric factors result in the staggered configuration of the trimethylphosphine ligands across the metal bond.

The reason for synthesizing $MoWCl_4(PMe_3)_4$ was to examine an unbridged quadruply bonded dimer with minimal ligand contribution to the metal-metal bond and to determine if there is some additional intrinsic metal-metal bond strength in the heteronuclear bond compared to the homonuclear bonds. A listing of the important bond distances of the three $M_2Cl_4(PMe_3)_4$ complexes is provided in Table II-5. The distances for $MoWCl_4(PMe_3)_4$ are those obtained after refining on the metal multipliers as discussed earlier. It is immediately apparent that the Mo-W quadruple bond of length 2.219(1) Å is not anomalously short as in the carboxylate dimers (1), but is instead 0.073 Å longer than the average, 2.146(2) Å, of the two homonuclear bonds. In these unbridged dimers then, the metal-metal bond distances do not point towards a stronger heteronuclear bond.

It is worth noting here that there exists one other series of quadruply bonded dimers for which the dimolybdenum, molybdenum-tungsten, ditungsten analogs have had structural determinations performed on them.

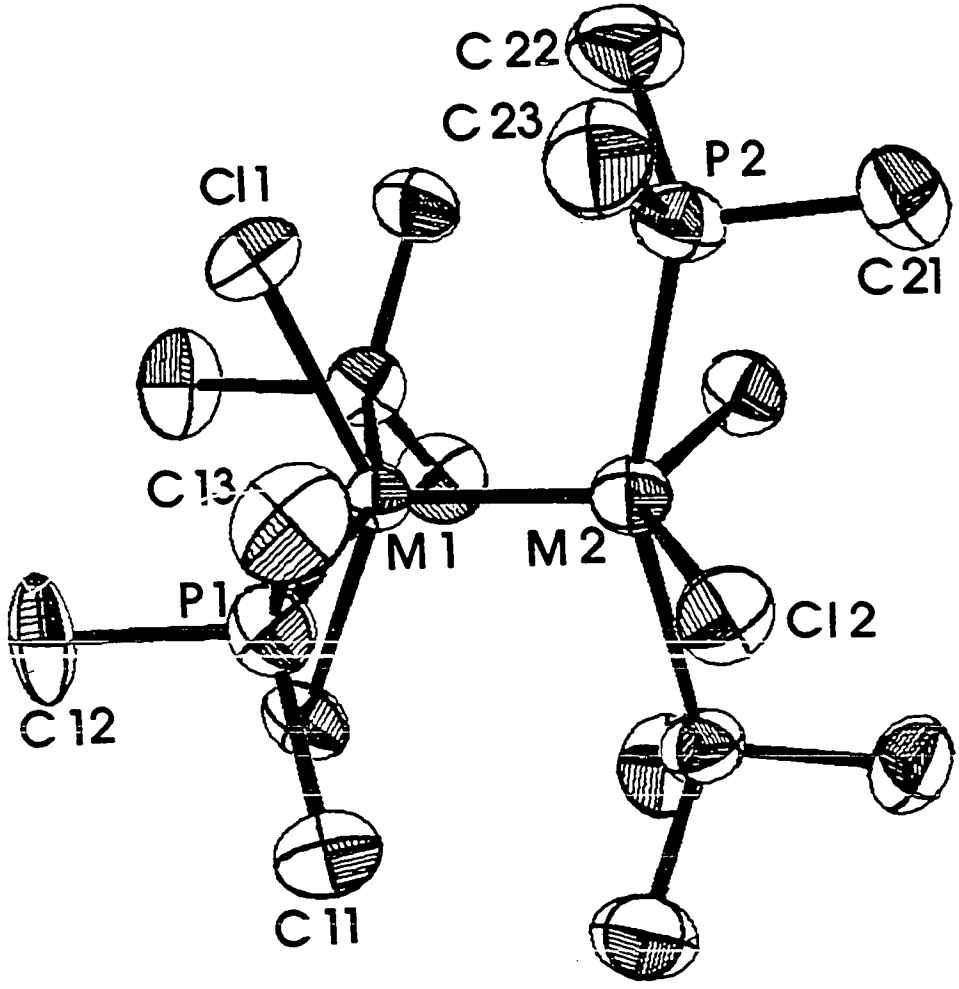

Figure II-1. ORTEP view of $MoWCl_4(PMe_3)_4$ molecule

Table II-5. Bond distances for $M_2Cl_4(PMe_3)_4$ compounds

	Bond Distances (Å)		
M_2 =	Mo_2	MoW	W_2
M-M	2.130(1)	2.219(1)	2.262(1)
M-Cl	2.415(1)	2.4105(25)	2.395(2)
	2.413(1)	2.4036(25)	2.389(2)
M-P	2.546(1)	2.5317(26)	2.509(2)
	2.544(1)	2.5245(25)	2.506(2)

This is the $M_2(mhp)_4$ series in which the anion of 2-hydroxy-6-methyl-pyridine (mhp) bridges the two metal atoms (25). The metal-metal bond distances for this series are d(Mo-Mo) = 2.065(1) Å, d(Mo-W) = 2.091(1) Å and d(W-W) = 2.161(1) Å (25). The heteronuclear bond falls 0.022 Å below the average, 2.113(2) Å, of the homonuclear bond lengths, indicative perhaps that the heteronuclear bond in this series is somewhat stronger than expected.

From examination of metal-metal bond distances only, the issue of intrinsically greater heteronuclear bond strength in quadruply bonded dimers becomes confusing. The three series discussed exhibit heteronuclear bond lengths 1) shorter than both homonuclear bonds ($M_2(O_2CR)_4$ (1)), 2) greater than the average of the homonuclear bonds ($M_2Cl_4(PMe_3)_4$)

and 3) less than the average of the homonuclear bonds ($M_2(mhp)_4$ (25)). The question of heteronuclear bond strength will be discussed further after the presentation of relevant spectral data.

Another interesting feature of the $M_2Cl_4(PMe_3)_4$ series is the gradual decrease in M-L bond lengths from $Mo_2Cl_4(PMe_3)_4$ to $W_2Cl_4(PMe_3)_4$. This is easily seen in Figure II-2 in which percent molybdenum or tungsten character is plotted against M-Cl and M-P bond lengths. Error bars of $\pm 3\sigma$ are drawn for each data point. For the homonuclear dimers, the two points for the M-Cl and the M-P distances correspond to the two phosphorous atoms in each molecule. Since the two metal-atom multipliers were allowed to vary for $MoWCl_4(PMe_3)_4$, the M-L distances are plotted both before and after this was done. With a fixed 50:50 ratio of Mo to W character for each metal, the M-L distances are d(MoW1-C11) = 2.407(3) Å, d(MoW1-C12) = 2.410(3) Å, d(MoW1-P1) = 2.524(3) Å and d(MoW2-P2) = 2.528(4) Å. When the metal-atom multipliers are allowed to vary, the refinement converged with one metal atom having 60.2% W and 39.8% Mo character, and the other having 32.6% W and 67.4% Mo character. The sum of the multipliers is $0.980 \pm 0.015(3\sigma)$, a value slightly below the theoretical value of 1.0 expected for a MoW dimer free of any $Mo_2Cl_4(PMe_3)_4$. This slightly low value is probably an artifact of the approximations made when using averaged scattering factors for disordered metal atoms, because a ^{31}P NMR spectrum of the sample used in the structure determination showed no $Mo_2Cl_4(PMe_3)_4$ to be present. Varying the metal multipliers has a small effect on the ligands producing a shift to greater separations of the respective M-L distances. The resulting M-L

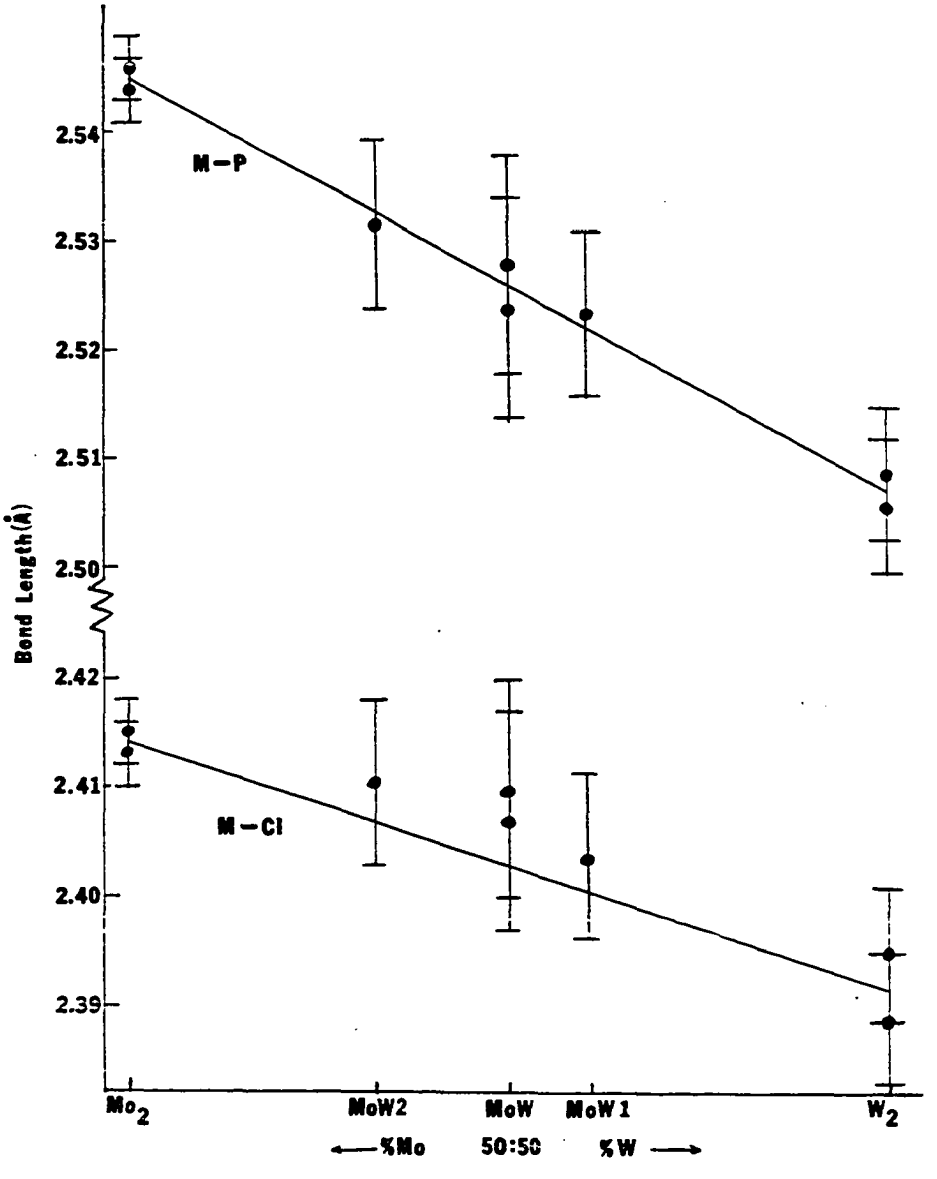

Figure II-2. Metal-ligand bond distances plotted against metal character

distances are those given in Table II-5. Plotted against the molybdenum and tungsten character of the metal atoms, the M-P bond distances fall on the straight line drawn through the M-P bond distances of the homonuclear dimers. The M-Cl heteronuclear bond distances are a little longer than predicted from the homonuclear distances; however, they show the expected decrease in bond distances with increasing tungsten character. Both the M-P and M-Cl bonds in the heteronuclear dimer should represent a weighted average of the W-L and Mo-L bonds, and this is borne out in the plot.

The fact that the M-L distances for the heteronuclear dimer are consistent with those expected from the metal atom multipliers (especially for the M-P distances) lends support to the possibility that there is some ordering of the metal atoms in the heteronuclear structure. In all previous structure determinations of symmetric multiply bonded heteronuclear dimers, $MoW(piv)_4$ (1), $MoW(mhp)_4$ (26) and Rb_3MoWCl_8H (1), no such ordering was reported. In the one electron oxidized complexes, $MoW(piv)_4I{\cdot}CH_3CN$, there is complete order of the metal atoms since the iodide is bound to the tungsten in the molecule (12). The factors which may lead to a partial ordering in $MoWCl_4(PMe_3)_4$ are probably due to crystal packing effects. Examination of the two independent M-P and M-Cl distances in each of the homonuclear dimers reveals that they differed from each other, although by less than 3σ. These differences, if real, are most likely a result of crystal packing effects. The heteronuclear dimer is partially ordered in a fashion that places the shorter M-L bonds of higher tungsten character in the same positions as the shorter M-L bonds of the homonuclear dimers. By this partial orientation of the

heteronuclear dimer, some repulsive intermolecular interactions may be reduced. Examination of intermolecular distances does not give any obvious indication of this, but the closest intermolecular contacts involve hydrogen atoms which are only in calculated positions.

An opposite point of view is that the differences in the heteronuclear M-L bond distances are not due to the tungsten or molybdenum character of the metal atoms, but are instead a result of the crystal packing effects which give differences in the M-L bond lengths in the homonuclear dimers. The heteronuclear M-P bonds provide an argument against this interpretation. In the homonuclear dimers, the two independent M-P distances are essentially equal yet they differ by approximately 3σ in the heteronuclear dimer, indicating an additional factor influencing these bonds, such as metal character.

Caution must be used when drawing conclusions about the metal atoms from the differences in the heteronuclear M-L bond lengths, since the two M-P and the two M-Cl bonds are within 3σ of each other, respectively. The refined metal multipliers in conjunction with these M-L comparisons, however, indicate that the partial metal atom order is a real phenomenon.

UV-Visible Spectra

The absorption energies and the extinction coefficients for the $\delta \rightarrow \delta^*$ transitions in the $M_2Cl_4(PMe_3)_4$ series are given in Table II-6. The two values given for $Mo_2Cl_4(PMe_3)_4$ correspond to those measured in this lab and those obtained by Cotton and co-workers (17). The energy of the $\delta \rightarrow \delta^*$ transition in $MoWCl_4(PMe_3)_4$ falls between those of the homonuclear dimers and is nearer the energy for $W_2Cl_4(PMe_3)_4$. This is in

accord with the metal-metal bonds in the dimers -- the Mo-W bond length is closer to d(W-W) than to d(Mo-Mo).

Table II-6. $M_2Cl_4(PMe_3)_4$ $\delta \rightarrow \delta^*$ transitions[a]

M_2 =	Mo_2	MoW	W_2
λ_{max} (nm)	581(2.80)[b]	632(2.77)[b]	657(4.2)[c]
	582(3.4)[c]		

[a]Extinction coefficients ($x10^3$ M^{-1} cm^{-1}) are given in parentheses.

[b]This work.

[c]Reference 17.

Since the energy of the $\delta \rightarrow \delta^*$ transition is an indication of the δ overlap, it is apparent, both from these transition energies and the metal-metal bond distances, that $W_2Cl_4(PMe_3)_4$ has the least δ overlap of the series. The heteronuclear dimer has only slightly greater δ overlap than $W_2Cl_4(PMe_3)_4$, and has less than that expected from the average of the homonuclear complexes. The degree of δ overlap in these complexes will be discussed more fully later.

Infrared and Raman Spectra

The symmetry of the ligands in all three dimers is D_{2d}. The total symmetry of the homonuclear dimers is still D_{2d} when the metals are included, whereas the heteronuclear dimer has a lower total symmetry of C_{2v} as a result of the asymmetry of the metal atoms. In D_{2d} symmetry,

there are three M-Cl normal stretching modes of symmetries $A_1 + B_2 + E$. The stretching modes of B_2 and E symmetries are expected to be infrared and Raman active, and the one of A_1 symmetry should only be Raman active. The metal-metal stretching mode which is of A_1 symmetry also should be only Raman active. Lowering the symmetry to C_{2v} for the heteronuclear dimer causes a change of the symmetries of the M-Cl stretching modes to $2A_1 + B_1 + B_2$. All these modes will be both infrared and Raman active. The metal-metal stretching mode in the heteronuclear dimer is of A_1 symmetry and is both infrared and Raman active. Figure II-3 shows the far-infrared spectra of these dimers.

Assignment of the bands is aided by examination of the far-infrared spectra of related dimolybdenum complexes. Some of these are provided in Table II-7. The spectra of the trimethylphosphine containing complexes are complicated by the fact that there are two C-P-C bending modes of symmetries A_1 and E in the same spectral region as the M-Cl stretching modes (27). The tributylphosphine and triethylphosphine complexes do not have these bending modes in the spectral region of interest. Two M-Cl stretches are found for $Mo_2Cl_4(PEt_3)_4$ and $Mo_2Cl_4(PBu_3)_4$ (5) as expected from the symmetry of the molecules. The spectrum of $Mo_2Cl_4(PMe_3)_4$ exhibits three bands in this same region, although four bands are expected: two M-Cl stretches and two C-P-C bends. By comparison with frequencies of the M-Cl stretching modes in the other dimolybdenum complexes, the bands at 329 cm^{-1} and 285 cm^{-1} are assignable to M-Cl stretches. Upon replacement of Cl with Br, the band at 285 cm^{-1} is shifted to 226 cm^{-1}; however, the band at 329 cm^{-1} is only reduced in

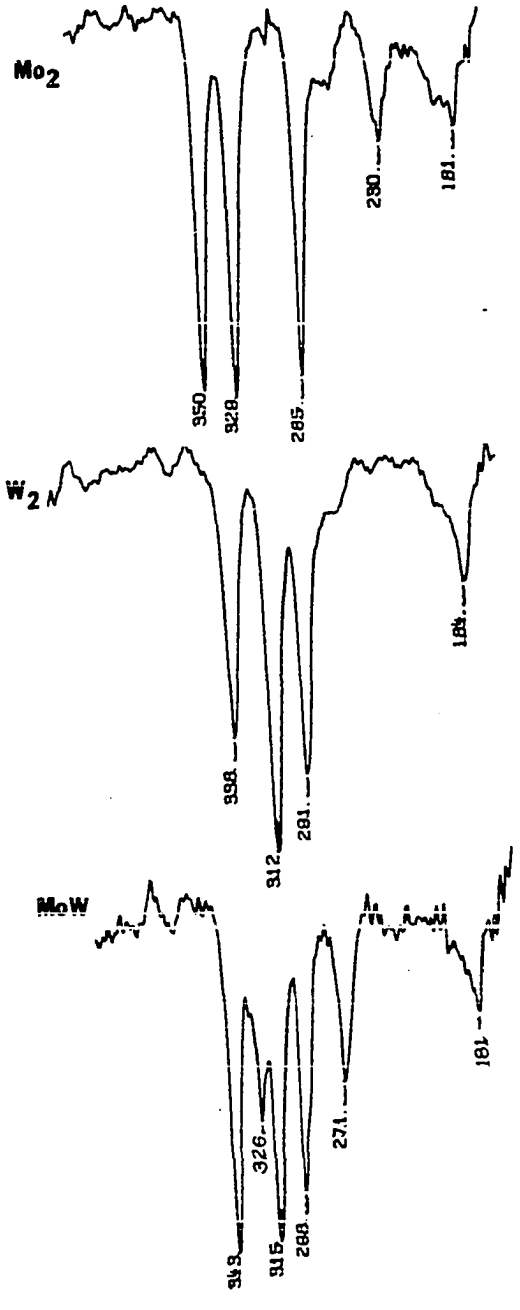

Figure II-3. Far-infrared spectra of $M_2Cl_4(PMe_3)_4$ series

Table II-7. Infrared spectra of $Mo_2X_4(PR_3)_4$ complexes[a]

Complexes	Assignment: C-P-C bend		Assignment: M-X Stretch		Reference
$Mo_2Cl_4(PMe_3)_4$	351 s	329 s	329 s	285 s	This work
$Mo_2Br_4(PMe_3)_4$	345 s	330 m	263 s	226 s	This work
$Mo_2Cl_4(PBu_3)_4$	---	---	326 m	278 m	5
$Mo_2Br_4(PBu_3)_4$	---	---	260 m	---	5
$Mo_2Cl_4(PEt_3)_4$	---	---	332 s	282 m	This work

[a]Relative intensities are given as s, strong; m, medium.

intensity, and a new band appears at 263 cm^{-1}. These shifts in the metal-halide stretching frequencies (M-Br $\tilde{=}$ 0.8 x M-Cl) are the same observed for the tributylphosphine dimers, from 326 cm^{-1} to 260 cm^{-1}. The fact that the band at 329 cm^{-1} in the trimethylphosphine dimer is only reduced in intensity upon replacement of Cl with Br indicates that in the chloride complex this band is either a combination band composed of a M-Cl stretching mode and a C-P-C bending mode, or the result of the accidental overlap of these two vibrational modes. In the bromide complex, this band, which appears at 330 cm^{-1}, is of only C-P-C bending character.

Based on the assignments discussed above, the various bands in the $M_2Cl_4(PMe_3)_4$ series are listed in Table II-8 along with their assignments.

Table II-8. Infrared spectra of $M_2Cl_4(PMe_3)_4$ complexes[a]

Complex	Assignment						
	C-P-C bend		M-X stretch		M-Cl bend or M-P stretch		M-M stretch
$Mo_2Cl_4(PMe_3)_4$	351 s	329 s	329 s	285 s	230 m	181 m	---
$W_2Cl_4(PMe_3)_4$	338 s	312 s	312 s	291 s	---	184 m	---
$MoWCl_4(PMe_3)_4$	343 s	315 s	315 s	298 s	---	181 m	326 m
			271 m				

[a]Relative intensities are given as s, strong; m, medium.

For all these complexes, the low energy C-P-C bending-mode band is also assigned as the high energy M-Cl stretching-mode band. The bands below 240 cm^{-1} have been tentatively assigned to M-Cl bending or M-P stretching modes. The spectral region composed of M-Cl stretching modes and C-P-C bending modes are very similar for the three complexes except that the heteronuclear dimer possesses two additional bands. These bands occur at 326 cm^{-1} and 271 cm^{-1} and are assigned to the M-Cl stretching mode of A_1 symmetry and the metal-metal stretching mode, respectively. Similar bands are not observed in the homonuclear dimers for the reasons of symmetry discussed above. The assignment of the band at 271 cm^{-1} is based on the work of San Filippo and Sniadoch (28) in which the same band assignment is made to a weak band at 282 cm^{-1} observed in the Raman spectrum of $Mo_2Cl_4(PBu_3)_4$. The Raman spectrum of $MoWCl_4(PMe_3)_4$, which is discussed

more fully below, shows bands at 322 cm^{-1} and 267 cm^{-1}, corresponding to these same two infrared bands after taking into account a 4 cm^{-1} correction. The observation of these bands in the infrared and Raman spectra provide further confirmation of the assignments made for these bands.

Table II-9 summarizes the important data obtained from the Raman spectra of the $M_2Cl_4(PR_3)_4$ (14,28) complexes as well as the $M_2(mhp)_4$ (25) series. The relative force constants are calculated using a simple harmonic oscillation approximation based only on the metal atoms and ignores the ligand contributions to the force constants. An interesting

Table II-9. Frequencies and relative force constants for M-M' stretching modes

Compound	ν (cm^{-1})	k (mdyn/Å)	Reference
$MoWCl_4(PMe_3)_4$	322(3)	3.84	This work
$Mo_2Cl_4(PMe_3)_4$	354(6)	3.54	This work
$Mo_2Cl_4(PBu^n_3)_4$	350(1)	3.46	(28)
$W_2Cl_4(PBu^n_3)_4$	260(10)	3.65	(14)
$Cr_2(mhp)_4$	556(3)	4.73	(25)
$CrMo(mhp)_4$	504(3)	5.03	(25)
$Mo_2(mhp)_4$	425(3)	5.10	(25)
$MoW(mhp)_4$	384(3)	5.45	(25)
$W_2(mhp)_4$	284(3)	4.71	(25)

observation is that in both series of complexes the Mo-W stretching force constant is the highest. The W-W force constant is higher than the Mo-Mo force constant in the $M_2Cl_4(PMe_3)_4$ series and vice versa in the $M_2(mhp)_4$ series. The anomalously large Mo-W force constants are possible evidence for some additional strength in the heteronuclear metal-metal bond.

Another feature of the Raman spectrum of $MoWCl_4(PMe_3)_4$ worthy of note is that the intensity of the metal-metal stretch is considerably lower than that seen for $Mo_2Cl_4(PMe_3)_4$. A similar effect has been observed for pentachlorobis(2,5-dithiahexane)dirhenium which possesses an asymmetric arrangement of ligands. The metal-metal stretching mode for this dimer is seen in both the infrared and Raman spectra; however, the Raman intensity is of lower intensity than that found for the Raman intensities of other dirhenium complexes having metal-metal stretching modes with Raman activity only (28).

^{31}P NMR Spectra

The trimethylphosphine ligands in the homonuclear dimers are all chemically equivalent and as such should give a single resonance in their proton decoupled ^{31}P NMR spectra. The heteronuclear dimer, on the other hand, provides an interesting situation in which the trimethylphosphine ligands are in exactly the same ligand environment as those in the homonuclear dimers, but two of these ligands are bound to tungsten and the other two are bound to molybdenum. This will give two chemically inequivalent phosphorus atoms. The difference in the chemical shifts of these two phosphorus atoms will result only from the differences in their interactions with the metal to which they are bound. Also, by comparing

these two inequivalent phosphorus atoms in the heteronuclear dimer to the chemical shifts of the phosphorus atoms in the homonuclear dimers, it should be possible to determine if there are any anomalous properties apparent in the heteronuclear dimer.

Figure II-4 shows the proton decoupled ^{31}P NMR spectra of the three dimers. The phosphorus atoms in each of the homonuclear dimers appear as a sharp singlet. There is very little difference in the resonance frequencies of the ^{31}P signals for the dimolybdenum and ditungsten complexes which appear at -8.32 ppm and -7.31 ppm, respectively, relative to H_3PO_4. The small shift to lower field in going from the dimolybdenum complex to the ditungsten complex is actually contradictory to the expected higher field shift when descending down a group (29); however, this expected shift must be viewed skeptically since it is only a qualitative observation and is usually applied to organometallic complexes.

The W-P ($I = 1/2$ for ^{183}W; natural abundance = 14.3%) coupling in $W_2Cl_4(PMe_3)_4$ is not easily seen. Magnification of the regions on either side of the central ^{31}P resonance brings out weak resonances at ca. 119, 97 and 49 Hz on either side of the central resonance. There should be two resonances from W-P coupling, one from direct coupling between the phosphorus atom and the tungsten atom to which it is bound ($^1J(W,P)$), and the other resulting from coupling across the metal-metal bond to the other tungsten ($^3J(W,P)$). The value of 119 Hz is appropriate for $^1J(W,P)$ (29). No previous values are available for $^3J(W,P)$; however, from the heteronuclear dimer's spectra discussed below, 97 Hz is probably too high for

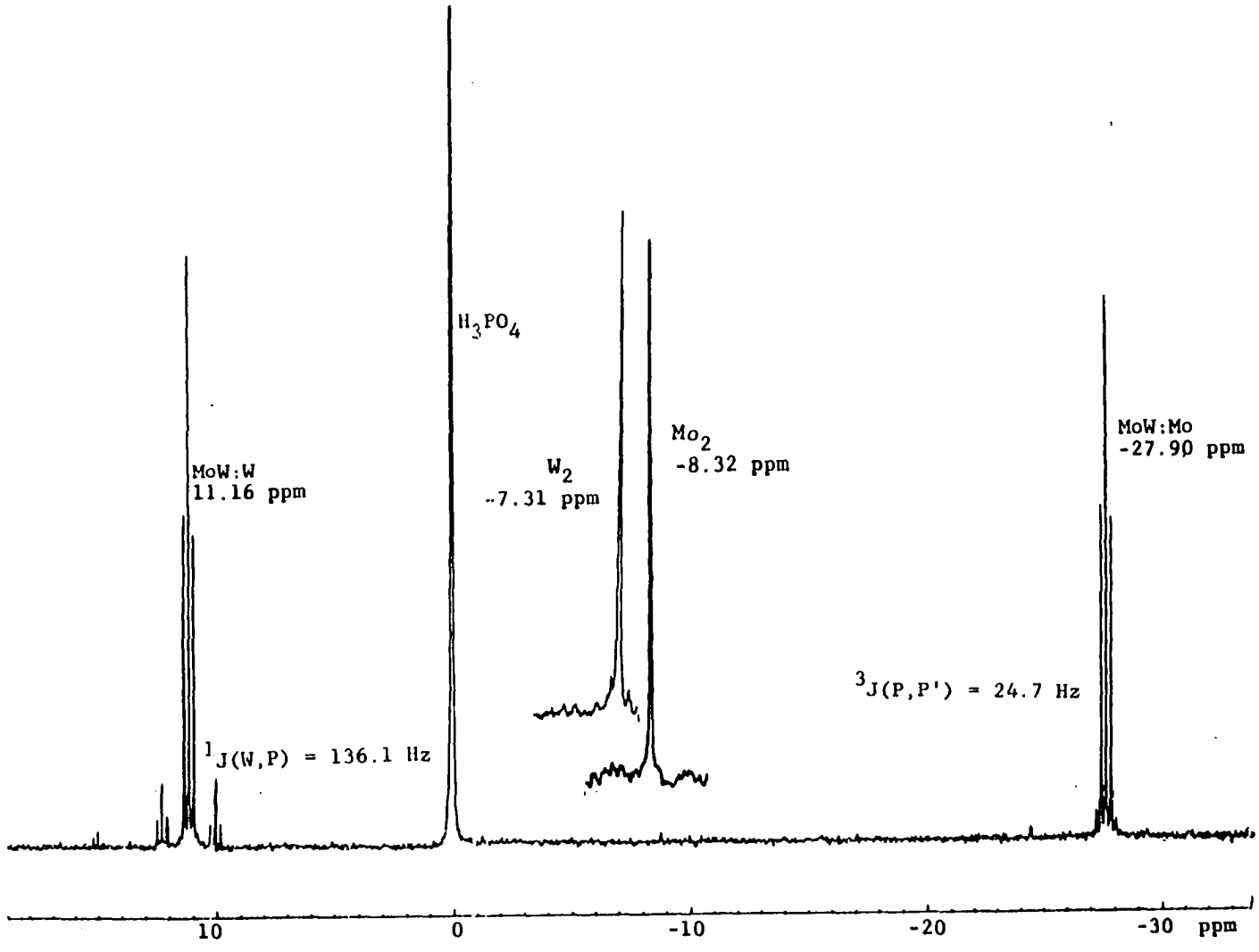

Figure II-4. Proton decoupled ^{31}P NMR of $M_2Cl_4(PMe_3)_4$ series

such a coupling process, whereas 49 Hz is reasonable. It is not possible, however, to unequivocally assign these weak resonances to particular W-P couplings.

The heteronuclear dimer's proton decoupled ^{31}P spectrum shows a number of interesting features. Each of the phosphorus resonances is split by the two chemically inequivalent phosphorus atoms on the other metal atom into a 1:2:1 triplet with $^{3}J(P,P') = 24.7$ Hz. This is a P-P coupling across the metal-metal quadruple bond. The only other example of P-P coupling through a quadruple bond is found for the phosphine substituted molybdenum dimer $Mo_2Me_4(PEt_3)_3(PMe_2Ph)$ in which the coupling constants are 21.5 and 21.2 Hz for $^{3}J(PEt_3,PEt_3^{i})$ and $^{3}J(PEt_3,PMe_2Ph)$, respectively (30). These values are quite comparable to the coupling constant obtained for the heteronuclear dimer and are in the range expected for a P-P coupling between two phosphorus atoms bound cis to a single metal atom (29). Coupling constants for trans phosphorus atoms on a single metal are much larger (> 100 Hz) than cis bound phosphorus atoms (29). One other example of P-P coupling through a metal-metal multiple bond is found in the literature. This is in the metal-metal double bonded dimer $Ta_2Cl_6(PMe_3)_4$ in which $^{3}J(P,P') = 2.46$ Hz (31).

The assignment of the resonance at 11.16 ppm to the trimethylphosphine bound to the tungsten atom is based on the observed W-P coupling of 136.1 Hz. The other resonance at -27.90 ppm is assigned to the trimethylphosphine bound to the molybdenum atom. No obvious $^{3}J(W,P)$ is seen for the phosphorus atoms bound to molybdenum, although small spikes are noticeable on both sides of the triplet. These spikes may be the

outside portions of the resonances resulting from this coupling. If this is the case, then the central resonance for $^{3}J(W,P)$ would be approximately under the two side resonances of the triplet, implying a $^{3}J(W,P)$ value of ca. 24 Hz.

Perhaps the most unexpected result from the ^{31}P NMR spectra of the heteronuclear dimer is the difference in the chemical shifts of the two resonances. These are dramatic shifts when compared to the two homonuclear resonances. This is an indication of some unusual bonding characteristics in the heteronuclear dimer. One possible explanation for this shift in the resonance frequencies is a charge separation in the heteronuclear dimer in which some electron density is transferred from tungsten to molybdenum. This suggestion is not too unreasonable considering that tungsten appears to have a stronger preference than molybdenum for the formation of complexes with the metal in the +3 oxidation state over complexes in the +2 oxidation state as exemplified by the difficulty encountered in the eventual syntheses of quadruply bonded tungsten dimers (32). An even better example of this preference is seen in the structure of $MoW(piv)_4I \cdot CH_3CN$ in which the iodine atom is bound to the tungsten atom giving the latter a formal oxidation state of +3 while molybdenum remains in the +2 oxidation state. This charge separation which would result in tungsten having a slightly higher effective charge and molybdenum having a slightly lower effective charge should affect the chemical shifts of the phosphorus atoms. Prediction of the expected chemical shift direction for such a charge separation is not

possible since ^{31}P resonance frequencies are determined for the most part by the paramagnetic contributions which are difficult to calculate (29).

From simple diamagnetic screening considerations, the observed chemical shifts are appropriate for this charge separation. The phosphorus atoms bound to tungsten should experience a deshielding and subsequent downfield shift due to the higher charge on the tungsten which would withdraw electron density from these phosphorus atoms. The opposite would be true for the phosphorous atoms on molybdenum. It is probably the case, however, that the observed chemical shifts are due to the paramagnetic contribution which are perturbed by this suggested charge separation and that these shifts only fortuitously fit with diamagnetic considerations.

X-ray Photoelectron Spectra

The results of the x-ray photoelectron spectra (XPS) are given in Table II-10. Binding energies are referenced to the C1s binding energy taken as 285.0 eV. The chlorine $2p_{3/2}$ and phosphorus 2s binding energies are essentially identical throughout the series. This is somewhat disappointing since it was expected that the ligands in $W_2Cl_4(PMe_3)_4$ would possess higher binding energies than those in $Mo_2Cl_4(PMe_3)_4$ because of the shorter W-L bonds. It is not possible to distinguish ligands bound to molybdenum from those on tungsten in the heteronuclear dimer.

The only unusual result is found for the $3d_{5/2}$ binding energies of molybdenum in the homonuclear and heteronuclear complexes. The lower binding energy of 228.7 eV for the molybdenum in $MoWCl_4(PMe_3)_4$ is an indication of a lower effective charge on molybdenum. This lower binding

Table II-10. X-ray photoelectron results for $M_2Cl_4(PMe_3)_4$[a]

	Binding Energies (eV)			
	Mo $3d_{5/2}$	W $4f_{7/2}$	Cl $2p_{3/2}$	P 2s
Mo_2	229.2(1.7/3.1)	---	198.7(1.6/1.6)	131.6(1.9)
MoW	228.7(1.7/3.2)	32.2(1.8/2.1)	198.7(1.6/1.6)	131.5(1.9)
W_2	---	32.2(1.7/2.1)	198.8(1.6/1.6)	131.6(2.0)

[a]FWHM (eV) for all orbitals and spin-orbit splittings (eV) for p, d and f orbitals are given in parentheses as (FWHM/SOS).

energy is in accord with the charge separation in the heteronuclear dimer discussed in the ^{31}P NMR section. The fact that no increase in W $4f_{7/2}$ binding energy is observed for the heteronuclear dimer may be a result of the larger number of total electrons in tungsten which will tend to reduce the shifts in core level binding energies with small changes in the effective charge on tungsten. From these results, it appears that the charge distribution between the metals and the ligands is the same in all the dimers. It is only for the heteronuclear dimer that an asymmetric charge distribution between the metals is present.

CONCLUSIONS

Before discussing the heteronuclear metal-metal quadruple bond, a presentation of some insights into the differences in the dimolybdenum and ditungsten quadruple bonds is needed. The W-W quadruple bond is considerably longer than the Mo-Mo quadruple bond in all compounds in which both molybdenum and tungsten examples are known (32). Since both molybdenum and tungsten have essentially equal atomic radii, the reason for the greater length of the ditungsten bond must be something other than atomic radii differences. Examination of the metal-ligand bonds in analogous molybdenum and tungsten compounds reveals that in all cases the tungsten-ligand bonds are shorter than, or about the same length as, corresponding molybdenum-ligand bonds (3,17,26,33,34). A possible explanation of these differences in metal-metal and metal-ligand bond lengths is the greater relativistic perturbations of tungsten. This relativistic pertubation is such that for s and p orbitals there is a decrease in the orbital radii and an increase in the ionization potentials (35,36). The d orbitals are affected mainly by the increased screening abilities of these relativistically contracted s and p orbitals, and therefore, have increased radii and decreased ionization potentials (35,36). Since metal-ligand bonds are mostly of s and p character, tungsten with more extensively contracted s and p orbitals, possesses shorter metal-ligand bonds than does molybdenum. Similarly, the relativistic extension of tungsten's 5d orbitals enables them to form more effective metal-metal bonds at larger metal-metal separations. This is exemplified by the $M_2Cl_9^{3-}$ series for Cr, Mo and W (37). In $Cr_2Cl_9^{3-}$,

d(Cr-Cr) = 3.12 Å (32), indicating that the contracted 3d orbitals of chromium are unable to form effective metal-metal bonds. The dimolybdenum anion with d(Mo-Mo) = 2.65 Å (32) is interpreted as possessing one σ bond, but no π bonds. Finally, in the ditungsten anion the W-W bond length is 2.41 Å (32), indicative of a multiple metal-metal bond. The W-W bonding consists of a σ bond and two π bonds. This π bonding occurs in the tungsten anion, but not in the molybdenum anion, because of the greater relativistic extension of the W 5d orbitals compared to the Mo 4d orbitals.

These relativistic effects are the reason for tungsten forming compounds of higher oxidation states, in particular W(III) complexes. The reduced ionization potential of the 5d orbitals and increased strength of the W-L bond, resulting from the contracted 6s and 6p orbitals, drive tungsten to form complexes with tungsten in higher oxidation state and with more ligands bound to tungsten.

This concept can be applied to the metal-metal quadruple bonds. The greater extension of the W 5d orbitals enables tungsten to achieve good d orbital overlap at metal-metal separations greater than can be achieved by similar molybdenum compounds. This allows the tungsten complex to relieve some of the ligand-ligand repulsion which occurs between eclipsed ligands across the metal bond. The molybdenum dimers must force these eclipsed ligands closer together to achieve effective d orbital overlap. The equilibrium metal-metal distances are determined by both d orbital overlap and ligand-ligand repulsions with tungsten dimers having longer equilibrium metal-metal distances for the reasons discussed above.

One result of tungsten's longer metal-metal quadruple bond distances is that the δ interaction is greatly reduced. The fact that $W_2Cl_4(PMe_3)_4$ has the lowest energy $\delta \rightarrow \delta^*$ transition is direct evidence of this decreased δ interaction. An indication of the strength of the δ bond in quadruply bonded tungsten dimers is found by comparison of the two isomers of $W_2Cl_4(dppe)_2$ (dppe = bis(diphenylphosphino)ethane (38)). In the green isomer of $W_2Cl_4(dppe)_2$ with d(W-W) = 2.280(1) Å, the bis(diphenylphosphino)ethane ligands are chelating to one tungsten atom each, and all the ligands are still in an eclipsed configuration across the metal-metal bond (38). On the other hand, the brown isomer with d(W-W) = 2.314(1) Å, possesses bridging ligands (38). These bridging ligands force all the ligands to adopt a staggered configuration across the metal-metal bond as observed for $Re_2Cl_4(dppe)_2$, which possesses only a triple bond (39). The staggered configuration eliminates the possibility of a δ bond. The difference of 0.034 Å between the W-W distances in these two isomers can be taken as a reasonable approximation of the δ contribution to the bond length in tungsten dimers. This difference is in accord with that found from comparing the W-W triple bonds with an average length of ca. 2.29 Å in Chisholm's W(III) unbridged dimers (34) and the W-W quadruple bond of 2.262(1) Å in $W_2Cl_4(PMe_3)_4$ (17). The contribution that the δ bond makes to the Mo-Mo bond lengths in the molybdenum quadruply bonded dimers can be approximated by reference to Chisholm's Mo(III) unbridged, triply bonded dimers, where the average Mo-Mo separation is ca. 2.22 Å (34) compared to $Mo_2Cl_4(PMe_3)_4$ with d(Mo-Mo) = 2.130(1) (17). The contribution to the molybdenum quadruple bond length is ca. 0.09 to 0.10 Å. The δ bond in the

molybdenum dimers is apparently a significant factor in the Mo-Mo bond; however, in the tungsten dimers this interaction is not as important nor as strong as in the molybdenum dimers and can be lost if ligand strain is great enough.

These approximate contributions made to the metal-metal bonds by the δ interaction apply only to unbridged dimers. The δ interaction is expected to be stronger for both ditungsten and dimolybdenum complexes when bridging ligands similar to the carboxylate ligands are present. These ligands hold the metals close together and do not exhibit large ligand-ligand repulsions across the metal bond.

The structure of $MoWCl_4(PMe_3)_4$ implies that the heteronuclear quadruple bond can be viewed as an approximate average of the homonuclear quadruple bonds, although having bond characteristics nearer the W-W bond. The heteronuclear dimer's uv-visible spectrum is consistent with this since the $\delta \rightarrow \delta^*$ transition falls at an energy between the two homonuclear transitions and slightly closer to the W-W transition.

The δ interaction in the heteronuclear dimer is expected to be an average of those in the homonuclear dimers. There are no good examples of unbridged heteronuclear dimers which possess a triple bond; therefore, it is difficult to approximate the contribution of the δ interaction to the heteronuclear quadruple bond. Attempting to compare $MoW(piv)_4$ and $MoW(piv)_4I{\cdot}CH_3CN$ with heteronuclear bonds of 2.080(1) Å (1) and 2.194(2) Å (12), respectively, is not a good example because of both the bridging pivalate ligands and the anomalously short Mo-W bond in $MoW(piv)_4$. The only reasonable compound for comparison to $MoWCl_4(PMe_3)_4$

is the heteronuclear tetramer $Mo_2W_2Cl_8(PMe_3)_4$ (40). In this complex, there are bonds assigned as single and triple bonds of lengths 2.842(1) Å and 2.276(1) Å, respectively (40). This triple bond distance when compared to the quadruple bond length of 2.219(1) Å in $MoWCl_4(PMe_3)_4$ implies that the δ interaction shortens the Mo-W bond by 0.057 Å. This value is reasonable when compared to the δ contributions found for the homonuclear dimers. The use of the tetramer's triple bond for obtaining this value must be viewed with caution since the ligand arrangement in this tetramer allows for some residual δ bonding to remain in this bond, although this residual bonding is expected to be small.

Even though there appear to be no unusual features in the structure of $MoWCl_4(PMe_3)_4$, certain anomalies are found in the ^{31}P NMR and XPS spectra. These have been tentatively interpreted as resulting from a charge separation in the complex. The drive for tungsten to achieve a slightly higher effective charge can be traced back to the relativistic effects discussed above. The relativistic increase of the ionization potential of the W 5d orbitals may make tungsten less electronegative than molybdenum, thus providing a driving force for this charge transfer. Calculations of the ionization potentials for the gaseous ions of Mo(II) and W(II) give differing results depending on the methods used; however, they do give a W(II) ionization less than the Mo(II) ionization by ca. 1.0 eV (41).

The Mo-W distance in the heteronuclear dimer $MoWCl_4(PMe_3)_4$ does not give any obvious explanation for the unusually short Mo-W bond in $MoW(piv)_4$ as was initially hoped. It may be, however, that the charge

separation, as proposed for $MoWCl_4(PMe_3)_4$ is the reason for this short Mo-W distance. It has been known for some time that the bond energy of a molecule composed of two elements with differing electronegativities is greater than either of the two homonuclear analogs. For example, the bond energy of ClF is 61 kcal/mole, which is greater than the bond energies of Cl_2 and F_2 with respective values of 57.9 and 36.6 kcal/mole (42). An explanation forwarded for this phenomenon is that such bonds between atoms of differing electronegativity are stabilized by ionic resonance (42), the wavefunction for the system being of the form:

$$\psi_{AB} = a\,\psi_{A-B} + b\,\psi_{A^+B^-} + c\,\psi_{A^-B^+}$$

The ionic terms $\psi_{A^+B^-}$ and $\psi_{A^-B^+}$ stabilize the system beyond that expected solely from the covalent contribution ψ_{A-B}. The degree of ionic stability will depend upon what contribution such ionic terms make to the total description of the system.

For the metal-metal homonuclear bonds the ionic contributions will be minimal. The heteronuclear metal-metal bond will have a larger ionic contribution because of the small difference in the effective electronegativities of Mo(II) and W(II). The fact that the experimental evidence points toward the presence of a charge separation in the heteronuclear bond provides support that such a stabilization may occur. The wavefunction for the Mo-W quadruple bond can be described by:

$$\psi_{MoW} = a\,\psi_{Mo-W} + b\,\psi_{Mo^-W^+} + c\,\psi_{Mo^+W^-}$$

The covalent term ψ_{Mo-W} will not be too different from that in the homonuclear dimers. The second term will contribute a significant amount to the Mo-W bond if the charge separation is actually present in the heteronuclear dimers. The last term should contribute very little to the bonding. This ionic resonance could be the reason for the anomalously short Mo-W bond in $MoW(piv)_4$. The additional stability imparted to the Mo-W bond by this ionic resonance should shorten the bond. It may also be the reason for $MoW(mhp)_4$ having a Mo-W distance below the average of the homonuclear bond lengths. The Mo-W bond in $MoW(mhp)_4$ may be prevented from decreasing further by the greater number of electrons in tungsten's core (32). At the separations reached with the mhp ligand, these core-core repulsions may become significant and limit the approach of the two metals. For $MoWCl_4(PMe_3)_4$, similar ionic resonance factors should be in effect, however, the Mo-W distance appears to be influenced more in this case by the equilibrium reached between the ligand-ligand repulsions and the metal-metal d orbital overlap.

Theoretical calculations have been performed on $Mo_2Cl_4(PMe_3)_4$ and $W_2Cl_4(PMe_3)_4$ (43). The calculated molecular orbital energies agree reasonably well with the photoelectron spectra. The results for the metal-metal and metal-ligand molecular orbitals are essentially those expected from the arguments presented here. One important result from the calculations is that relativistic corrections have a much greater effect on the character and energy of the molecular orbitals for $W_2Cl_4(PMe_3)_4$ than for $Mo_2Cl_4(PMe_3)_4$ as expected. The calculations do not, however, give any additional insight into the nature of the heteronuclear bond.

The synthesis and characterization of $MoWCl_4(PMe_3)_4$ has not answered the question of why anomalies are seen in certain of the heteronuclear dimers. It has, however, led to some of the tentative explanations made above. It is important to point out that these explanations are only speculation based on examination of molecular structures, spectral data and a few theoretical calculations. It is apparent that a good description of the Mo-W quadruple bond will require consideration of a number of factors. In particular, relativistic effects must be invoked, and these may in fact be the underlying reason for the changes in bonding from Mo-Mo to Mo-W to W-W.

REFERENCES CITED

1. Katovic, V.; McCarley, R. E. J. Am. Chem. Soc. 1978, 100 5586.

2. Cotton, F. A.; Extine, M.; Gage, L. D. Inorg. Chem. 1978, 17, 172.

3. Sattelberger, A. P.; McLaughlin, K. W. J. Am. Chem. Soc. 1981, 103, 2880.

4. Brencic, J. V.; Cotton, F. A. Inorg. Chem. 1970, 9, 351.

5. San Filippo, J.; Sniadoch, H. J.; Grayson, R. L. Inorg. Chem. 1974, 13, 2121.

6. Katovic, V.; McCarley, R. E. Inorg. Chem. 1978, 17, 1268.

7. Katovic, V.; McCarley, R. E., Iowa State University, Ames, Iowa, unpublished results.

8. Klofta, T.; Carlin, R. T.; McCarley, R. E., Iowa State University, Ames,Iowa, to be submitted for publication.

9. Carlin, R. T. Ph.D. Dissertation, Iowa State University, Ames, Iowa, 1982; Section I.

10. Luly, M. H. "APES, A Fortran Program to Analyze Photoelectron Spectra", 1979, U. S. DOE Report IS-4694.

11. McCarley, R. E.; Templeton, J. L.; Colburn, T. J.; Katovic, V.; Hoxmeier, R. J. Adv. Chem. Ser. 1976, 150, 318.

12. Katovic, V.; Templeton, J. L.; Hoxmeier, R. J.; McCarley, R. E. J. Am. Chem. Soc. 1975, 97, 5300.

13. Schaefer, M. A. Ph.D. Dissertation, Iowa State University, Ames, Iowa, 1971.

14. Sharp, P.; Schrock, R. R. J. Am. Chem. Soc. 1980, 102, 1430.

15. Rohrbaugh, W. J.; Jacobson, R. A. Inorg. Chem. 1974, 13, 2535.

16. Jacobson, R. A. J. Appl. Crystallogr. 1976, 9, 115.

17. Cotton, F. A.; Extine, M. W.; Felthouse, T. R.; Kolthammer, B.W.S.; Lay, D. G. J. Am. Chem. Soc. 1981, 103, 4040.

18. Lawton, S. L.; Jacobson, R. A. Inorg. Chem. 1968, 13, 2124.

19. Karcher, B. A. Ph.D. Dissertation, Iowa State University, Ames, Iowa, 1981.

20. Hanson, H. P.; Herman, F.; Lea, J. D.; Skillman, S. Acta Crystallogr. 1960, 17, 1040.

21. Templeton, D. H. in "International Tables for X-ray Crystallography , 1st ed.; Macgillary, C. H. and Rieck, G. D., Eds.; Kynock Press: Birmingham, England, 1962; Vol. III, page 215.

22. This structural determination yielded final residuals of R = 0.066 and R_w = 0.088. The data set was deemed to be of poor quality due to instrumentation problems during data collection. The positional parameters of all nonhydrogen atoms were essentially those obtained for the structure refinement discussed in the text. A redetermination was performed to obtain smaller standard deviations.

23. Powell, D. R.; Jacobson, R. A. "FOUR: A General Crystallographic Fourier Program", 1980, U. S. DOE Report IS-4737.

24. Lapp, R. L.; Jacobson, R. A. "ALLS, A Generalized Crystallographic Least Squares Program", 1979, U. S. DOE Report IS-4737.

25. Bursten, B. E.; Cotton, F. A.; Cowley, A. H.; Hanson, B. E.; Lattman, M.; Stanley, G. G. J. Am. Chem. Soc. 1979, 101, 6244.

26. Cotton, F. A.; Hanson, B. E. Inorg. Chem. 1978, 17, 3237.

27. Maslowsky, E., Jr. "Vibrational Spectra of Organometallic Compounds", John Wiley and Sons: New York, 1977; page 8.

28. San Filippo, J., Jr.; Sniadoch, H. J. Inorg. Chem. 1973, 12, 2326.

29. Pregosin, S.; Kunz, R. W. "^{31}P and ^{13}C NMR of Transition Metal Phosphine Complexes", Diehl, P., Fluck, E. and Kosfeld, R., Eds.; Springer-Verlag: New York, 1979.

30. Girolami, G. S.; Mainz, V. V.; Andersen, R. A. J. Am. Chem. Soc. 1981, 103, 3953.

31. Sattelburger, A. P.; Wilson, R. B., Jr.; Huffman, J. C. Inorg. Chem. 1982, 21, 2392.

32. Cotton, F. A.; Walton, R. A. "Multiple Bonds Between Metal Atoms", John Wiley and Sons: New York, 1982; and references cited therein.

33. Cotton, F. A.; Norman, J. G. J. Coord. Chem. 1971, 1, 161.

34. Chisholm, M. H. Transition Met. Chem. 1978, 3, 321 and references therein.

35. Pitzer, K. S. Accts. Chem. Res. 1979, 12, 271.

36. Pyykko, P.; Desclaux, J. P. Accts. Chem. Res. 1979, 12, 276.

37. Summerville, R. H.; Hoffman, R. J. J. Amer. Chem. Soc. 1979, 101, 3821.

38. Cotton, F. A.; Felthouse, T. R.; Lay, D. G. J. Am. Chem. Soc. 1980, 102, 1431.

39. Cotton, F. A.; Stanley, G. G.; Walton, R. A. Inorg. Chem. 1978, 17, 2099.

40. Carlin, R. T. Ph.D. Dissertation, Iowa State University, Ames, Iowa, 1982, Section I.

41. Fraga, S.; Karwowski, J.; Sexena, K.M.S. "Handbook of Atomic Data", Elsevier Scientific Publishing Company: New York, 1976; pages 263 and 265.

42. Huheey, J. E. "Inorganic Chemistry: Principles of Structure and Reactivity", Harper and Row: New York, 1972; page 155.

43. Cotton, F. A.; Hubbard,J. L.; Lichtenburger, D. L.; Shim, I. J. Am. Chem. Soc. 1982, 104, 679.

SECTION III. SYNTHESIS OF MIXED-METAL (Mo-W) RECTANGULAR CLUSTERS. CRYSTAL STRUCTURE OF $Mo_2W_2Cl_8(PMe_3)_4$ and ^{31}P NMR STUDY OF $Mo_2W_2Cl_8(PBu^n_3)_4$

INTRODUCTION

The recent synthesis of the quadruply bonded dimer $MoWCl_4(PMe_3)_4$ (1) sparked interest in the possibility for the preparation of the tetramer $Mo_2W_2Cl_8(PR_3)_4$. The homonuclear analogs, $Mo_4Cl_8(PR_3)_4$ (2,3,4) and $W_4Cl_8(PR_3)_4$ (3,4) have both been prepared. These homonuclear tetramers have a rectangular framework of metal atoms with two unbridged, short sides and two long sides bridged by two chlorines or bromines. Each metal has a distorted square planar coordination. The bond distances in the rectangle suggests that the short, unbridged edges are M-M triple bonds and the long, halide-bridged edges are M-M single bonds.

The formation of these tetramers is unique because it can be viewed as a cycloaddition of two dimers (2). This cycloaddition involves loss of the δ component of the quadruple bond in each dimer and formation of two single bonds which join the dimers together. The reaction is believed to be initiated by loss of phosphine ligand with subsequent formation of the metal-metal single bonds (2).

Using similar techniques as those used to prepare the homonuclear tetramers (2,4), it has been possible to synthesize $Mo_2W_2Cl_8(PMe_3)_4$ and $Mo_2W_2Cl_8(PBu_3)_4$. The characterization of these mixed-metal tetramers has been accomplished using ^{31}P NMR spectra, uv-visible spectra and an x-ray single-crystal study.

EXPERIMENTAL

Materials

All reaction products were handled in Schlenk vessels under a nitrogen atmosphere or under vacuum.

Tetrahydrofuran and cyclohexane were dried and handled as discussed earlier (1). Methanol was dried over sodium methoxide and vacuum distilled onto Molecular Sieves (4Å) for storage. Trimethylphosphine and tri-n-butylphosphine were obtained from Alpha Products and Strem Chemicals, respectively, and were used without further purification. Chlorotrimethylsilane was obtained from Fisher Scientific Company and was used without further purification. Aluminum trichloride obtained from Fisher Scientific Company was purified by sublimation.

Physical Measurements

Infrared and uv-visible spectra were obtained as described earlier (5). Samples for ^{31}P NMR study were dissolved in $CDCl_3$ and sealed in vacuo in 10 mm NMR tubes along with a capillary containing a H_3PO_4 standard. The ^{31}P NMR spectra were obtained using a Bruker WM-300 Spectrometer. X-ray powder diffraction data were obtained using an Enraf Nonius Delft triple focusing Guinier x-ray powder diffraction camera with Cu K_{α_1} radiation (λ = 1.54056 Å).

Syntheses

$MoW(O_2CCMe_3)_4$

This extremely air-sensitive compound was prepared in limited quantities by a muti-step procedure devised by V. Katovic *et al.* (6).

$Mo_2W_2Cl_8(PMe_3)_4$)

Using a N_2 dry box, $MoW(O_2CCMe_3)_4$ (0.22 g, 0.32 mmol) and $AlCl_3$ (0.2 g, 1.5 mmol) were introduced into a 100 mL reaction flask. Trimethylphosphine (0.06 mL, 0.6 mmol) and 30 mL of THF were then vacuum distilled into the flask. The reaction mixture was stirred at reflux for one day. Upon filtration, a blue-green filtrate (indicating a significant amount of dimer formation) and a small quantity of a yellow-green solid were obtained. This yellow-green solid was extracted with the mother liquor under reduced pressure. The mother liquor was refiltered giving insoluble yellow-green crystals which were suitable for x-ray single-crystal analysis.

$Mo_2W_2Cl_8(PBu^n_3)_4$

$MoW(O_2CCMe_3)_4$ (0.5 g, 0.73 mmol), $AlCl_3$ (0.39 g, 2.9 mmol) and PBu_3 (0.35 mL, 1.4 mmol) were refluxed under nitrogen in 20 mL of THF for *ca.* one day. The dark-green solution was filtered; however, no solid was obtained. The solvent was removed *in vacuo* giving a green tar to which was added 15 mL of methanol. Filtering of the methanol solution gave a dark-green filtrate and a yellow-green solid. The methanol solution was discarded. The yellow-green solid was dried *in vacuo* and then extracted

with cyclohexane to obtain crystals. Indexing two of these crystals confirmed them to be isomorphous with the corresponding PBu^n_3 derivatives of the molybdenum (7) and tungsten (4) homonuclear tetramers (8). The crystals, however, exhibited weak diffracting characteristics, and so no single-crystal x-ray data were collected.

$Mo_4Cl_8(PMe_3)_4$

$Mo_2(OCCH_3)_4$ (1.0 g, 2.3 mmol), $AlCl_3$ (1.25 g, 9.4 mmol) and PMe_3 (5.2 mmol obtained by heating 1.13 g $AgI \cdot PMe_3$) were stirred under nitrogen in 30 mL THF for 18 hours. The reaction mixture was filtered, and the resulting light-green solid was washed with deoxygenated methanol and dried in vacuo. Comparison of x-ray powder patterns of this product and of the mixed-metal PMe_3 tetramer confirmed them to be isomorphous.

Collection and Treatment of X-ray Data

The crystal selected was irregularly shaped with dimensions 0.2 x 0.14 x 0.2 mm. It was mounted in a 0.3 mm glass capillary and placed on a 4-circle diffractometer designed at the Ames Laboratory (9). Initial indexing was performed by inserting 11 reflections obtained from four ω-oscillation photographs into the automatic indexing program ALICE (10). The unit cell was determined to be tetragonal.

Final lattice parameters were obtained from least-squares refinement of 9 reflections with $2\theta > 30°$. The lattice parameters obtained were $a = 12.6443(8)$ Å, $c = 11.2854(9)$ Å, $V = 1804.3(2)$ $Å^3$ and $Z = 2$.

Two full octants, hkl and $\bar{h}\bar{k}l$, were collected with periodic monitoring of three standard reflections. A total of 3730 reflections

were collected. These were corrected for Lorentz and polarization effects and standard deviations were calculated (11). Reflections with $I > 3\sigma_I$ were retained giving a total of 2888 reflections which were subsequently averaged using the centrictetragonal relationships $hk\ell = kh\ell = \bar{h}\bar{k}\ell = \bar{k}\bar{h}\ell$ to 844 independent reflections. An empirical absorption correction ($\mu = 81.4\ cm^{-1}$) was applied using a ϕ-scan technique at $\chi = 90°$ (12).

Structure Solution and Refinement

Systematic extinctions for h00, h = 2n + 1; 0k0, k = 2n + 1; and 001, l = 2n + 1, uniquely determined the space group as the accentric group $P4_22_12$. All refinements were carried out using either block-matrix or full-matrix least-squares procedures minimizing the function $\Sigma\omega(|F_o|-|F_c|)^2$, where $\omega = 1/\sigma_F 2$ (13). Scattering factors for all non-metals were obtained from Hanson et al. (14).

A sharpened Patterson map (15) revealed the position of the one independent metal atom. This metal atom was input using a scattering factor table calculated by averaging the molybdenum and tungsten tables of Hanson et al. (14). The real and imaginary parts of anomalous dispersion were calculated also by averaging together the appropriate molybdenum and tungsten tables (16). Refining on only the metal atom gave residuals of $R = \Sigma\left||F_o|-|F_c|\right|/\Sigma|F_o| = 0.269$, and $Rw = [\Sigma\omega(|F_o|-|F_c|)^2/\omega|F_o|^2]^{1/2} = 2.359$. Using a combination of least-squares refinements (13) and Fourier synthesis (15) techniques, all non-hydrogen atoms were located and refined to residuals of R = 0.045 and Rw = 0.078.

At this point an accentric data set was generated in which only the relation hkl = $\bar{h}\bar{k}$l was used in averaging the data (in centric tetragonal systems: hkl = k$\bar{h}$l = $\bar{h}\bar{k}$l = $\bar{k}\bar{h}$l). This accentric data set consisted of 1522 independent reflections. With this data set, refinements using xyz and -x,-y,-z coordinates gave respective residuals of R = 0.0475 and Rw = 0.0764, and R = 0.0470 and Rw = 0.0757. Because of the very small differences in the residuals for the left and right handed models, refinement using accentric data was felt to be unwarranted, and so the centric data were used for the remainder of the refinement.

From a difference Fourier synthesis (15), it was possible to locate most of the hydrogens on the methyl carbons; however, after assigning them fixed isotropic B values of 7.0 $Å^2$, attempts to refine the positional parameters of these methyl hydrogens were unsuccessful. Therefore, idealized hydrogen positions were calculated near the observed positions setting d(C-H) = 0.95 Å and H-C-H = 109.47°. These positional parameters as well as the isotropic B values of 7.0 $Å^2$ were held constant throughout the remainder of the refinement. Including these fixed hydrogens in the refinement gave lower residuals of R = 0.040 and Rw = 0.047, and lowered the residuals of the low angle data by ca. 1 to 2%.

At this point, another difference Fourier synthesis revealed the presence of a diffuse and highly disordered THF molecule. Summation over the positive residual electron density showed there to be ca. one THF molecule per tetramer unit. Using three carbon atoms (C1s, C2s, C3s) in general positions with multipliers of 0.25, 0.25 and 0.5 a reasonable fit to the THF electron density was obtained. Inclusion of this THF molecule

in the refinement gave R = 0.035 and Rw = 0.045 and dramatically improved the low angle data (sin $\theta/< 0.2$) by several percent.

A secondary extinction correction was applied using an option in the least-squares program which enables refinement on a secondary extinction factor to be performed (13). A secondary extinction factor of 0.00020(5) was obtained. Final residuals after full-matrix least-squares refinement were R = 0.034 and Rw = 0.045. The final difference Fourier synthesis was clean with the largest peak of 0.8 $e^-/Å^3$ found between intracluster metal atoms. Peaks of ca. 0.5 $e^-/Å^3$ were seen in the region of the THF molecule.

A check of the metal character was performed by allowing the metal multiplier to vary. Refinement converged with a metal multiplier of 0.964(13), a value within 3σ of full occupancy indicating essentially a 50:50 mixture of molybdenum and tungsten in the tetramer as expected. Therefore, the metal multiplier was held at 1.0 for the final refinement discussed above.

Positional and thermal parameters are given in Tables III-1, III-2 and III-3, and bond distances and angles are provided in Table III-4. ORTEP drawings of the molecule and of the unit cell are shown in Figures III-1 and III-2, respectively.

Table III-1. Positional parameters for $Mo_2W_2Cl_8(PMe_3)_4 \cdot THF$ nonhydrogen atoms[a]

Atom	X	Y	Z
MOW	0.08243(5)	0.07636(5)	0.10069(5)
CLt	0.1092(3)	0.2489(3)	0.1922(3)
CLb	-0.1037(3)	0.1084(3)	0.1453(3)
P	0.2806(3)	0.0669(3)	0.1243(3)
C1	0.361(1)	0.181(1)	0.085(1)
C2	0.349(1)	-0.043(1)	0.051(2)
C3	0.314(2)	0.047(2)	0.284(2)
C1S	0.434(3)	0.504(4)	0.081(3)
C2S	0.530(6)	0.412(5)	0.009(9)
C3S	0.545(5)	0.583(5)	0.035(6)

[a]Estimated standard deviations are given in parentheses for the last significant figures.

Table III-2. Thermal parameters for $Mo_2W_2Cl_8(PMe_3)_4 \cdot THF$ nonhydrogen atoms[a,b]

Atom	B_{11}	B_{22}	B_{33}	B_{12}	B_{13}	B_{23}
MOW	2.732(36)	2.670(35)	2.983(31)	-0.237(19)	-0.026(29)	-0.217(28)
CLt	4.73(19)	3.36(16)	5.10(16)	-0.93(14)	-0.11(14)	-1.41(15)
CLb	3.07(16)	3.18(16)	4.47(13)	-0.39(9)	0.66(14)	-1.10(13)
P	2.81(16)	3.89(18)	5.14(18)	-0.26(13)	00.79(14)	-0.07(16)
C1	3.3(6)	4.0(7)	7.5(10)	-1.1(5)	-0.9(7)	1.7(7)
C2	2.7(6)	5.9(9)	10.8(13)	0.2(6)	-0.3(7)	-0.3(9)
C3	7.1(11)	9.3(13)	5.9(10)	-1.0(9)	-3.1(8)	0.2(9)
	B[c]					
C1S	7.1(9)					
C2S	6.7(17)					
C3S	5.3(16)					

[a]Estimated standard deviations are given in parentheses for the last significant figures.

[b]B_{ij} are defined by $\exp[-1/4(B_{11}h^2a^{*2} + B_{22}j^2b^{*2}...2B_{23}k\ell b^*c^*)]$.

[c]Isotropic temperature factors, B, are given in $Å^2$.

Table III-3. Calculated positional parameters for hydrogen atoms in $Mo_2W_2Cl_8(PMe_3)_4$ molecule[a]

Atom	X	Y	Z
H11	0.36399	0.19662	0.00486
H12	0.43054	0.17311	0.11646
H13	0.33050	0.24369	0.12535
H21	0.36413	-0.09504	0.11331
H22	0.41311	-0.01810	0.02075
H23	0.30549	-0.07226	-0.00518
H31	0.30395	-0.02300	0.30822
H32	0.26353	0.09077	0.33058
H33	0.38154	0.07135	0.29996

[a]All hydrogen atoms are assigned isotropic thermal parameters of 7.0 $Å^2$.

Table III-4. Bond distances (Å) and angles (Deg) for $Mo_2W_2Cl_8(PMe_3)_4$ molecule[a]

Distances	
MoW-MoW	2.275(1)
MoW-MoW	2.842(1)
MoW-Clt	2.437(4)
MoW-Clb	2.405(4)
MoW-Clb	2.440(4)
MoW-P	2.523(4)
P-C1	1.82(1)
P-C2	1.83(2)
P-C3	1.86(2)

Angles			
MoW-MoW-MoW	89.90(0)	MoW-P-C1	119.3(5)
MoW-MoW-Clt	135.24(10)[b]	MoW-P-C2	117.0(5)
MoW-MoW-Clt	113.45(9)	MoW-P-C3	109.5(6)
MoW-MoW-Clb	53.52(9)[b]	C1-P-C2	103.4(7)
MoW-MoW-Clb	54.67(9)[b]	C1-P-C3	102.2(8)
MoW-MoW-Clb	99.66(8)	C2-P-C3	103.2(9)
MoW-MoW-Clb	99.66(8)		
MoW-MoW-Clb	104.21(8)		
MoW-MoW-P	98.09(9)		
MoW-MoW-P	134.13(10)[b]		
Clt-MoW-Clb	84.14(13)		
Clt-MoW-Clb	139.93(12)		
Clb-MoW-Clb	103.05(12)		
Clt-MoW-P	81.94(13)		
Clb-MoW-P	79.68(12)		
Clb-MoW-P	160.72(12)		
MoW-Clb-MoW	71.81(10)		

[a]Estimated standard deviations are given in parentheses for the last significant figures.

[b]Angles for which MoW-MoW vector is the long MoW-MoW separation in the tetramer.

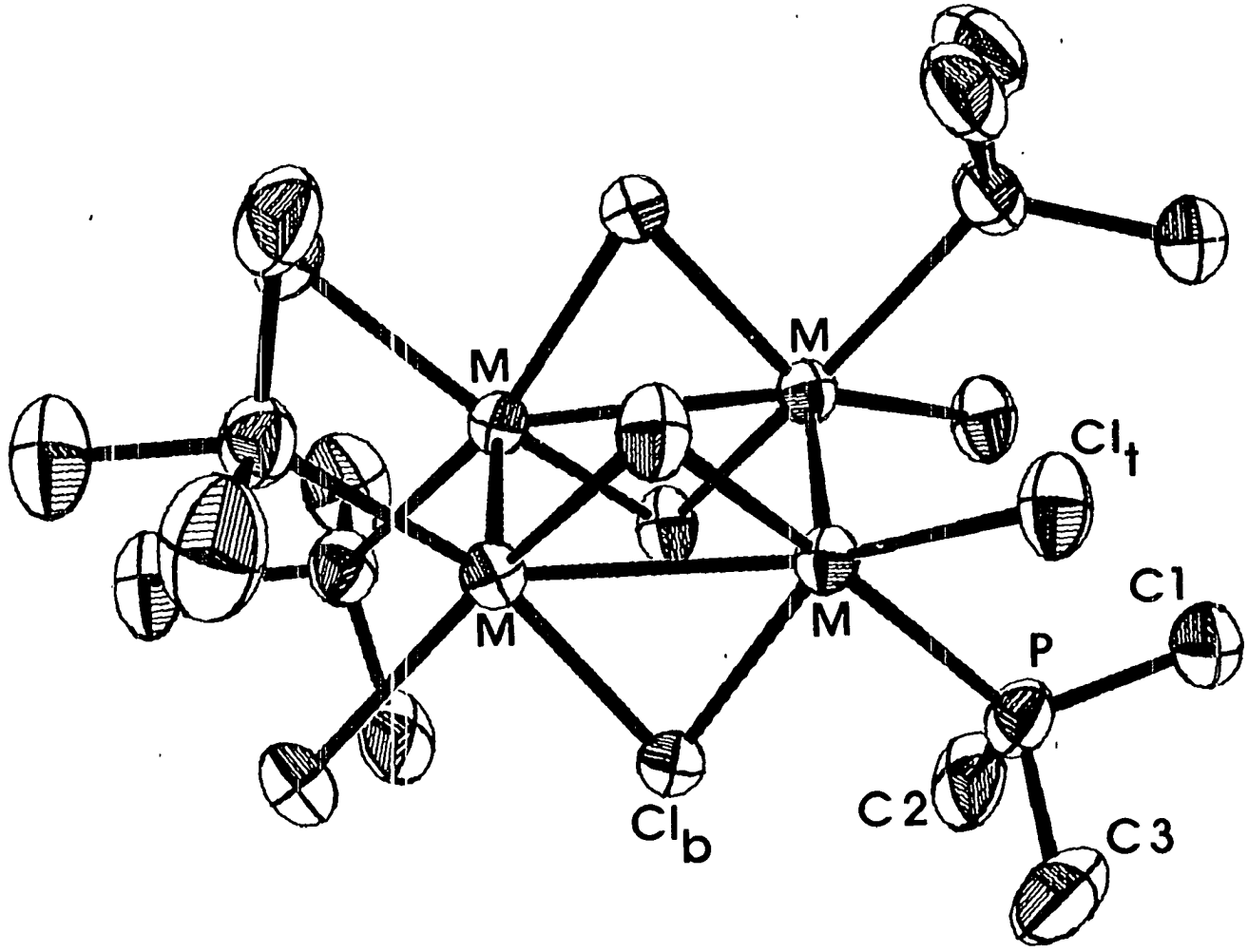

Figure III-1. ORTEP drawing of $Mo_2W_2Cl_8(PMe_3)_4$ molecule

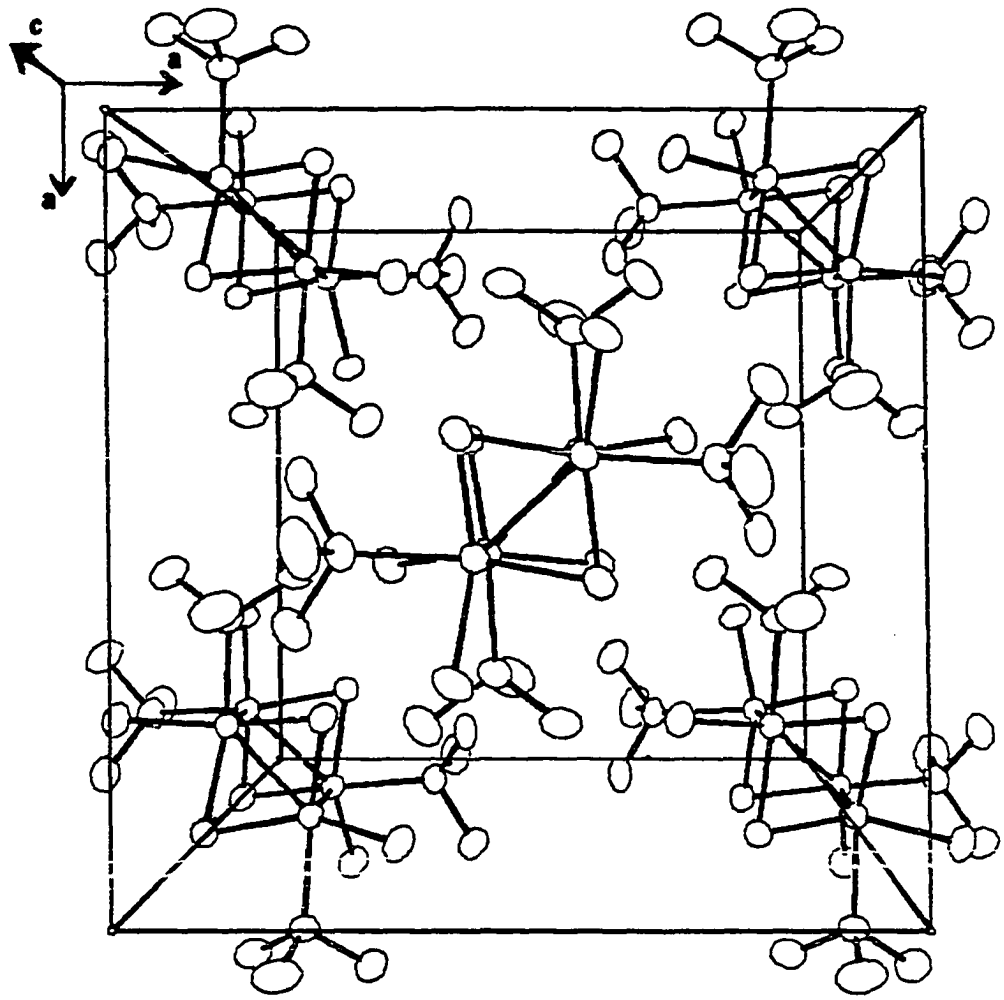

Figure III-2. Unit cell of $Mo_2W_2Cl_8(PMe_3)_4$ viewed down c-axis

RESULTS AND DISCUSSION

Crystal Structure

The basic structure of the mixed-metal tetramer is essentially that expected from examination of the other homonuclear tetramers (2,3,4). The metal atoms form a rectangle with two long M-M bonds, 2.842(1) Å, and two short M-M bonds, 2.275(1) Å. As has been discussed for the homonuclear cases, the heteronuclear rectangle can be viewed as being formed by the cycloaddition of two quadruply bonded dimers of formulation $MoWCl_4(PR_3)_4$ (1). The long M-M bond is formed by σ overlaps of the dxy orbitals on the metal atoms with subsequent loss of the δ interactions in the dimer units, reducing the quadruple bonds to formal triple bonds. In Table III-5, are listed the important parameters for comparison of the heteronuclear tetramer to the homonuclear tetramers (4,7). The PBu^n_3 homonuclear tetramers were chosen because the ligand arrangement about these tetramers is of D_{2d} symmetry, the same as in the mixed-metal tetramer.

An examination of the M-L bond lengths for the series of tetramers in Table III-5 reveals three apparent anomalies in the mixed-metal PMe_3 tetramer: 1) short M-P bond; 2) long M-Clt bond; 3) long M-Clb bond.

The M-P bond of 2.520(4) Å is actually equal to the average M-P bond length in $MoWCl_4(PMe_3)_4$ (1). The M-P distance is that expected when compared to the M-P distances found in the analogous molybdenum and tungsten dimers (1). Apparently, M-PMe_3 bonds are 0.1 to 0.2 Å shorter than M-PBu^n_3 bonds in these compounds; therefore, the shortness of the M-P bond in the heteronuclear tetramer is due to the bonding characteristics of PMe_3 and not to the metals present.

Table III-5. Tetramer bond distances (Å) and angles (Deg)[a]

	$Mo_2W_2Cl_8(PMe_3)_4$	$Mo_4Cl_8(PBu^n_3)_4$[b]	$W_4Cl_8(PBu^n_3)_4$[c]
$M\text{-}M_{short}$	2.275(1)	2.214(4)	2.309(2)
$M\text{-}M_{long}$	2.842(1)	2.904(3)	2.840(1)
M-Clt	2.437(4)	2.406(6)	2.400(5)
M-Clb (cis P)	2.405(4)	2.406(6)	2.396(5)
(trans P)	2.440(4)	2.417(6)	2.417(5)
M-P	2.523(4)	2.551(4)	2.530(5)
M-M-M	89.90(0)	89.94(1)	89.93(3)
M-Clb-M	71.81(10)	74.04(16)	72.3(1)
Clb-M-Clb	103.05(12)	100.48(18)	102.8(2)

[a]Estimated standard deviations are given in parentheses for last significant figures.

[b]Reference 7.

[c]Reference 4.

Because the M-PMe_3 bond is considerably shorter than the M-PBu^n_3 bonds, PMe_3 should have a greater *trans* effect than PBu^n_3. This is most likely the reason for the unusually long M-Clb bond in the mixed-metal tetramer, since it is this bond which is *trans* to PMe_3. This same *trans* effect is seen in the other tetramers, but to a lesser degree. The other M-Clb bond, *trans* to Clt, in the mixed-metal tetramer is an average of the corresponding M-Clb bond lengths in the Mo and W tetramers.

There is no apparent reason for the unusually long M-Clt distance in the mixed-metal tetramer, except that it too may be a result of bonding properties of PMe_3.

A discussion of the metal-metal bond distances in the heteronuclear tetramer based solely on its crystal structure would be ambiguous because of the inability to distinguish between Mo and W atoms in the structure. Although the triple bonds will both be Mo-W bonds, the two single bonds could be either two Mo-W bonds, or one Mo-Mo bond and one W-W bond. The ^{31}P NMR results discussed next distinguishes between these two metal isomers.

^{31}P NMR Spectra

Because of the low solubility of $Mo_2W_2Cl_8(PMe_3)_4$ in all common organic solvents, it was impossible to obtain a ^{31}P NMR spectrum of this tetramer. Using the tri-n-butylphosphine heteronuclear tetramer, however, solubility in $CDCl_3$ was sufficient to obtain a spectrum. The full proton decoupled ^{31}P spectrum of $Mo_2W_2Cl_8(PBu^n_3)_4$ is shown in Figure III-3. It consists of two doublets centered at 9.04 and 9.88 ppm, and two multiplets centered at 3.48 and 14.02 ppm. The two multiplets correspond

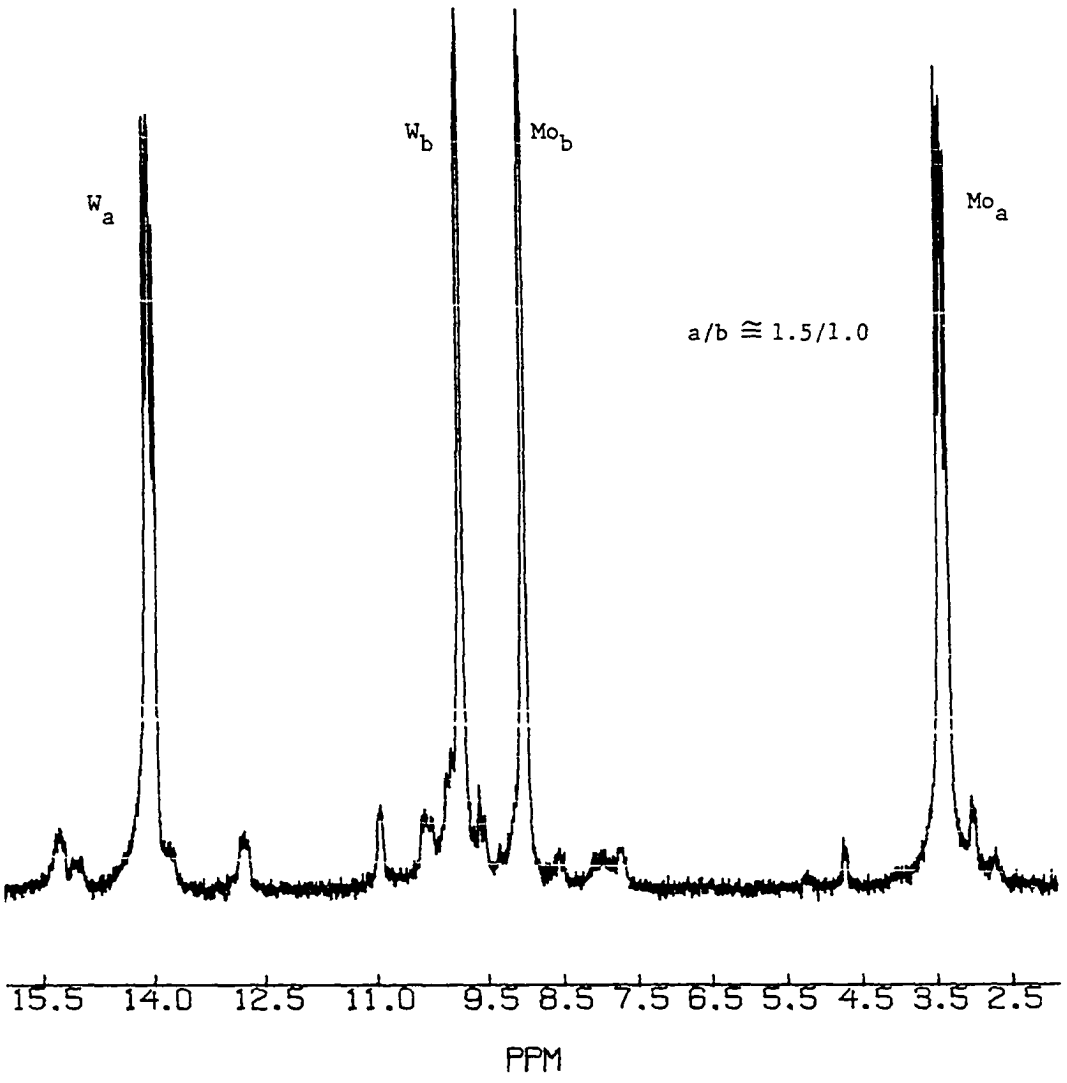

Figure III-3. Full proton decoupled ^{31}P NMR spectrum of $No_2W_2Cl_8(PBu^n_3)_4$

to one isomer, isomer a, of the tetramer, and the two doublets result from the presence of another isomer, isomer b. The relative concentrations of isomer a to isomer b is ca. 1.5 to 1.0. Assignment of these resonances requires examination of both the P-P' and W-P couplings.

The multiplets are in fact doublets of doublets with P-P' coupling constants of 8.5 and 5.9 Hz. This is apparent from Figure III-4 which shows a magnified view of the multiplet centered at 14.02 ppm. To obtain such a coupling scheme, it is necessary to have an isomeric arrangement of metal atoms in which Mo and W alternate around the tetramer as shown in the Figure III-4 insert. In this isomer, each phosphorus atom on tungsten will see two equivalent phosphorus atoms bound to molybdenum. Because the two molybdenums are bonded differently to tungsten, the coupling constants of each phosphorus atom on tungsten to the phosphorus atoms on the two molybdenum will be different, thus giving rise to the observed doublet of doublets. The same coupling scheme is seen for the phosphorus atoms bound to molybdenum. Unambiguous assignment of the two coupling constants to coupling across the single or triple bond is not possible. Coupling across a heteronuclear quadruple bond has been found to be 24.7 Hz in $MoWCl_4(PMe_3)_4$ (1). The two coupling constants observed in this tetrameric isomer have similar values. It would seem most likely that the larger of the two coupling constants should be assigned to the coupling across the triple bond. This assignment can only be made tentatively since the presence of the bridging chlorine atoms across the single bond may increase the coupling process across this longer bond.

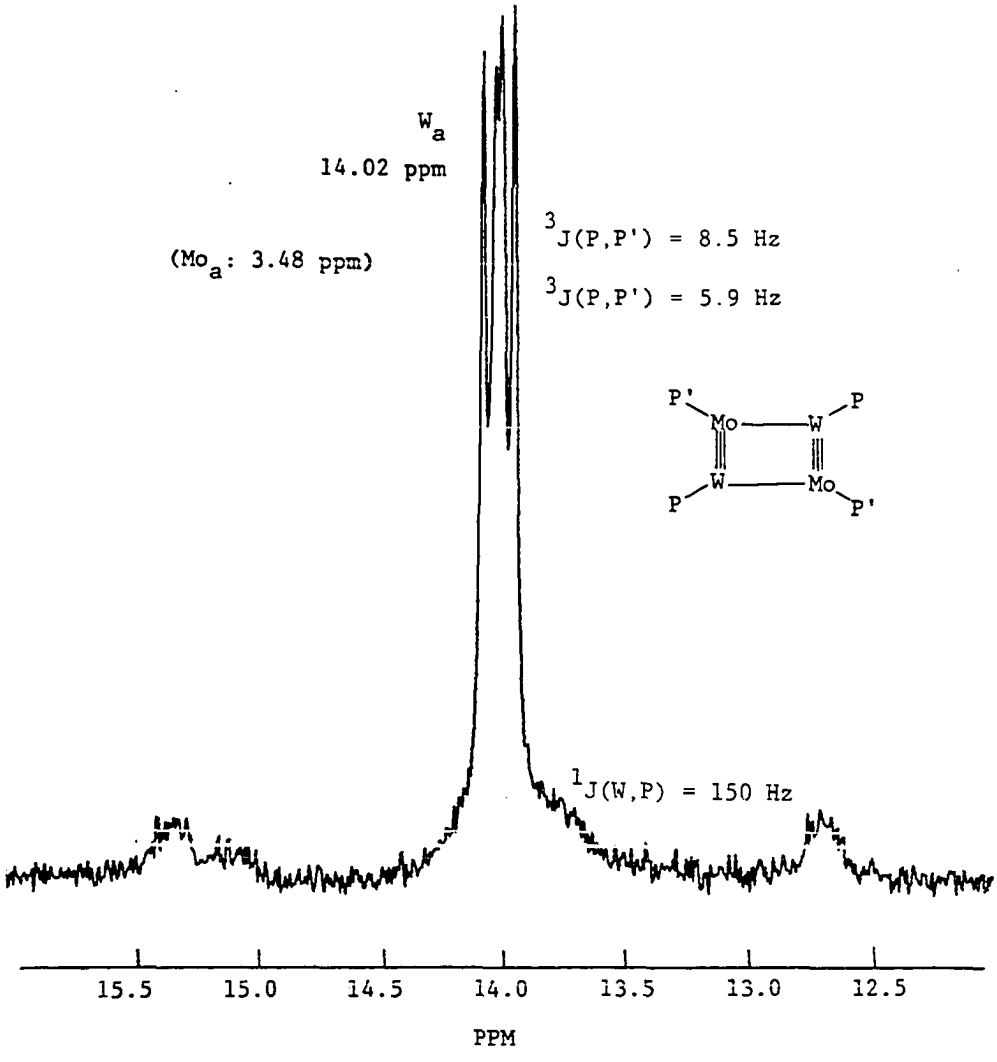

Figure III-4. Magnified view of multiplet centered at 14.02 ppm showing P-P´ coupling resulting from isomer a of $Mo_2W_2Cl_8(PBu^n_3)_4$. The other resonance for isomer a is at 3.48 ppm

Figure III-5 shows a magnified view of the resonances assigned to isomer b. The single P-P' coupling constant of 3.2 Hz observed for the two doublets can be explained by an isomeric arrangement of metal atoms in which the long bonds of the tetramer consist of one Mo-Mo bond and one W-W bond. With this arrangement, the two equivalent phosphorus atoms on the tungsten see each other across the long bond resulting in no coupling across this bond; however, they do couple across the triple bond to one of the two equivalent phosphorus atoms on molybdenum. It is somewhat surprising that such a low P-P' coupling constant is found for this isomer. It is less than one-half the lower of the two coupling constants found in isomer a. The P-P' coupling constants across the triple bond in both isomers are expected to have comparable values, yet the results do not support this, regardless of which coupling constant is assigned to the P-P' coupling across the triple bond in isomer a.

Assignment of resonances to phosphorus atoms bound to tungsten or to molybdenum can be made by looking for the presence of W-P coupling. For isomer a the resonance at 14.02 ppm is unambiguously assigned to phosphorus bound to tungsten since W-P coupling resonances are observed at ca. 150 Hz on both sides of the main resonance. (Although a sharp resonance is seen on the downfield side of the resonance at 3.48 ppm, it must be due to an impurity, because no corresponding resonance is found on the upfield side.) This value is in accord with other one-bond W-P coupling constants (17). The assignments for isomer b are not straightforward because of excessive noise and extraneous peaks in this region. The resonance at 134 Hz downfield from the doublet at 9.88 ppm has the sharpest peak profile

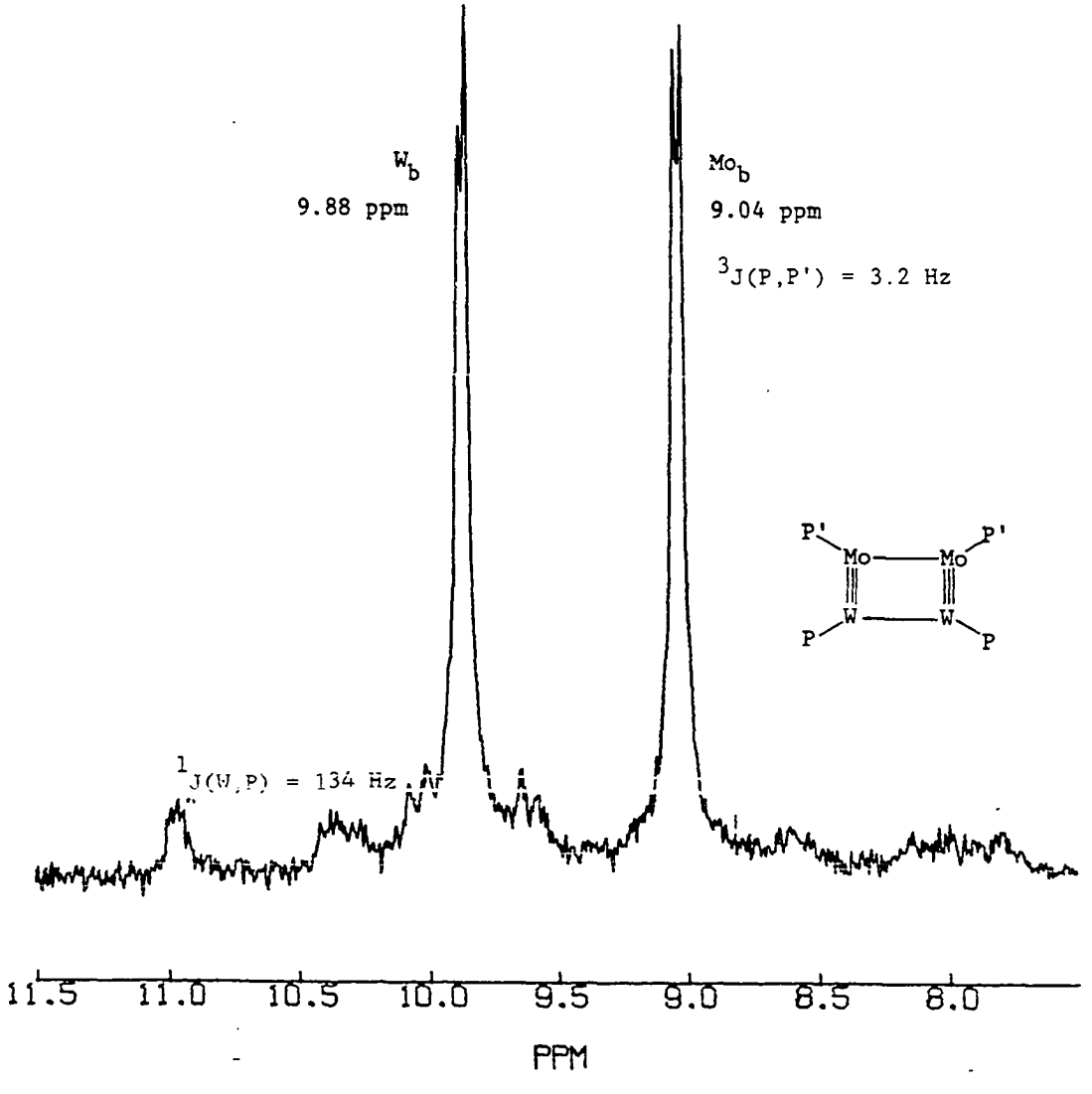

Figure III-5. Magnified view of resonances resulting from isomer b of $Mo_2W_2Cl_8(PBu^n_3)_4$

and is at a resonance frequency appropriate for a W-P coupling; therefore, the resonance at 9.88 ppm is tentatively assigned to the phosphorus atoms bound to tungsten with a W-P coupling constant of 134 Hz. The corresponding peak on the upfield side may be obscured because it would fall just on the high-field side of the main resonance at 9.04 ppm.

The formation of two metal tetrameric isomers is not totally unexpected. From statistical considerations alone, an exact 50:50 mixture of the two isomers is predicted. Apparently, there is some driving force which produces a larger fraction of isomer a over isomer b. Speculation into what these driving forces may be will be presented later.

The discussion above assumes that the resonances in the ^{31}P NMR spectrum are due to two metal isomers. If there were two types of phosphine arrangements in $Mo_2W_2Cl_4(PBu^n_3)_4$, this could also account for the spectrum. To confirm that this is not the case, a ^{31}P NMR spectrum was taken of $Mo_4Cl_8(PBu^n_3)_4$ (2) in $CDCl_3$. The spectrum showed only a sharp singlet at 14.06 ppm, indicating the presence of only one phosphine isomer for this tetramer. From a rough indexing of a single-crystal of $Mo_2W_2Cl_8(PBu^n_3)_4$ (8), it was determined that it has essentially the same unit cell as $Mo_4Cl_8(PBu^n_3)_4$ (7). These two tetramers should, therefore, be isostructural and since the molybdenum homonuclear tetramer exhibits only one arrangement of phosphine ligands, by analogy so should the heteronuclear tri-n-butylphosphine tetramer.

UV-Visible Spectra

The relevant uv-visible spectra are shown in Figures III-6, III-7 and III-8. Since the concentrations of most of the solutions used in

obtaining the spectra were not determined, the plotted absorption intensities of the curves in each figure are not representative of their relative extinction coefficients. Valuable information can be drawn from comparison of the relative curve shapes and the position of absorption maxima.

Figure III-6 plots the uv-visible spectra of the three PBu^n_3 tetramers (4). It is immediately apparent that the spectra of the heteronuclear and of the tungsten homonuclear tetramers are almost identical at wavelengths below 350 nm. They both exhibit a large maximum at ca. 297 nm with a shoulder on the low energy side. The molybdenum tetramer's uv-visible spectrum shows a maximum at 312 nm with no low energy shoulder. At wavelengths above 350 nm, the spectrum of the heteronuclear tetramer appears to be an average of the spectra of the homonuclear tetramers.

In Figure III-7, plots of both the PMe_3 and PBu^n_3 heteronuclear tetramers' spectrum are shown together. They are essentially identical exhibiting maxima at 296 and 297 nm, respectively.

The final figure, Figure III-8, shows the spectra of the two PMe_3 tetramers, $Mo_4Cl_8(PMe_3)_4$ and $Mo_2W_2Cl_8(PMe_3)_4$. The $Mo_4Cl_8(PMe_3)_4$ spectrum is anomalous because of the absorptions at 273 and 344 nm. No such absorptions are found for $Mo_4Cl_8(PBu^n_3)_4$. The peaks at 307 and 417 nm in the $Mo_4Cl_8(PMe_3)_4$ spectrum correspond to absorptions at 312 and 435 nm, respectively, in the spectrum of $Mo_4Cl_8(PBu^n_3)_4$.

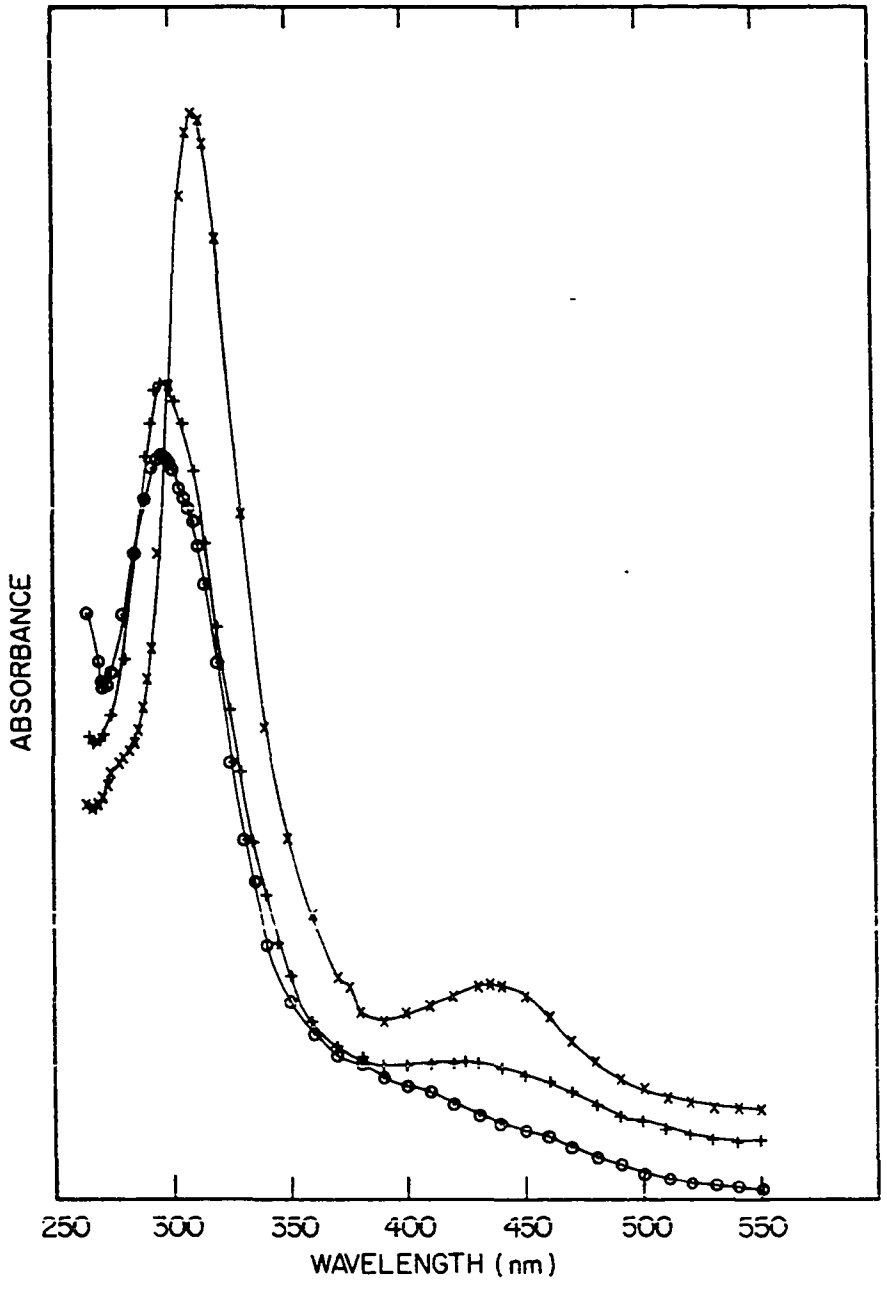

Figure III-6. $Mo_4Cl_8(PBu^n_3)_4$ (x), $Mo_2W_2Cl_8(PBu^n_3)_4$ (+) and $W_4Cl_8(PBu^n_3)_4$ (o) uv-visible spectra

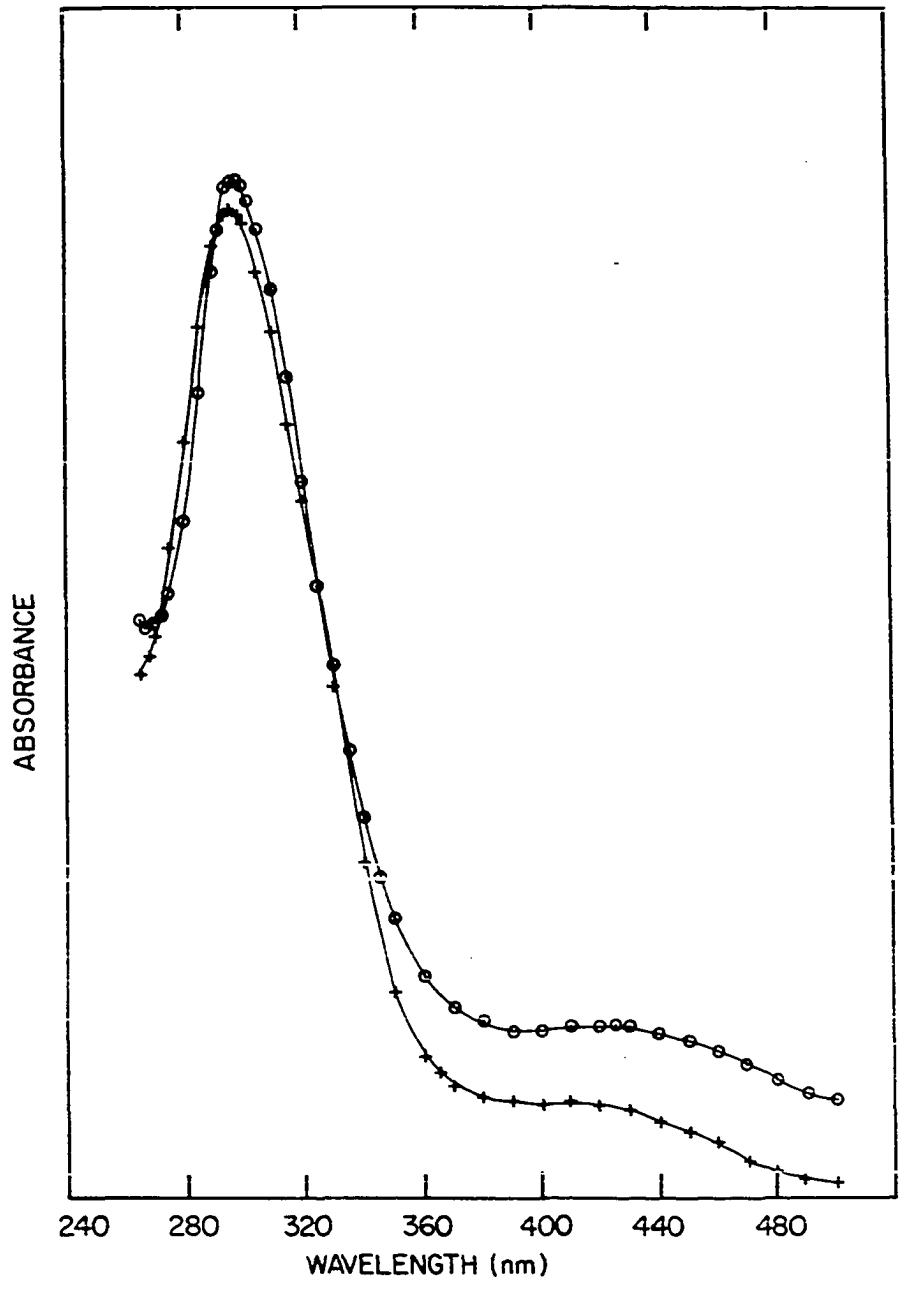

Figure III-7. $Mo_2W_2Cl_8(PMe_3)_4$ (+) and $Mo_2W_2Cl_8(PBu^n_3)_4$ (o) uv-visible spectra

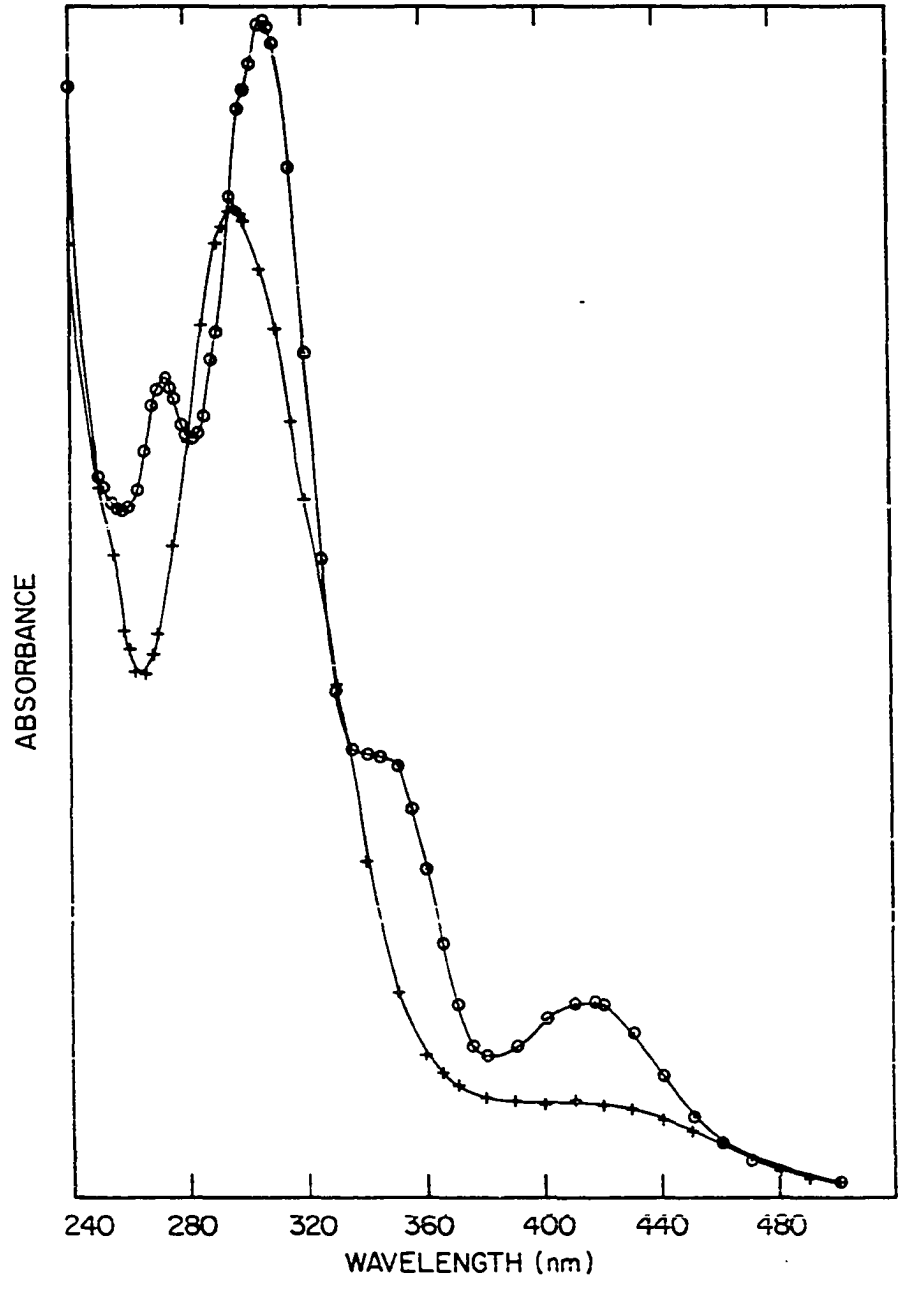

Figure III-8. $Mo_4Cl_8(PMe_3)_4$ (o) and $Mo_2W_2Cl_8(PMe_3)_4$ (+) uv-visible spectra

CONCLUSIONS

Several features of the heteronuclear tetramer deserve careful consideration. Foremost of these are the metal isomer distribution and the relation of the mixed-metal metal-metal bond distances to those found in the homonuclear tetramers.

From statistical reasoning alone, the metal isomer distribution is predicted to be a 50:50 mixture of the two metal isomers discussed earlier. The fact that the ratio of isomer a to isomer b in the tri-n-butylphosphine tetramer is ca. 1.5 to 1.0 leads to the speculation that there are some driving forces favoring isomer a. Two possible explanations are forwarded here. One explanation for the ratio of tetramers is that the formation of two heteronuclear single bonds is favored over that of two homonuclear bonds. This concept is in agreement with the hypothesis already forwarded for Mo-W quadruply bonded heteronuclear dimers that the heteronuclear quadruple bond is intrinsically stronger than the average of the two homonuclear bonds (1). Also, the presence of a charge separation between molybdenum and tungsten which has been proposed for the heteronuclear dimers (1) may cause this observed tetramer distribution. The charge separation proposed for $MoWCl_4(PMe_3)_4$ is such that a small quantity of electron density is transferred from tungsten to molybdenum. If such a phenomenon is occurring in the tetramers, then isomer a would probably have a lower total energy because of its symmetrical distribution of these charges. These factors may be acting concurrently, or it may be that none of these simple explanations are valid, and the true reason for the relative tetramer concentrations is more obscure.

A charge separation argument was also used to explain the chemical shift difference in the phosphorous atoms bonded to tungsten and molybdenum in $MoWCl_4(PMe_3)_4$. Using charge separation arguments to explain the chemical shifts in the two heteronuclear tetramer isomers, it might be expected that in isomer b the accumulation of charge on one side of the tetramer would reduce the amount of electron density transferred from tungsten to molybdenum, thus, giving more nearly equal chemical shifts for the two types of phosphorous atoms. For isomer a, the charge transfer from tungsten to molybdenum may be greater because of the symmetrical distribution of the resulting charge separations, and therefore, the observed ^{31}P chemical shifts should be larger than in isomer b. As in the discussion of the charge separation for $MoWCl_4(PMe_3)_4$ (1), these arguments must be viewed with considerable caution. It must be emphasized that the chemical shifts of ^{31}P nuclei are strongly dependent upon the paramagnetic contributions which are difficult to calculate, and so predictions of ^{31}P NMR chemical shifts are tentative at best.

A discussion of the metal-metal bond distances in the heteronuclear tetramer must take into consideration the presence of two isomers. In the discussion presented below it is assumed that the ratio of metal isomers is about the same in the PMe_3 heteronuclear tetramer as that found by ^{31}P NMR for the PBu^n_3 heteronuclear tetramer. Also, it is assumed that a difference in phosphine ligands does not affect the metal-metal distances significantly allowing comparison of $Mo_2W_2Cl_8(PMe_3)_4$ to $Mo_4Cl_8(PBu^n_3)_4$ (7) and $W_4Cl_8(PBu^n_3)_4$ (4).

Examination of Table III-4 shows that the longest M-M long-bond is found in $Mo_4Cl_8(PBu^n_3)_4$, with $Mo_2W_2Cl_8(PMe_3)_4$ and $W_2Cl_8(PBu^n_3)_4$ having essentially equal M-M long-bonds. This can be rationalized by examining the shorter M-M triple bonds in the tetramers. In $Mo_4Cl_8(PBu^n_3)_4$, the Mo-Mo triple bond is about the same length as observed in Chisholm's Mo_2L_6 compounds (L = NR_2, OR, Me, Cl, etc.), where the average Mo-Mo triple bond is ca. 2.22 Å (18). This is in spite of the greater ligand-ligand repulsions expected from the eclipsed ligands in the tetramers. This may be an indication that some residual interaction remains in the molybdenum tetramer's Mo-Mo triple bond. This partial bonding would be achieved at the expense of the Mo-Mo long bond because it is the dxy orbital on each metal which is used for both the interaction and the long bond formation (2). In $W_4Cl_8(PBu^n_3)_4$, the W-W triple bond is longer by ca. 0.02 Å than the average W-W triple bond of 2.29 Å found in the ditungsten analogues (18) of the Mo_2L_6 compounds, demonstrating the expected M-M lengthening resulting from the increased repulsions of the eclipsed ligands in the tetramers.

The fact that the M-M long-bond in $Mo_2W_2Cl_8(PMe_3)_4$ is about the same length as in the tungsten tetramer can be explained in terms of this competition for the dxy orbital. Examination of the M-M distances in the $M_2Cl_4(PMe_3)_4$ series (1) shows that the MoW bond length is closer to the W-W bond length than to the Mo-Mo bond length. Since the ditungsten compound apparently has a lower degree of δ interaction than does the dimolybdenum compound (1), the mixed-metal dimer should possess a weaker δ interaction than the average of its homonuclear analogues. In forming

the mixed-metal tetramer then, the dxy orbital is more available for forming the long bonds between coupling dimers. The strength of the M-M long bonds in the various tetramers should be such that $Mo_4Cl_8(PBu^n_3)_4$ will have the weakest bond due to the residual δ interaction, and $W_4Cl_8(PBu^n_3)_4$ will have the strongest. The long M-M bond in the mixed-metal tetramer will be nearer that of the W-W long bond but still intermediate between the two homonuclear tetramers.

The similarities in the heteronuclear and tungsten tetramers are further borne out by the uv-visible spectra already discussed. These two tetramers have nearly identical spectra, whereas the molybdenum tetramer's uv-visible spectrum is somewhat different.

The importance of residual δ bonding in the tetramers can also be used to explain the metal thermal ellipsoids in the $Mo_2W_2Cl_8(PMe_3)_4$ structure refinement. Before performing the ^{31}P NMR study on the tri-n-butylphosphine heteronuclear tetramer, it was assumed that the nearly isotropic shape of the refined anisotropic thermal ellipsoids obtained for the metal atoms meant that the only metal isomer present was one in which Mo and W alternated around the ring to give a symmetric arrangement with the two long bonds being Mo-W single bonds, and therefore of equal length. The ^{31}P NMR experiment shows that actually two metal isomers are present for $Mo_2W_2Cl_8(PBu^n_3)_4$, one with alternating metal atoms and the other isomer having long bonds consisting of one Mo-Mo and one W-W bond. If only the type of metals involved in the long M-M bonds was the factor determining the length of these bonds, then the asymmetric tetramer would be distorted such that the Mo-Mo and the W-W long bonds would be ca.

2.90 Å and 2.84 Å, respectively. Disordering of this distorted tetramer with the symmetric tetramer should produce anisotropic thermal ellipsoids elongated along the long M-M bond axes. On the other hand, using only the residual δ bond argument, the long M-M bonds in the asymmetric tetramer should be equal to each other and equal to those in the symmetric tetramer since the degree of bonding in the long bond would be dependent only on the amount of δ bonding remaining in the short bonds, which would be the same for both isomers. Based upon the thermal parameters, the distortion of the asymmetric tetramer is not observed. This implies that the distortion in the asymmetric tetramer is small due to the relative importance of the residual bond considerations, and/or that because of the higher percentage of symmetric tetramer expected to be present in the PMe_3 derivative, as indicated by the ^{31}P NMR experiment on the PBu^n_3 tetramer, the structural features resulting from this distortion are not seen in the structure refinement.

An additional factor which results in shorter M-M long-bonds for W-W is the relativistic extension of the W 5d orbitals (19). A discussion of the effect of such an extension on various Mo-Mo, Mo-W and W-W dimers has been presented (1). The extension of the W 5d orbitals will allow for better overlap at the distance found for the W-W long bonds. The Mo 4d orbitals do not experience significant relativistic extension and are not as effective in bonding at longer distances. The effect on the heteronuclear tetramer of this relativistic perturbation of tungsten will depend upon which metal isomer is considered. For the symmetric isomer, the Mo-W long bond overlap should be an average of the overlaps found for

the long bonds of the two homonuclear tetramers. The asymmetric isomer on the other hand will experience the distortion discussed above.

REFERENCES CITED

1. Carlin, R. T. Ph.D. Dissertation, Iowa State University, Ames, Iowa, 1982; Section II.

2. Ryan, T. R.; McCarley, R. E. Inorg. Chem. 1982, 21, 2072.

3. McCarley, R. E.; Ryan, T. R.; Torardi, C. C. "Reactivity of Metal-Metal Bonds"; Chisholm, M. H., Ed.; American Chemical Society: Washington, D.C., 1981, ACS Symp. Ser. No. 155, page 41.

4. Ryan, T. R. Ph.D. Dissertation, Iowa State University, Ames, Iowa, 1981; Sections II and III.

5. Carlin, R. T. Ph.D. Dissertation, Iowa State University, Ames, Iowa, 1982; Section I.

6. Katovic, V.; Templeton, J. L.; Hoxmeier, R. J.; McCarley, R. E. J. Am. Chem. Soc. 1975, 97, 5300.

7. Lii, K. H.; McCarley, R. E., Iowa State University, Ames, Iowa, unpublished results.

8. Average lattice parameters obtained from indexing two crystals of $Mo_2W_2Cl_4(PBu^n_3)_4$ were: a = 27.45 Å, b = 37.00 Å, c = 14.60 Å, $\alpha = 89.15^0$, $\beta = 88.8^0$, $\gamma = 91.4^0$. The homonuclear tetramers' unit cells are orthorhombic ($\alpha=\beta=\gamma=90^0$) with the following dimensions. $Mo_4Cl_8(PBu^n_3)_4$, a = 26.654(3) Å, b = 36.403(3) Å, c = 14.437(3) Å, reference 6; $W_4Cl_8(PBu^n_3)_4$: a = 26.990(9) Å, b = 36.302(9) Å, c = 14.293(6) Å, reference 4.

9. Rohrbaugh, W. J.; Jacobson, R. A. Inorg. Chem. 1974, 13, 2535.

10. Jacobson, R. A. J. Appl. Crystallogr. 1976, 9, 115.

11. Lawton, S. L.; Jacobson, R. A. Inorg. Chem. 1968, 13, 2124.

12. Karcher, B. A. Ph.D. Dissertation, Iowa State University, Ames, Iowa, 1981.

13. Lapp, R. L.; Jacobson, R. A. "ALLS: A Generalized Crystallographic Least Squares Program", 1979, U. S. DOE Report IS-4737.

14. Hanson, H. P.; Herman, F.; Lea, J. D.; Skillman, S. Acta Crystallogr. 1960, 17, 1040.

15. Lapp, R. L.; Jacobson, R. A. "FOUR: A General Crystallographic Fourier Program", 1980, U. S. DOE Report IS-4737.

16. Templeton, D. H. in "International Tables for X-ray Crystallography", 1st ed.; Macgillary, C. H. and Rieck, G. D., Eds.; Kynoch Press: Birmingham, England, 1962; Vol. III, page 215.

17. Pregosin, S.; Kunz, R. W. "^{31}P and ^{13}C NMR of Transition Metal Phosphine Complexes", Diehl, P., Fluck, E. and Kosfeld, R.; Eds.; Springer-Verlag: New York, 1979.

18. Chisholm, M. H. Transition Met. Chem. 1978, 3, 321, and references cited therein.

19. Pitzer, K. S. Accts. Chem. Res. 1979, 12, 271.

SUMMARY

The tungsten(III)-tungsten(III) dimer $W_2(\mu\text{-}H)(\mu\text{-}Cl)Cl_4(pyridine)_4$ and its 4-ethylpyridine analog have been synthesized from a quadruply bonded tungsten dimer. Its formulation can be viewed as an oxidative addition of HCl across a tungsten-tungsten quadruple bond. By comparison to the metal-metal double bond distances found in tungsten(IV)-tungsten(IV) dimers, the tungsten-tungsten bond in the 4-ethylpyridine complex is tentatively assigned as a double bond.

The synthesis and characterization of $MoWCl_4(PMe_3)_4$ has been accomplished. The molybdenum-tungsten bond distance is slightly longer than the average of the metal-metal distances in the homonuclear analogs. The ^{31}P NMR of this complex shows the presence of one of the few known P-P′ couplings across a metal-metal multiple bond. Certain of the anomalous characteristics of this heteronuclear dimer are proposed to result from the possible presence of an intramolecular charge separation between molybdenum and tungsten.

Two rectangular heteronuclear tetramers, $Mo_2W_2Cl_8(PMe_3)_4$ and $Mo_2W_2Cl_8(PBu^n_3)_4$ have been synthesized. A structure determination of the PMe_3 derivative indicates that it is very similar to the previously determined molybdenum and tungsten tetramers. The structure consists of two triply bonded units joined together by two metal-metal single bonds to form a rectangle of metal atoms. From a ^{31}P NMR spectrum of the PBu^n_3 tetramer, it has been determined that there are two isomers present differing only by the arrangement of the metal atoms around the rectangle.

ADDITIONAL LITERATURE CITED

1. Cotton, F. A.; Walton, R. A. "Multiple Bonds Between Metal Atoms"; John Wiley and Sons: New York, 1982; and references cited therein.

2. Cotton, F. A.; Fanwick, P. E.; Niswander, R. H.; Sekutowski, J. C. J. Am. Chem. Soc. 1978, 100, 4725.

3. Stephenson, T. A.; Wilkinson, G. J. Chem. Soc. 1964, 2538.

4. Cotton, F. A.; Niswander, R. H.; Sekutowski, J. C. Inorg. Chem. 1978, 17, 3541.

5. Sattelburger, A. P.; McLaughlin, K. W. J. Am. Chem. Soc. 1981, 103, 2880.

6. Demarco, D.; Nimry, T.; Walton, R. A. Inorg. Chem. 1980, 19, 575.

7. Anderson, L. B.; Cotton, F. A.; Demarco, D.; Fang, A. Ilsley, W. H.; Kolthammer, W. S.; Walton, R. A. J. Am. Chem. Soc. 1981, 20, 5078.

8. Sharp, P. R.; Schrock, R. R. J. Am. Chem. Soc. 1980, 102, 1430.

9. Collins, D. M.; Cotton, F. A.; Koch, S.; Millar, M.; Murillo, C. A. J. Am. Chem. Soc. 1977, 99, 1259.

10. Cotton, F. A.; Koch, S.; Mertis, K.; Millar, M.; Wilkinson, G. J. Am. Chem. Soc. 1977, 99, 4989.

11. Collins, D. M.; Cotton, F. A.; Koch, S.; Millar, M.; Murillo, C. A. Inorg. Chem. 1978, 17, 2017.

12. Sattelberger, A. P.; McLaughlin, K. W.; Huffman, J. C. J. Am. Chem. Soc. 1981, 103, 2880.

13. Santure, D. J.; Huffman, J. C.; Sattelberger, A. P. J. Am. Chem. Soc. to be published.

14. Cotton, F. A.; Wang, W. Inorg. Chem. 1982, 21, 3859.

15. Katovic, V.; Templeton, J. L.; Hoxmeier, R. J.; McCarley, R. E. J. Am. Chem. Soc. 1975, 97, 5300.

16. Katovic V.; McCarley, R. E. J. Am. Chem. Soc. 1978, 100, 5586.

17. Cotton, F. A.; Extine, M.; Gage, L. D. Inorg. Chem. 1978, 17, 172.

18. Katovic, V.; McCarley, R. E. Inorg. Chem. 1978, 17, 1268.

19. Ryan, T. R.; McCarley, R. E. Inorg. Chem. 1982, 21, 2072.

20. McCarley, R. E.; Ryan, T. R.; Torardi, C. C. "Reactivity of Metal-Metal Bonds"; Chisholm, M. H., Ed.; American Chemical Society: Washington, D.C., 1981; ACS Symp. Ser. No. 155, page 41.

ACKNOWLEDGEMENTS

I would like to express my appreciation for all the advice and guidance given to me by Dr. R. E. McCarley. In addition, my fellow graduate co-workers provided invaluable friendship and help for which I am most grateful. I would also like to thank all the members of Dr. R. A. Jacobson's research group for their patient and amiable consultations.

Of course, I must thank all my close friends here who made my graduate career a memorable and enjoyable portion of my life. Lastly, and most importantly, I want to thank my parents, Robert and Betty Carlin, for their love and encouragement throughout my academic career.